

Sigurd Harstad

Bulk oil-water pipe separation: performance of MPPS prototype with spiked oil

Masteroppgave i Petroleumsteknologi

Veileder: Milan Stanko

Februar 2021

Sigurd Harstad

Bulk oil-water pipe separation: performance of MPPS prototype with spiked oil

Masteroppgave i Petroleumsteknologi
Veileder: Milan Stanko
Februar 2021

Norges teknisk-naturvitenskapelige universitet
Fakultet for ingeniørvitenskap
Institutt for geovitenskap og petroleum



NTNU

Kunnskap for en bedre verden

Sammendrag

Vann produseres vanligvis sammen med hydrokarboner under utvinning av olje og gass. Når et felt modnes, forventes den produserte vannmengden å stige. Vannet må skilles fra olje og gassen og behandles før det slippes ut eller injiseres i bergartene.

Ved NTNU er det en forskningsgruppe som jobber med undervanns produksjon og prosessering kalt SUBPRO, som forsker på separering av olje-vann ved bruk av rør separator konsept som er tenkt plassert på havbunnen. En prototype av en slik separator er blitt utviklet og bygget, som del av et PhD prosjekt. Væskene benytte i de første eksperimentene på prototypen var Exxsol™ D60 og desilert vann tilsatt salt.

I denne avhandling vil ytelsenes til separator prototypen undersøkes, med en ny olje-vann blanding med mer realistisk egenskaper skal separeres, en væskeblanding som er mer lik hva en kan forvente fra en produksjonsbrønn.

For å studere effekten av å tilsette råolje til Exxsol™ D60 har på seperasjon av væskeblanding, ble det gjennomført seperasjonstester i glassflasker. Exxsol™ D60 ble tilsatt råolje i mengder av 200, 300, 400, 500, 600, 700, 800 ppm. De ulike blandingene av Exxsol™ D60 og råolje ble blandet med destillert vann tilsatt 3,4 vekt% NaCl, i vannkutt på 25, 50 og 75%. Resultatene indikerer at ved å tilsette råolje til Exxsol™ D60 øker signifikant tiden for at grenseflaten mellom de to væskene forblir ved samme høyde. Og øker signifikant tiden som krevers for at væske skilles, for vannkutt 25% og 50%. For eksempel økes tiden før væskene skilles ved vannkutt 25% fra 51 s for 200 ppm råolje i Exxsol™ D60 til 2 min og 21 s for 800 ppm i Exxsol™ D60. Det var ingen signifikant endring for vannkutt 75%.

Eksperimenter ble utført på prototypen ved å separere Exxsol™ D60 og destillert vann tilsatt 3,4 vekt% NaCl og ved å separere Exxsol™ D60 tilsatt 185 ppm råolje og destillert vann tilsatt 3,4 vekt% NaCl. Dette for å undersøke hvordan det å tilsette råolje til Exxsol™ D60 påvirket ytelsen til separator prototype.

Kurver for dreneringspotensiale for et enkelt tappepunkt ble frembrakt og sammenlignet for de ulike væskene benyttet. Resultatene viser at når Exxsol™ D60 var tilsatt råolje var ytelsene dårligere for lik total strømningsrate og vannkutt inn til separatorene. Vannet som ble hentet ut av separatorene hadde signifikant høyere andel olje i seg. En nedgang i vannkutt hentet ut fra separatorene fra 1% oppimot 30% ble beregnet.

Kurver for dreneringspotensiale ble sammenlignet kurver gitt av en forenklet numerisk modell som tidligere er utviklet. Denne modeller ser på ulike strømningsmønstre og hvordan en tenkte tapping av disse vil påvirker kurver for dreneringspotensiale. Observasjoner tyder på at modellen samsvarer med kurver for dreneringspotensiale når rent vann tappes. Modellen for emulsjon dekker ikke alle de ulike utviklingene av kurver for dreneringspotensiale som ble sett når emulsjon ble tappet.

Summary

Water is typically produced simultaneously with hydrocarbons during oil and gas extraction. As fields mature the amount of water produced is expected to rise. The water needs to be separated from the oil and gas and treated before disposal to the environment or re-injection into formations.

At NTNU there is a research program on subsea production and processing called SUBPRO that conducts research on bulk separation of oil-water using a pipe separator concept for placement on the seabed. A prototype of this separator was developed and build during a PhD research project. The test fluids used for the first experimental campaigns were Exxsol™ D60 and distilled water with salt.

In this thesis, the author will examine the performance of the prototype separator when separating a new oil-water mixture with more realistic separating characteristics, that are closer to what can be expected from a well stream.

To study the effect of adding crude to Exxsol™ D60 on the separation performance prior to experiments on the prototype separator, bottle separation tests with Exxsol™ D60 spiked with X amounts of crude oil (200, 300, 400, 500, 600, 700, 800 ppm) and distilled water w/ 3,4 wt% NaCl at water cut 25, 50 and 75% were performed. The results indicate that adding crude oil to Exxsol™ D60 increases significantly the time required for the interface to form and remain at a stable level and for separation to be completed for water cuts of 25% and 50%, e.g at water cut 25% separation time increased from 51 s for Exxsol™ D60 + 200 ppm crude to 2 min and 21 s for Exxsol™ D60 + 800 ppm crude. The was no significant change in separation time for a water cut of 75%.

Experiments were performed on the prototype separator with Exxsol™ D60 mixed with distilled water w/ 3,4 wt% and Exxsol™ D60 + 185 ppm crude mixed with distilled water w/ 3,4 wt% to study the effect of adding crude to Exxsol™ D60 on the prototype separator performance.

Drainage potential curves for a single tapping point were generated and compared between the Exxsol™ D60 and Exxsol™ D60 + 185 ppm crude. Results show that when the Exxsol™ D60 was spiked with crude, for the same operating conditions, the extracted water stream had a significantly higher oil content than for Exxsol™ D60, a drop in water cut tapped from the separator of 1 % upwards to 35 % was observed. Thus the performance of the prototype separator was worse when separation Exxsol™ D60 spiked with 185 ppm crude and distilled water w/ 3,4 wt%.

The experimental drainage potential curves were compared to the output of a simple numerical model programmed previously by the author that considers the flow pattern approaching the tapping point. The model-generated curves fit the experimental curves for tapping of pure water, but tapping of different oil-water emulsions was not completely captured the model-generated curves.

Acknowledgments

I would like to start by expressing my deepest gratitude to my supervisor, Associate Professor Milan Stanko, for all his help, giving valuable feedback, and sharing his vast knowledge. It has been a pleasure. Secondly, I would like to give thanks to Ph.D. candidate Hamidreza Asaadian, for our cooperation, his help, and all the fun times we had working together. I would like to thank SUBPRO for letting me use the MPPS setup.

A special thanks to Noralf Vedvik, Steffen Wærnes Moen for helping me get the MPPS up and running, and show me how to operate it.

Thanks to Heiner Schümann, Roger Overå, for different kinds of theoretical and practical help.

Students and PhD candidates in "Milans research group" has my gratitude, for inspiring me with their own work.

Thanks to all taxpayers in Norway, paying for all my years of tuition-free education.

Lastly I would like to thank all of my friends at NTNU, UiB, UiS and in Tekna Student for brightening up my days, in different ways.

Livet er et lære, man må alltid lære - Mayo

Life is a lesson, one must always learn - Mayo

Table of Contents

Sammendrag	i
Summary	i
Acknowledgments	ii
Table of Contents	v
List of Tables	vii
List of Figures	xi
Nomenclature	xii
1 Introduction	1
1.1 Motivation	1
1.2 Objective	3
1.3 Methodology	3
1.4 Software	4
1.4.1 Excel®	4
1.4.2 LabVIEW™	4
2 Theoretical framework	5
2.1 Density	5
2.2 Viscosity	5
2.3 Gravity-driven fluid separation	6
2.4 Flow patterns of multiphase flow in pipes	8
2.4.1 Stratified flow	9
2.4.2 Dispersed flow	9
2.4.3 Emulsion flow	10
2.5 Stability of emulsion	11
2.6 Drainage potential	11
2.7 Estimation of experimental errors	12
2.7.1 Root sum squared	13
2.7.2 Propagation of errors	13

2.8	Systematic and random error	14
2.8.1	Random error	14
2.8.2	Systematic error	15
2.9	Five number summary	16
2.10	Numerical model of drainage potential of a single tapping point	17
2.10.1	Assumptions	17
2.10.2	Drainage potential curve model	18
2.10.3	Width function	19
2.10.4	Water volume fraction distributions	20
2.10.5	Numerical solving	26
3	Bottle separation tests	29
3.1	Method	29
3.2	Bottle separation test results	32
4	Experimental campaigns	35
4.1	Design	35
4.2	Regulation	37
4.3	Instrumentation and measurements	38
4.3.1	Data acquisition system	39
4.3.2	Systematic error in experimental campaign	40
4.3.3	Random error in experimental campaign	40
4.3.4	Calibration	40
4.4	Exxsol™ D60 campaign	41
4.5	Exxsol™ D60 + 185 ppm crude oil campaign	42
5	MPPS experimental results	43
5.1	Drainage potential for unspiked oil and spiked oil at equal inlet conditions	44
5.2	Drainage potential for fixed WC inlet and same fluid mixture over a range total flow rates	55
6	Project thesis numerical modeling results	63
6.1	Drainage potential curves from numerical modeling	63
7	Discussion	71
7.1	Bottle separation tests results	71
7.2	MPPS experimental results	72
7.3	Comparison between experimental and model-generated drainage potential curves	73
8	Conclusion	77
8.1	Recommendation for further work	78
	Bibliography	79
	Appendix A - Calibration certificate for Micro Motion F200 and Sitrans FC430	83

Appendix B - Re-calibration statement	94
Appendix C - Risk assessment for laboratory experiments (Norwegian)	96
Appendix D - Risk assessment for MPPS experiments (Norwegian)	100
Appendix E - Documentation for laboratory equipment	107
DURAN®YOUTILITY Laboratory Bottle 125 ml	107
SARTORIUS CPA6202S	110
heidolph MR Hei-Standard	117
Appendix F - MATLAB script	119
Drainage potential curve script	119
Step water volume fraction function script	124
Step water volume fraction function script	125
Step water volume fraction function script	126
Uniform volume fraction function script	127
Linear transition from water to oil script	127
Linear transition from water to oil with phase contamination script	129
Width function script	130
Bisection Method script	130

List of Tables

3.1	Test matrix for bottle separation tests	29
4.1	Pump specifications	37
4.2	Recorded parameters	38
4.3	WC calculated related to the corresponding tags in the PI&D of Fig.4.3	39
4.4	Systematic error components [26]	40
4.5	Unspiked Exxsol™ D60 Experimental campaign test matrix	41
4.6	Unspiked Exxsol™ D60 Experimental campaign infill test matrix	42
4.7	Spiked Exxsol™ D60 Experimental campaign test matrix	42
4.8	Spiked Exxsol™ D60 Experimental campaign infill test matrix	42

List of Figures

1.1	Ratio[-] of produced water [m ³] and produced oil [m ³] [5]	2
2.1	Illustration of fluid viscosity [13]	5
2.2	Forces acting on a liquid droplet submerged in a fluid [14]	6
2.3	Design of gravity separator [22]	8
2.4	Stratified flow [18]	9
2.5	Stratified flow with mixing over interface [18]	9
2.6	Dispersed flow, less dense dispersed in dense liquid [18]	10
2.7	Dispersed flow, dispersed liquid in both phases [18]	10
2.8	Emulsion flow, water dispersed in oil	10
2.9	Emulsion flow, oil dispersed in water	11
2.10	Tapping of stream illustration	11
2.11	Drainage potential curve illustration	12
2.12	Illustration of relationships between the true value and random and systematic errors [12]	14
2.13	Pipe section with fluid split along $y=h$	17
2.14	Flowchart for adjusting the solution generated	20
2.15	Uniform water volume fraction in pipe for inlet WC 30%,50%,70%	21
2.16	Step water volume fraction in pipe for inlet WC 30%,50%,70%	22
2.17	Step water volume fraction with uniform contamination, WC inlet 50%, OiW 5%, WiO 5% and for WC inlet 50%, OiW 1%, WiO 10%	23
2.18	Step water volume fraction with random contamination, WC inlet 50%, mean OiW 5%, mean WiO 5%	24
2.19	Linear transition water volume fraction, for WC inlet 50% transition zone 0,1; WC inlet 50% transition zone 0,2 and WC inlet 50% transition zone 0,4	25
2.20	Linear transition water volume fraction, for WC inlet 50% transition zone 0,4 OiW 5%, WiO 10%	26
3.1	Photo of the separation bottle depicting Exxsol™ D60 w/ 300 ppm crude oil, WC 50% The black line is interface of clean oil, the brown layer between clean oil and transparent water at the bottom is an emulsion layer. Photo taken at T_{in} , time when separation of the phases was completed	30

3.2	Photo of the separation bottle depicting Exxsol™ D60 w/ 300 ppm crude oil, WC 50% The black line is interface of clean oil and transparent water at the bottom. Photo taken at T_{sep} , time when separation of the phases was completed	31
3.3	Time recorded for fixed interface, T_{in} at Crude concentration of 200, 300, 400, 500, 600, 700, 800 ppm in Exxsol™ D60, at WC 25%, 50%, 75%	32
3.4	Time recorded phase separation, T_{sep} at Crude concentration of 200, 300, 400, 500, 600, 700, 800 ppm in Exxsol™ D60, at WC 25%, 50%, 75%	33
4.1	MMPS prototype [26]	36
4.2	MMPS prototype dimensions [mm] [26]	36
4.3	PI&D experimental system setup	38
5.1	Drainage potential for spiked oil and distilled water w/ 3.4 wt% NaCl and unspiked oil and distilled water w/ 3.4 wt% NaCl at WC inlet 30%, total flow rate of 300 L/min.	44
5.2	Drainage potential for spiked oil and distilled water w/ 3.4 wt% NaCl and unspiked oil and distilled water w/ 3.4 wt% NaCl at WC inlet 50%, total flow rate of 300 L/min.	45
5.3	Drainage potential for spiked oil and distilled water w/ 3.4 wt% NaCl and unspiked oil and distilled water w/ 3.4 wt% NaCl at WC inlet 70%, total flow rate of 300 L/min.	46
5.4	Drainage potential for spiked oil and distilled water w/ 3.4 wt% NaCl and unspiked oil and distilled water w/ 3.4 wt% NaCl at WC inlet 90%, total flow rate of 300 L/min. Picture of flow of unspiked oil top left, picture of flow of spiked oil bottom left	47
5.5	Drainage potential for spiked oil and distilled water w/ 3.4 wt% NaCl and unspiked oil and distilled water w/ 3.4 wt% NaCl at WC inlet 30%, total flow rate of 500 L/min. Picture of flow of unspiked oil top right, picture of flow of spiked oil bottom left	48
5.6	Drainage potential for spiked oil and distilled water w/ 3.4 wt% NaCl and unspiked oil and distilled water w/ 3.4 wt% NaCl at WC inlet 50%, total flow rate of 500 L/min. Picture of flow of unspiked oil top left, picture of flow of spiked oil bottom left	49
5.7	Drainage potential for spiked oil and distilled water w/ 3.4 wt% NaCl and unspiked oil and distilled water w/ 3.4 wt% NaCl at WC inlet 70%, total flow rate of 500 L/min. Picture of flow of unspiked oil top left, picture of flow of spiked oil bottom left	50
5.8	Drainage potential for spiked oil and distilled water w/ 3.4 wt% NaCl and unspiked oil and distilled water w/ 3.4 wt% NaCl at WC inlet 90%, total flow rate of 500 L/min. Picture of flow of unspiked oil top left, picture of flow of spiked oil bottom left	51
5.9	Drainage potential for spiked oil and distilled water w/ 3.4 wt% NaCl and unspiked oil and distilled water w/ 3.4 wt% NaCl at WC inlet 30%, total flow rate of 700 L/min. Picture of flow of unspiked oil bottom right, picture of flow of spiked oil bottom left	52

5.10	Drainage potential for spiked oil and distilled water w/ 3.4 wt% NaCl and unspiked oil and distilled water w/ 3.4 wt% NaCl at WC inlet 50%, total flow rate of 700 L/min. Picture of flow of unspiked oil top left, picture of flow of spiked oil bottom left	53
5.11	Drainage potential for spiked oil and distilled water w/ 3.4 wt% NaCl and unspiked oil and distilled water w/ 3.4 wt% NaCl at WC inlet 70%, total flow rate of 700 L/min	54
5.12	Drainage potential for unspiked oil and distilled water w/ 3.4 wt% NaCl at WC inlet 30%, total flow rate of 300, 500, 700 L/min	55
5.13	Drainage potential for spiked oil and distilled water w/ 3.4 wt% NaCl, WC inlet 30%, total flow rates 300, 500, 700 L/min	56
5.14	Drainage potential for unspiked oil and distilled water w/ 3.4 wt% NaCl at WC inlet 50%, total flow rates 300, 500, 700 L/min	57
5.15	Drainage potential for spiked oil and distilled water w/ 3.4 wt% NaCl at WC inlet 50%, total flow rates 300, 500, 700 L/min	58
5.16	Drainage potential for unspiked oil and distilled water w/ 3.4 wt% NaCl at WC inlet 70%, total flow rates 300, 500, 700 L/min	59
5.17	Drainage potential for spiked oil and distilled water w/ 3.4 wt% NaCl at WC inlet 70%, total flow rates 300, 500, 700 L/min	60
5.18	Drainage potential for unspiked oil and distilled water w/ 3.4 wt% NaCl at WC inlet 90%, total flow rates 300, 500 L/min	61
5.19	Drainage potential for spiked oil and distilled water w/ 3.4 wt% NaCl at WC inlet 90%, total flow rates 300, 500 L/min	62
6.1	Drainage potential curve given step water volume fraction function distribution $\alpha(y)$ WC inlet 70% [16]	64
6.2	Drainage potential curve given step water volume fraction function distribution $\alpha(y)$ with uniform contamination OiW 5%, WiO 5% WC inlet 30%, 50%, 70%, 90% [16]	65
6.3	Drainage potential curve given step water volume fraction function distribution $\alpha(y)$ with uniform contamination OiW 1% WiO 1%, OiW 5% WiO 5%, OiW 10% WiO 10%, OiW 20% WiO 20%, WC inlet 50% [16]	66
6.4	Drainage potential curve given linear transition water volume fraction function distribution $\alpha(y)$ given normalized width of transition zone 0,4 WC inlet 30%, 50%, 70%, 90% [16]	67
6.5	Drainage potential curve given linear transition water volume fraction function distribution $\alpha(y)$ given normalized width of transition zone 0,1 , 0,2 , 0,4 , 0,8 WC inlet 50% [16]	68
6.6	Drainage potential curve given linear transition water volume fraction function distribution $\alpha(y)$ with uniform contamination OiW 1% WiO 1%, OiW 5% WiO 5%, OiW 10% WiO 10%, OiW 20% WiO 20% given normalized width of transition zone 0,4 WC inlet 50% [16]	69

Nomenclature

Greek

α	Volume fraction	[-]
ϵ	Separation efficiency	[%]
μ	Dynamic viscosity	[cP]
ν	Kinematic viscosity	[m^2/s]
ρ	Density	[kg/m^3]
τ	Shear stress	[N/m^2]

Other

A	Area	[m ²]
C_1	Calculated result	
D_d	Droplet diameter	[m]
D_{in}	Inner diameter of vessel/ pipe	[m]
F	Force	[N]
F_B	Buoyancy force	[N]
F_D	Drag force	[N]
F_G	Gravitational force	[N]
g	Gravitational acceleration	[m/s ²]
h_l	Height of liquid layer	[m]
H_w	Water holdup	[]
m	Mass	[kg]
m_i	measured quantity	
\bar{m}	mean value	
Q_1	first quartile	
Q_3	third quartile	
\dot{Q}	Volume flow rate	[m ³ /s]
r	Radius of pipe	[m]
T	Temperature	[° C]
T_{in}	Time for emulsion/water interface stabilized at fix height	[s]
T_{sep}	Time for emulsion/water to separate	[s]
t	Time	[s]
\bar{t}	t distribution	
UC_1	best estimate of uncertainty	
U_m	measurement error	
U_{rand}	random error	
U_{res}	resolution error	
U_{sys}	total systematic error	
U_t	transducer error	
u	Velocity	[m/s]
V	Volume	[m ³]
v	Velocity	[m/s]
y	Position in pipe	[m]

Abbreviations

ADC	analog to digital converter
ER	Extraction Rate
IFT	Interfacial tension
LBS	Least significant bit
LC	Level control
MMPS	Multiple Parallel Pipe Separator
NCS	Norwegian continental shelf
NTNU	Norwegian University of Science and Technology
OiW	Oil in Water
PC	Pressure control
PI&D	Pipe and Instrumentation Diagram
PLC	Programmable logic controller
ppm	Parts per million
ppmW	Parts per million weight
PTS	Petroleum Technical Center (senter)
RSS	Root sum squared
SD	Standard Deviation
SFI	Centre for Research-based Innovation
SPE	Society of Petroleum Engineers
SUBPRO	SUBSEA PRODUCTION AND PROCESSING
TBA	To be added
WC	Water Cut
WiO	Water in Oil
WT	Water tapped

Chapter 1

Introduction

1.1 Motivation

Water is typically produced simultaneously with hydrocarbons during oil and gas extraction. The water originates from connate water in the pores of the producing reservoir layers, water-bearing layers of the reservoir, dissolved in the hydrocarbons and external injection of water for pressure support and displacement of oil [10]. Water production on the Norwegian continental shelf (NCS) has ranged between 160-190 million Sm³ per year since 2004. For example in 2018, it was reported 133 million Sm³ water were released to the environment and 40,4 million Sm³ water were re-injected, resulting in 173,4 million Sm³ total produced water reported [5]. Produced oil in 2018 was reported to be 86,2 million Sm³, which gives a ratio of produced water to produced oil of 2,01. The general trend of the ratio of produced water to produced oil has been increasing steadily since 1994 (except for some years), reported by the Norwegian Oil and Gas Association as illustrated in **Fig. 1.1**. Fig. 1.1 show the ratio [-] produced water to produced oil on the y-axis from 1993 until 2018 on the NCS, whit year on the x-axis. The ratio of water produced to oil produced is expected to continue to rise in the future on the NCS. Handling of produced water is and will continue to be an important task for the operators, given the mature state of the NCS with many fields that produce high amounts of water and extended focus on discoveries close to existing infrastructure [6]. Tie-back to existing infrastructure limitations can create bottlenecks in the production system. Limiting the hydrocarbon production rates by the capacity to separate water and oil and capacity to treat produced water. Improving water-oil separation or adding more capacity will debottleneck the production system [26].

Prior to the disposal of produced water to the environment or re-injected into formation produced water needs to be separated from the hydrocarbons and treated. Governmental regulations limit the amount of oil in disposed water to 30 mg/L averaged over a month [3]. Water-oil separation is partly performed by a first stage bulk separator using gravity vessels where the oil content is reduced to 500 - 1000 ppmW [1]. Equipment for bulk liquid-liquid separation is placed on the subsea or topside on the offshore installations. Placing units subsea have several benefits compared to topside. The water-oil mixture travels a shorter

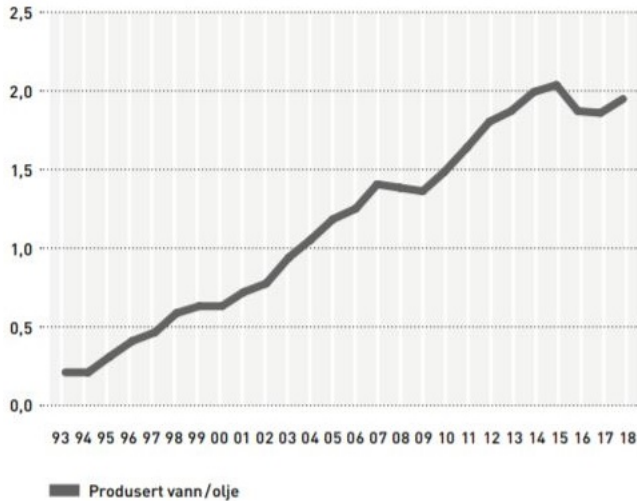


Figure 1.1: Ratio[-] of produced water [m³] and produced oil [m³] [5]

distance from the wellhead before separation, resulting in reduced pressure drop in flow lines [21],[24]. Reducing the water cut (WC) before boosting decreases the energy input potentially needed for boosting. Shorter transport lengths result in the fluid being subjected to less shear stress and the reduction of shear stress is beneficial to the separation process because it avoids the formation of fine emulsion and dispersion [26]. Another benefit is the flexibility a subsea installation provides, if needed bulk liquid-liquid separation units can be placed on the subsea without impact on weight and/or footprint limitation of an offshore topside structure. Subsea units can be installed, if needed without the operator leaving extra available space and weight carrying capacity in the field planning and development phase. Thus capital investments are reduced and parts of the investment are possibly postponed to a later phase of the lifespan of the field. The flexibility provides operators the opportunity to install subsea bulk liquid-liquid separators to combat increasing WC, and produce more oil in the late phases.

Skjefstad [27],[28] developed a parallel pipe bulk oil-water separator as part of the SUBPRO research center funded by the research council of Norway and 7 industrial partners [4]. A prototype of the separator was build and several experimental campaigns were conducted to quantify the performance of the separator, refine its design, evaluate the effect of surfactants and inlet choking, among others. The fluids employed were Exxsol™ D60 and distilled water with 3,4 wt% NaCl.

1.2 Objective

In this thesis, the author will examine the performance of the prototype of the separation concept proposed by Skjefstad, when separating a new oil-water mixture with more realistic separating characteristics. The ultimate goal is to measure the efficiency of the separator with an oil-water mixture closer to what can be expected from a well stream.

Some specific objectives of this research are:

- Quantify the variation in bottle separation time of a mixture of Exxsol™ D60 and water with 3,4 wt% NaCl when adding crude oil to the Exxsol™ D60 for different WC
- Use the results of bottle separation time to determine an appropriate Exxsol™ D60, crude oil mixture for testing on MPPS prototype

Experimental testing measuring separation performance of a single tapping point, variables measured are:

- Run a experimental campaign with Exxsol™ D60, also denoted "unspiked oil" and water with 3,4 wt% NaCl to form a benchmark
- Evaluate the results and collect more data points if deemed necessary
- Run a experimental campaign with Exxsol™ D60 + crude, also denoted "spiked oil" and water with 3,4 wt% NaCl
- Evaluate the results and collect more data points if deemed necessary

After completing data collecting, the following data analysis will be completed:

- Evaluate the results and investigate the effect on separator performance by adding crude to the Exxsol™ D60
- Compare drainage potential curves with the result from numerical modeling developed as part of project thesis [16]

1.3 Methodology

The methodology used in this project was mostly experimental, using instrumentation at Reservoir lab at Department of Geoscience and Petroleum and SUBPRO MPPS experimental setup located at "PTS Hallen" of Department of Geoscience and Petroleum. The following software was used

1.4 Software

1.4.1 Excel®

Microsoft® Excel® is software developed and sold by Microsoft® as part of the Office 365® package. Excel® is a spreadsheet program with the major benefit of displaying the values at all times, for easy manipulation. Excel® also has extensive and easy to customize plotting tools. Excel® was used in the project to store data from the experiments. Excel® calculation functions were used to calculate presented results from measured quantities, and to calculate estimated systematic and random error of the results. Excel® was also used to generate the plots provided in this thesis.

1.4.2 LabVIEW™

Laboratory Virtual Instrument Engineering Workbench is a system-design platform sold by National Instruments. A LabVIEW™ operation panel was developed by Skefstad. The LabVIEW™ operation panel was used in this work to regulate the MPPS experimental setup. And sample the data for the experimental campaigns.

Chapter 2

Theoretical framework

The content of sections 2.1, 2.2, 2.3, 2.4 and 2.6 was presented earlier by Harstad [16] as a part of *Bulk oil-water pipe separation: performance of single tap and spiking experiments*, and are restated as it forms the theoretical basis this project.

2.1 Density

Density of a fluid is according to Cengel, Cimbala [13], defined as mass per unit volume expressed in Eq. 2.1

$$\rho = \frac{m}{V} \quad (2.1)$$

By measuring the weight of a given volume, the bulk density of the fluid can be determined.

2.2 Viscosity

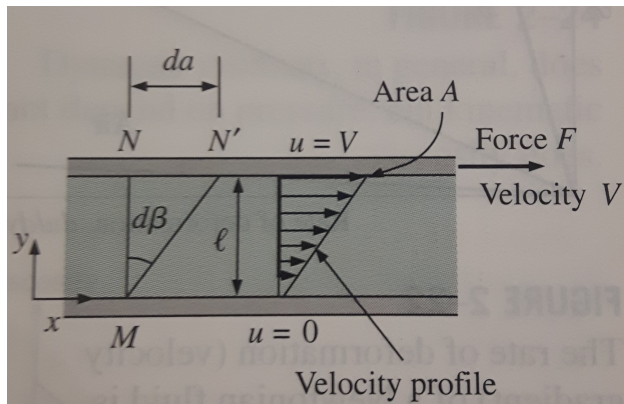


Figure 2.1: Illustration of fluid viscosity [13]

Fig. 2.1 illustrates a situation where two parallel plates are separated by fluid. The bottom plate is kept stationary, the other is subjected to a constant force F , parallel to the plates, the fluid is subjected to shear stress by the moving plate, given in Eq. 2.2.

$$\tau = \frac{F}{A} \quad (2.2)$$

In some fluids, e.g. water, oil, and air, the relationship between the shear stress and velocity profile of the fluid, $\frac{du}{dy}$ is linear. Such fluids are referred to as Newtonian fluids[13], and the relationship is expressed in Eq. 2.3

$$\tau = \mu \cdot \frac{du}{dy} \quad (2.3)$$

μ is the coefficient of viscosity or dynamic viscosity. Dynamic viscosity and density of fluid are related according to Eq. 2.4

$$\nu = \frac{\mu}{\rho} \quad (2.4)$$

ν is the kinematic viscosity.

2.3 Gravity-driven fluid separation

Immiscible fluids of different densities will separate into different layers, given sufficient time. A droplet of fluid is subjected to three forces; buoyancy force, F_B , drag force, F_D and gravitational force, F_G . Forces on a droplet submerged in a fluid illustrated in **Fig. 2.2** Assuming a circular droplet of diameter D_d the gravitational force is expressed in Eq. 2.5

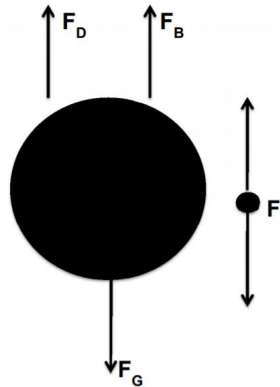


Figure 2.2: Forces acting on a liquid droplet submerged in a fluid [14]

$$F_G = m \cdot g \quad (2.5)$$

Rewritten for the gravitational force on a droplet is expressed in Eq. 2.6

$$F_G = \pi \cdot \frac{D_d^3}{6} \cdot \rho_d \cdot g \quad (2.6)$$

the buoyancy of an object fully submerged in a fluid is expressed in Eq. 2.7

$$F_B = V_{displaced} \cdot \rho_f \cdot g \quad (2.7)$$

Rewritten for the buoyancy of a fully submerged droplet in a fluid, is expressed in Eq. 2.8

$$F_B = \pi \cdot \frac{D_d^3}{6} \cdot \rho_f \cdot g \quad (2.8)$$

Drag force on a droplet given by Stokes law according to Zwanzig [29] given in Eq. 2.9

$$F_D = 6 \cdot \pi \cdot \mu_d \cdot \frac{D_d}{2} \cdot u_d \quad (2.9)$$

Balancing the forces in Eq. 2.10 and 2.11 assuming the buoyancy and drag force work in the same direction, opposite to the gravitational force.

$$F_G = F_D + F_B \quad (2.10)$$

$$\pi \cdot \frac{D_d^3}{6} \cdot \rho_d \cdot g = 6 \cdot \pi \cdot \mu_d \cdot \frac{D_d}{2} \cdot u_d + \pi \cdot \frac{D_d^3}{6} \cdot \rho_f \cdot g \quad (2.11)$$

The expression in Eq. 2.11 give a constant velocity u_d , that satisfy the force balance. This velocity is referred to as settling velocity or terminal velocity. Settling velocity of a droplet in a fluid expressed in Eq. 2.12 assuming drag given by Stokes law. Settling velocity is dependent on fluid properties, droplet properties, and droplet size.

$$u = \frac{D_d^2}{18} \cdot \frac{\rho_d - \rho_f}{\mu_f} \cdot g \quad (2.12)$$

Settling velocity for a water droplet in oil expressed in Eq. 2.13.

$$u_w = \frac{D_d^2}{18} \cdot \frac{\rho_w - \rho_o}{\mu_o} \cdot g \quad (2.13)$$

Settling velocity for an oil droplet in water expressed in Eq. 2.14.

$$u_o = \frac{D_d^2}{18} \cdot \frac{\rho_o - \rho_w}{\mu_w} \cdot g \quad (2.14)$$

The settling velocity defines the velocity at which a droplet travels in another fluid. If a droplet of fluid is submerged in a fluid of the same density the sum of forces equals zero and velocity is thus zero.

Settling velocity is used to determine the needed residence time to get phase separation. The maximum length traveled by a droplet is given by the height of the layer the droplet is submerged in h_l , given in Eq. 2.15

$$h_l = u_d \cdot t \quad (2.15)$$

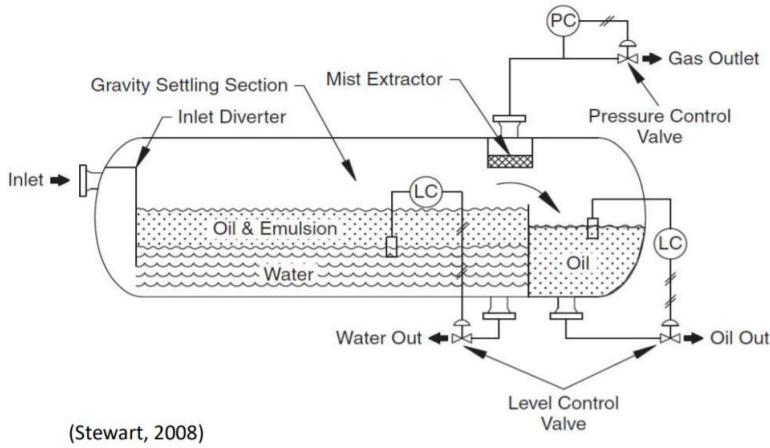


Figure 2.3: Design of gravity separator [22]

Rearranging for residence time in Eq. 2.16

$$t = \frac{h_l}{u_d} \quad (2.16)$$

Density difference is used to separate fluid in a gravity separator. A schematic illustration of gravity separator presented is in **Fig. 2.3**. Bulk separation of oil-water on the NCS is performed using gravity separation. Two or three separators are common in the North Sea according to Bothamley [9].

2.4 Flow patterns of multiphase flow in pipes

Liquid-liquid immiscible fluids flowing in the same pipe section will develop different flow patterns yielding different pressure loss and affect the separation of liquid phases, as presented by Trallero, Sarica, Brill [18]. According to Brauner [11] flow patterns are divided into four basic prototypes

1. Stratified layers with either smooth or wavy interface
2. Large slugs, elongated or spherical, of one liquid in the other
3. A dispersion of relatively fine drops of one liquid in the other
4. Annular flow, where one of the liquids forms the core and the other liquid flows in the annulus

However, in many cases, the flow pattern consists of a combination of these basic configurations. The naming and categorization of different liquid-liquid flow patterns is still a subject of debate.

Trallero, Sarica, Brill [18] identified six different oil-water flow patterns in an experimental study, these flow patterns are shortly described next. The reader is encouraged to consult the works of Trallero, Sarica, Brill [18] or Brauner [11] for further investigation of the subject of flow patterns.

2.4.1 Stratified flow

Stratified flow is flow in two distinguishable layers and separated by a smooth interface. The flow pattern is dominated by gravity, thus the phase of less density will occupy the upper part of the vessel of flow, illustrated in **Fig. 2.4**. Higher velocities of flow and higher shear at the interface may result in droplets breaking out and mixing across the liquid-interface. Stratified flow with mixing at the interface illustrated in **Fig. 2.5**

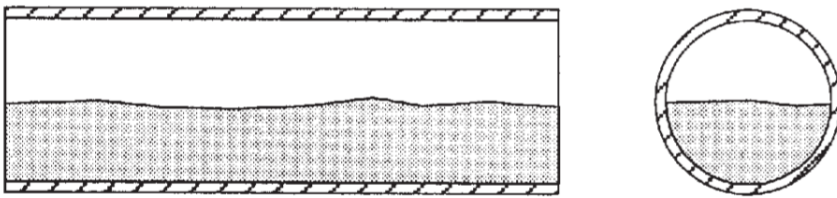


Figure 2.4: Stratified flow [18]

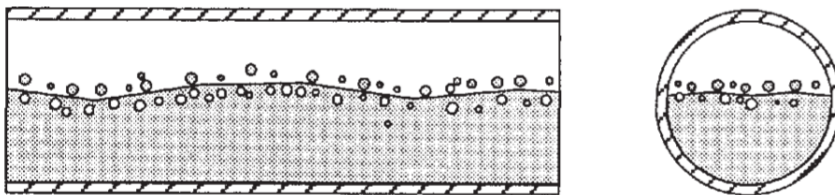


Figure 2.5: Stratified flow with mixing over interface [18]

2.4.2 Dispersed flow

Higher shear at the liquid interface results in droplets moving into the other liquid phase. The presence of the dispersed liquid affects the density, viscosity, and pressure drop of the hosting phase. One phase loses its continuity when all of the fluid is dispersed in the other fluid. Dispersed flow can consist of denser liquid dispersed in less dense liquid e.g. water dispersed in oil. Or less dense liquid dispersed in a denser liquid, e.g oil dispersed in water as illustrated in **Fig. 2.6**, or both as illustrated in **Fig. 2.7**

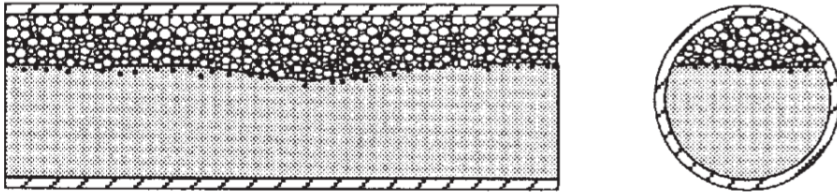


Figure 2.6: Dispersed flow, less dense dispersed in dense liquid [18]

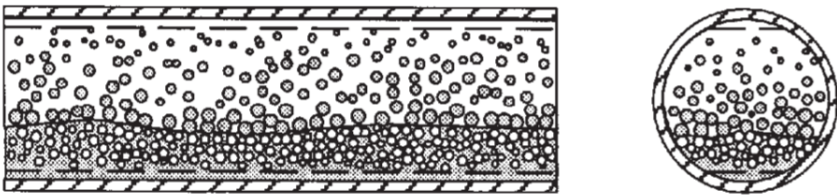


Figure 2.7: Dispersed flow, dispersed liquid in both phases [18]

If none of the liquids is fully dispersed in the other liquid, the dispersion can center around the liquid-interface and the flow pattern are of three-phase flow, with three distinguishable different layers flowing [15].

2.4.3 Emulsion flow

An emulsion is a stable mixture where one liquid is fully dispersed in another liquid. An emulsion can consist of denser liquid dispersed in less dense liquid e.g water dispersed in oil **Fig. 2.8**. Or less dense liquid in a denser liquid e.g oil dispersed in water **Fig. 2.9**

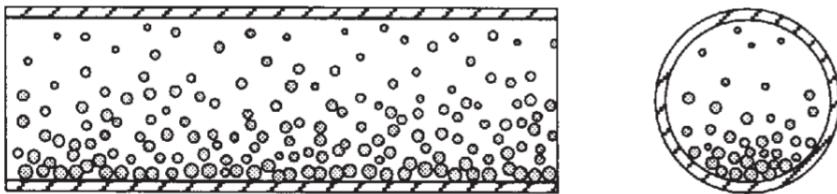


Figure 2.8: Emulsion flow, water dispersed in oil

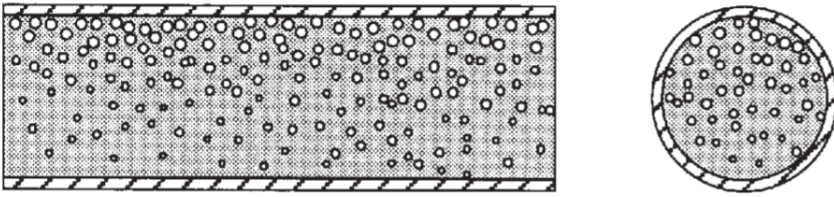


Figure 2.9: Emulsion flow, oil dispersed in water

2.5 Stability of emulsion

Emulsions are unstable and will, give time break down and separate into distinctive phases. Kokal [20] presents the following distinction in different types of emulsion. Lose, stable for a few minutes. Medium, stable for tens of minutes. And tight, stable for hours up to days.

Kokal [20] gives a number of factors affecting the stability of an emulsion.

- Presence of heavy polar components
- Fine solids in the fluids
- Temperature
- Droplet size and distribution
- Brine composition and pH

Kelesoglu [19] reports that heavy crude of the NCS forms a tight emulsion stable up to 3 week for WC 10, 20, 30, 40, 50, 55, 60, 65, and 70%

2.6 Drainage potential

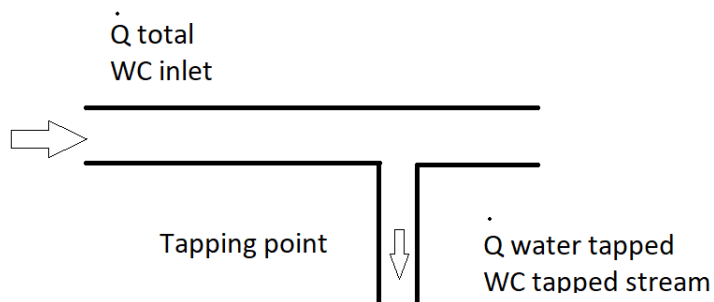


Figure 2.10: Tapping of stream illustration

Consider the oil-water separation configuration presented in **Fig. 2.10** where a mixture of oil and water, with total liquid flow rate \dot{Q}_{total} and water rate \dot{Q}_{Water} . There is a tapping point with the purpose of draining a water-rich portion of the total flow and an outlet of the oil-rich portion of the flow. A water-rich portion is extracted at the tapping point.

The tapped portion of the flow has a water rate, $\dot{Q}_{Water\ tapped}$, a total tapped liquid flow rate $\dot{Q}_{total\ tapped}$ and thus a WC_{tapped} . The percentage of total water flow tapped denoted Water Tapped (WT), can be calculated as in Eq. 2.17

$$WT[\%] = \frac{\dot{Q}_{Water\ tapped}}{\dot{Q}_{Water}} \cdot 100 \quad (2.17)$$

WC_{tapped} can be related to WT, this relation is referred to as drainage potential by Stanko [21]. The relation can be plotted to generate a drainage potential curve. An example of such a drainage potential curve is presented in **Fig. 2.11**. The drainage potential is expected to behave differently to an increase in WT, depending on the flow pattern in the pipe section.

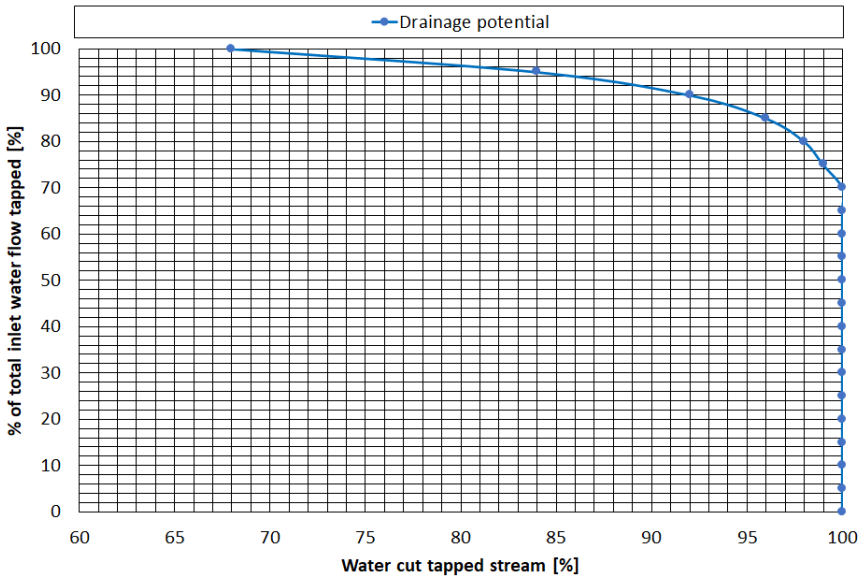


Figure 2.11: Drainage potential curve illustration

2.7 Estimation of experimental errors

In this work, errors were estimated using the principles outlined by Ratcliffe, Ratcliffe [12] and Ganji, Wheeler [8]. The reader is referred to these titles for a more detailed description of the topics. Statistical properties and definitions are extracted from Moore et al. [25]. The definitions and concepts needed to estimate and present errors for this work are summarized in the following sections.

2.7.1 Root sum squared

Root sum squared (RSS) is a mathematical operation used in the estimation of errors. An example provided in Eq. 2.18 for three values, a, b and c

$$RSS = \sqrt{a^2 + b^2 + c^2} \quad (2.18)$$

2.7.2 Propagation of errors

Experimental results of interest are calculated by combining one or more measured and/or known quantities. The errors in the measured quantities will affect the total estimated error of the calculated result. The magnitude of this effect is described as sensitivity to the one error [12]. An example is presented below to illustrate the concepts of propagation of error. If a calculated result C_1 is related to measured quantities m_{q1} , m_{q2} , m_{q3} as in Eq. 2.19.

$$C_1 = m_{q1} \cdot m_{q2} \cdot m_{q3}^2 \quad (2.19)$$

The sensitivity is expressed as the partial derivative of the calculated value with respect to the measured quantity. For the example presented in Eq. 2.19 the sensitivities are given in Eq. 2.20, Eq. 2.20, Eq. 2.22

$$\frac{\partial C_1}{\partial m_{q1}} = m_{q2} \cdot m_{q3}^2 \quad (2.20)$$

$$\frac{\partial C_1}{\partial m_{q2}} = m_{q1} \cdot m_{q3}^2 \quad (2.21)$$

$$\frac{\partial C_1}{\partial m_{q3}} = m_{q1} \cdot m_{q2} \cdot 2 \cdot m_{q3} \quad (2.22)$$

Relating the measured quantities of the example with errors Um_{q1} , Um_{q2} , Um_{q3} Ratcliffe, Ratcliffe [12] present a "best estimate of uncertainty" UC_1 as in Eq. 2.23.

$$UC_1 = \sqrt{(Um_{q1} \cdot \frac{\partial C_1}{\partial m_{q1}})^2 + (Um_{q2} \cdot \frac{\partial C_1}{\partial m_{q2}})^2 + (Um_{q3} \cdot \frac{\partial C_1}{\partial m_{q3}})^2} \quad (2.23)$$

2.8 Systematic and random error

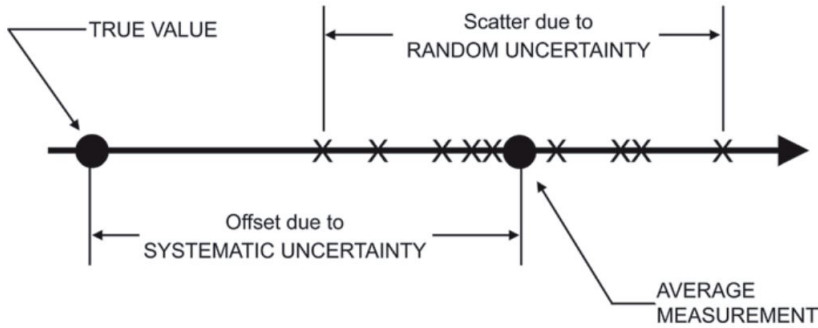


Figure 2.12: Illustration of relationships between the true value and random and systematic errors [12]

The systematic error is the measuring system's produced value offset from a true value. Random error is measurements scatter around average measurement [12], the difference of the two is illustrated in **Fig. 2.12**.

2.8.1 Random error

The random error can be expressed by Eq. 2.24 presented by Wheeler, Ganji [8].

$$\text{Random error} = \text{reading} - \text{average of reading} \quad (2.24)$$

When several measurements are recorded for a simple value. The random error should be accounted for by the following relation, Eq.2.25 according to Moffat [23].

$$U_{rand} = \pm \bar{t} \cdot SD \quad (2.25)$$

\bar{t} is t distribution and calculated by knowing the number of measurements, n and confidence interval, C . SD is the calculated standard deviation. Standard deviation can be calculated using the steps in Eq. 2.26 through Eq. 2.28 as presented by Moore et al. [25].

$$\bar{m} = \frac{\sum_{i=1}^n \cdot m_i}{n} \quad (2.26)$$

$$S = \frac{\sum_{i=1}^n \cdot (m_i - \bar{m})^2}{n - 1} \quad (2.27)$$

$$SD = \frac{S}{\sqrt{n}} \quad (2.28)$$

\bar{m} represents the average value of a measurement, m_i is the individual measurement point and n is the number of measurements.

2.8.2 Systematic error

The systematic error can be expressed by Eq. 2.29 presented by Wheeler, Ganji [8].

$$\text{Systematic error} = \text{average of reading} - \text{true value} \quad (2.29)$$

In this work, the systematic errors estimated for the measurement system and data acquisition system are affected by the resolution error U_{res} , transducer error, U_t , and measurement error, U_m . The concept and treatment of transducer error are beyond the scope of this work, the reader is directed to Sensors Terminology [7]. The measurement error, U_m represents error or uncertainty in the physical value measured before converting the measurement to a signal, electrical or other.

The total systematic error U_{sys} for the measurement system is determined using the expressing for the prorogation of error from Ratcliffe, Ratcliffe [12], as expressed in Eq. 2.30

$$U_{sys} = \sqrt{(U_{res})^2 + (U_t)^2 + (U_m)^2} \quad (2.30)$$

Resolution error

According to Wheeler, Ganji [8], converting continuous analog signal to digital signal represented in bits restricts the resolution of the value being represented. The least significant bit (LBS) represents the lowest resolution of the measured value represented in the converter bit signal. LSB can be calculated using Eq. 2.31 where n is the number of bits in the digital signal, $Analog_{max}$ is the maximum analog value output, and $Analog_{min}$ is the minimum analog value output.

$$LBS = \frac{Analog_{max} - Analog_{min}}{2^n} \quad (2.31)$$

An error in the represented digital value arises from the digital representation of the value have an LBS. This error is denoted Resolution error and can be expressed as in Eq. 2.32 where n is the number of bits in the digital signal, $Analog_{max}$ is the maximum analog value output, and $Analog_{min}$ is the minimum analog value output.

$$U_{res} = \pm 0.5 \cdot \frac{Analog_{max} - Analog_{min}}{2^n} \quad (2.32)$$

2.9 Five number summary

Moore et al. [25] state that a five-number summary can in cases where a data set has strong outliers, do a better job of representing the data set than the mean and standard deviation. A five-number summary consists of according to Moore et al. [25], a minimum value, first quartile Q_1 , median, third quartile Q_3 , and a maximum, that can be defined.

Minimum

The minimum is the lowest value recorded in a data set.

First quartile

The first quartile is the median of numbers in an ordered increasing list running from minimum to the median of the complete set.

Median

Median is the number in the center of numbers in an ordered increasing list running from minimum to maximum, if the set contains an even number of data points, the median is the mean of the two values in the center of the ordered increasing list.

Third quartile

The third quartile is the median of numbers in an ordered increasing list running from complete sets median to the maximum.

Maximum

The maximum is the highest value recorded in a data set.

2.10 Numerical model of drainage potential of a single tapping point

As part of the project thesis work, Harstad [16] developed a simplified numerical model to predict the shape of a drainage potential curve when tapping from a single tapping point, given a fractional distribution of fluids in a pipe section. The description of the model from this work [16], is included in Section 2.10 to form a basis for comparing experimental and model generate drainage potential curves.

In this section, the goal was to investigate the effect flow patterns have on the drainage potential curve. This study was performed using a numerical model, developed and programmed using the commercial software MatLab®

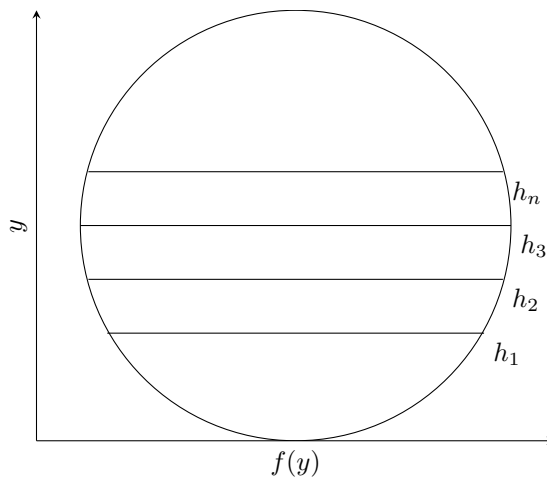


Figure 2.13: Pipe section with fluid split along $y=h$

2.10.1 Assumptions

To generate drainage potential curves from mathematical relations, the following assumptions were made to simplify the task.

- Uniform fluid velocity in the pipe. $v(y)$ fluid velocity is assumed to be the same for the whole pipe section and equal to the mixture velocity

$$v(y) = \frac{Q_o + Q_w}{A}$$

- No slip between the fluids
- Circular pipe
- No friction from the pipe wall to fluid.
- Immiscible fluids, no fluid interaction along the interface

- Simplified splitting of fluid flow. When draining a portion of the fluid from the pipe, the flow is assumed to be split along $y=h$ over the whole of the pipe body. All fluid under h is drained, all fluid over h is not drained. Splitting along h as illustrated in **Fig. 2.13**
- Steady state flow regime. Water volume fraction distribution in the flow $\alpha(y)$ and fluid velocity $u(y)$ do not change over time.

2.10.2 Drainage potential curve model

The area (A) of a pipe section was approximated using Eq. 2.33, given a function for the width $w(y)$ of the pipe as a function of y , distance from the lowest point of the pipe ($y=0$)

$$A = \int_0^{D_{in}} w(y) \cdot dy \quad (2.33)$$

Building on Eq. 2.33, the total water volume fraction, or water holdup H_w of the flow was calculated using Eq. 2.34 by introducing a function $\alpha(y)$ that give water volume fraction at position y . As a function of y , distance from the lowest point of the pipe ($y=0$).

$$H_w = \int_0^{D_{in}} w(y) \cdot \alpha(y) \cdot dy \quad (2.34)$$

WC of a flow was given by Eq. 2.35.

$$WC = \frac{\dot{Q}_{total\ water}}{\dot{Q}_{total\ liquid}} \quad (2.35)$$

By applying the no slip between fluids assumptions, WC of the flow was calculated Eq. 2.36 equal to the water holdup. This assumptions was applied for all the following relations, thus the terms WC, water volume fraction and water holdup are used interchangeably.

$$WC_{total\ calculated} = \int_0^{D_{in}} w(y) \cdot \alpha(y) \cdot dy \quad (2.36)$$

Volumetric flow rate in a pipe was expressed in Eq. 2.37.

$$\dot{Q} = A \cdot v \quad (2.37)$$

Combining Eq. 2.33 and Eq. 2.37 the volumetric flow rate, or total liquid flow rate, was expressed in Eq. 2.38.

$$\dot{Q}_{total\ liquid} = v \cdot \int_0^{D_{in}} w(y) \cdot dy \quad (2.38)$$

Total water flow rate in the pipe using expressed in Eq. 2.39.

$$Q_{total\ water} = v \cdot WC_{total} \cdot \int_0^{D_{in}} w(y) \cdot dy \quad (2.39)$$

Using the splitting of the flow outline in Fig. 2.13 along a $y=h$ the area of pipe from $y=0$ to $y=h$ was calculated using Eq. 2.40.

$$A_{pipe\ section} = \int_0^h w(y) \cdot dy \quad (2.40)$$

Using the same function $\alpha(y)$ for water volume fraction at position y gave WC for the drained portion of the flow by Eq. 2.41. The pipe was drained from $y=0$ to the horizontal line h , illustrated in Fig. 2.13. Flow in pipe area below h was assumed fully drained, flow above h was assumed not drained. To increase the volume of fluid drained, h was moved higher in the pipe section.

$$WC_{drained} = \int_0^h w(y) \cdot \alpha(y) \cdot dy \quad (2.41)$$

Combining Eq. 2.37 and Eq. 2.40 gave total liquid drained Eq. 2.42,

$$\dot{Q}_{liquid\ drained} = v \cdot \int_0^h w(y) \cdot dy \quad (2.42)$$

the total water drained in Eq. 2.43.

$$\dot{Q}_{water\ drained} = v \cdot WC_{drained} \cdot \int_0^h w(y) \cdot dy \quad (2.43)$$

The water drained was expressed in percentage of total water in Eq. 2.44

$$\% \dot{Q}_{water} = \frac{\dot{Q}_{water\ drained}}{\dot{Q}_{total\ water}} \cdot 100\% \quad (2.44)$$

2.10.3 Width function

The width $w(y)$, of a pipe segment was related to y using the the given relation Eq. 2.47, 2.48 and 2.50

$$r = \frac{D_{in}}{2} \quad (2.45)$$

For the lower half of the pipe, $y < \frac{D_{in}}{2}$

$$d = r - y \quad (2.46)$$

$$w(y) = 2 \cdot r \cdot \sin\left(\arccos\left(\frac{d}{r}\right)\right) \quad (2.47)$$

For the center-line of the pipe, $y = \frac{D_{in}}{2}$

$$w(y) = 2 \cdot r \quad (2.48)$$

For the upper half of the pipe, $y > \frac{D_{in}}{2}$

$$d = y - r \quad (2.49)$$

$$w(y) = 2 \cdot r \cdot \sin\left(\arccos\left(\frac{d}{r}\right)\right) \quad (2.50)$$

2.10.4 Water volume fraction distributions

Several water volume fraction functions $\alpha(y)$ were developed to simulate different water volume fraction distribution in the pipe. Functions was constructed to mimic the expected distribution of different flow patterns presented by Trallero, Sarica, Brill [18]. The different functions were developed using the WC inlet to system as input, more input variables were added when needed. The position of interface or point of "switch" of dominating phase calculated by the function. Workflow of the model presented in **Fig. 2.14**. Scripts are attached in appendix F.

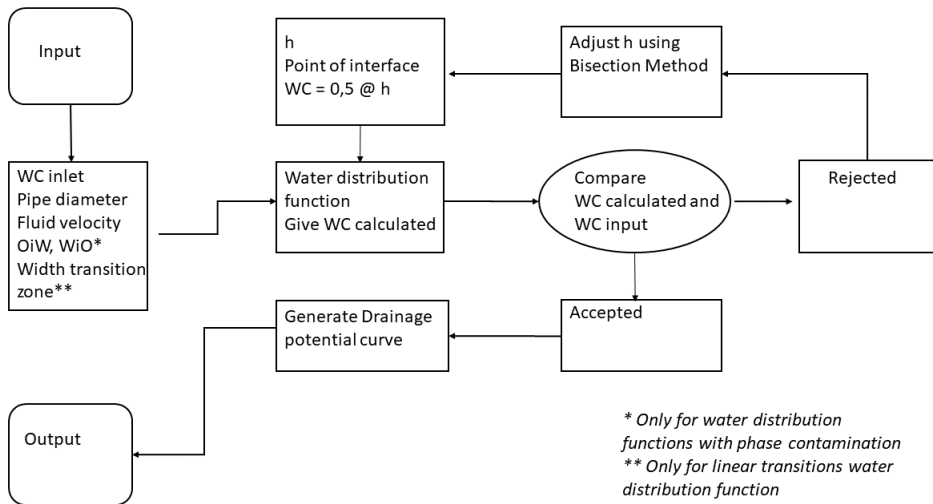


Figure 2.14: Flowchart for adjusting the solution generated

Uniform water volume fraction

Uniform water volume fraction in the pipe section gave the same water volume fraction over the whole pipe section. The water volume fraction at any position equals the WC input. Uniform water volume fraction function simulate a fully developed, uniformly distributed stable emulsion in the pipe. **Fig. 2.15** illustrate the water volume fraction distribution at normalized pipe position, for WC inlet of 30%, 50% and 70%

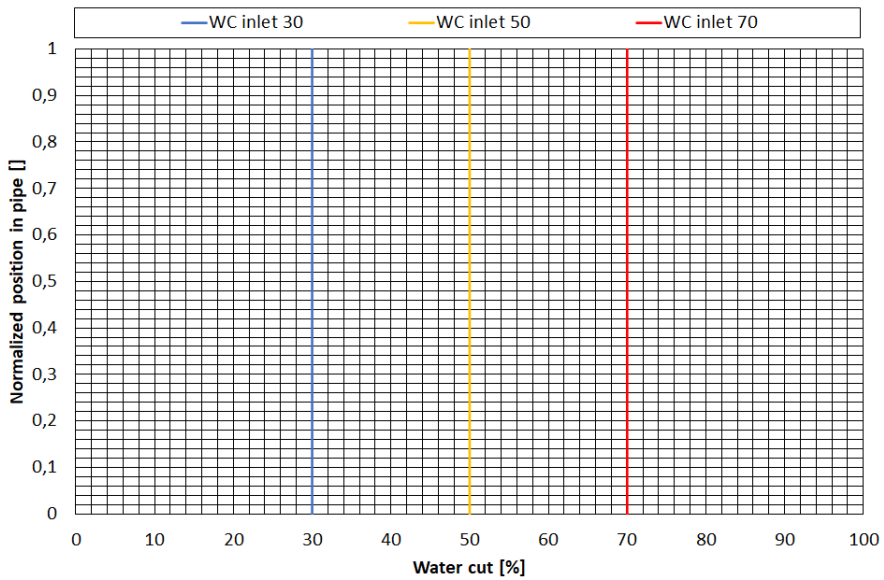


Figure 2.15: Uniform water volume fraction in pipe for inlet WC 30%,50%,70%

Step function water volume fraction

A step water volume fraction function gave water volume fraction of 100% for the portion of the pipe below the interface. A sharp interface and water volume fraction of zero for pipe position above the interface. Position of the interface was determined by the step function water volume fraction. Step water volume fraction function simulate a fully stratified flow. **Fig. 2.16** illustrate the water volume fraction distribution at normalized pipe position, for WC inlet of 30%, 50% and 70%

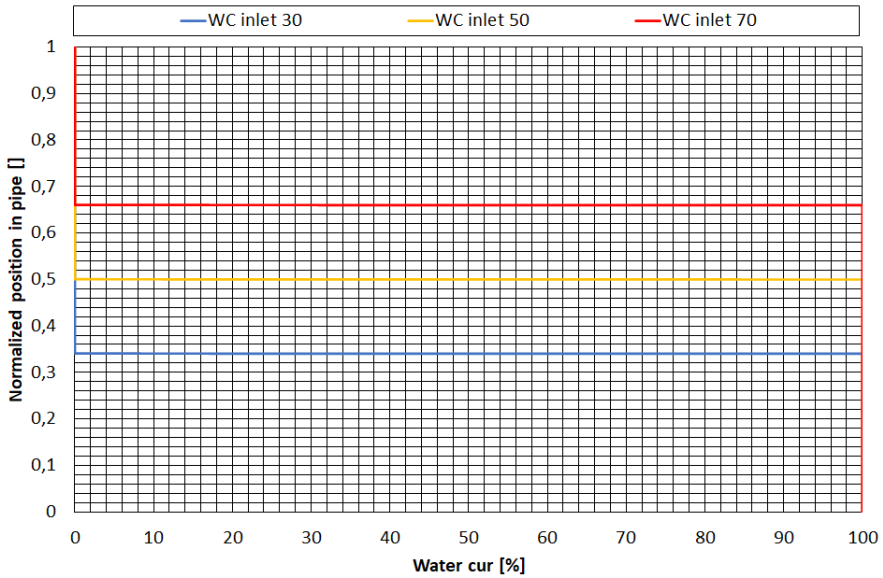


Figure 2.16: Step water volume fraction in pipe for inlet WC 30%,50%,70%

Step water volume fraction function uniform contamination

A step water volume fraction function with uniform phase contamination gave water volume fraction of 100% minus the OiW contamination below an interface. Water volume fraction of zero added the WiO contamination above the interface. WC input, OiW contamination and WiO contamination given as inputs to the function. Position of interface was determined by step water volume fraction with uniform phase contamination function. OiW and WiO can be different from each other. OiW and WiO can be chosen such that the function simulate dispersion of OiW and water flow pattern. The water volume fraction distribution can also simulate dispersion of WiO and water. **Fig. 2.17** illustrate the distribution at normalized pipe position, for WC inlet 50%, OiW 5%, WiO 5% and for WC inlet 50%, OiW 1%, WiO 10%

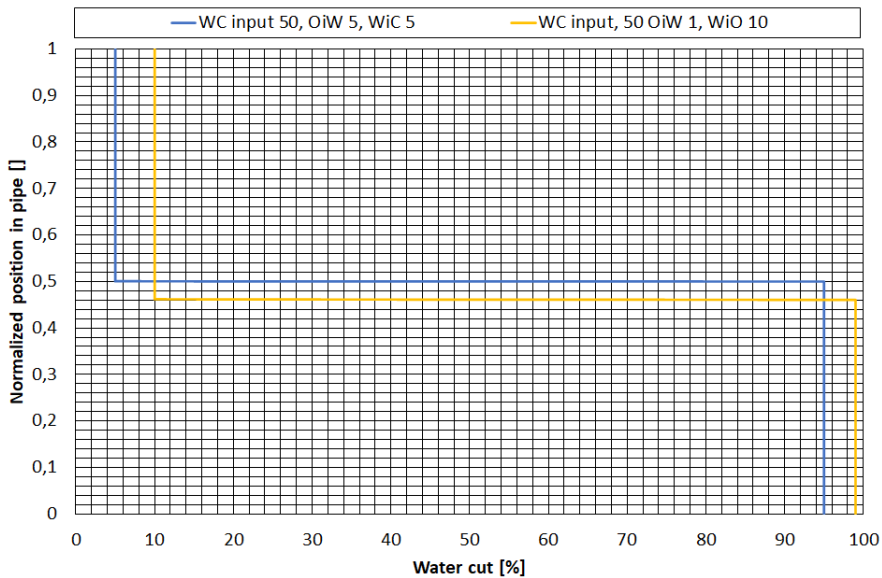


Figure 2.17: Step water volume fraction with uniform contamination, WC inlet 50%, OiW 5%, WiO 5% and for WC inlet 50%, OiW 1%, WiO 10%

Step water volume fraction function with random contamination

A step function with random contamination gave water volume fraction of 100% minus OiW contamination below the interface. A sharp interface and water volume fraction of zero plus the WiO contamination above the interface. The contamination was uniformly distributed around mean OiW and mean WiO contamination. WC input, mean OiW contamination and mean WiC contamination given as inputs to the function. Position of interface was determined by function. Mean OiW and mean WiO can be different. Step function water volume fraction with random contamination simulate stratified flow with contamination over interface. OiW and WiO can be increased such that the function simulate dispersion of OiW and water and simulate dispersion of WiO and water. **Fig. 2.18** illustrate the water volume fraction distribution at normalized pipe position, for WC inlet 50%, mean OiW 5%, mean WiO 5%

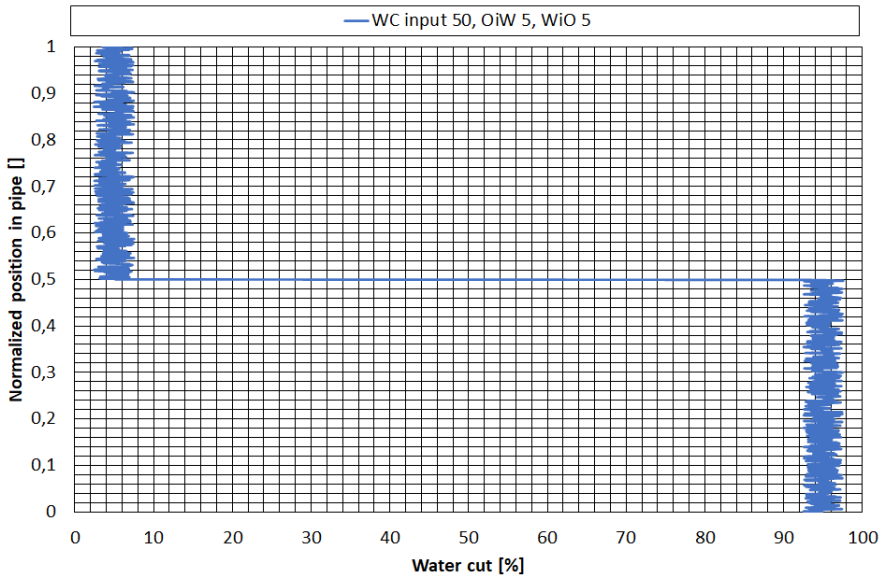


Figure 2.18: Step water volume fraction with random contamination, WC inlet 50%, mean OiW 5%, mean WiO 5%

Linear transition from water to oil

Linear transition function gave a straight line transition from water volume fraction 100%, to water volume fraction zero over a given normalized height fraction of the pipe segment. The height fraction of the transition zone is an input to the function. The position of the transition zone was determined by the linear transition function. Linear transition simulate flow pattern of three phase, with a dispersion phase between the water flow and the oil phase. **Fig. 2.19** illustrate the water volume fraction distribution at normalized pipe position, for WC inlet 50% and height fraction of transition zone as 0,1, 0,2 and 0,4 normalized pipe height fraction.

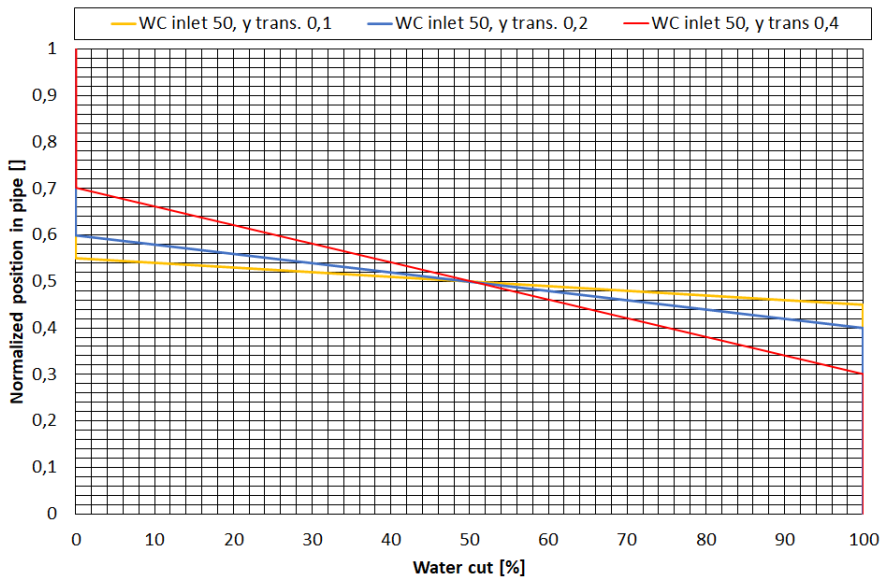


Figure 2.19: Linear transition water volume fraction, for WC inlet 50% transition zone 0,1; WC inlet 50% transition zone 0,2 and WC inlet 50% transition zone 0,4

Linear transition water to oil uniform phase contamination

Linear transition with phase contamination function gave a straight line transition from water volume fraction 100% minus OiW contamination, to zero plus the WiO contamination, over a given portion of the pipe segment. The height fraction of the transition zone is a input to the function. The position of the transition zone was determined by the linear transition with phase contamination function. Linear transition simulate a flow pattern of three phase, with a dispersion phase between the water flow and the oil phase. **Fig. 2.20** illustrate water volume fraction distribution at normalized pipe position, for WC inlet 50% and width of transition zone as 0,4 of the pipe, OiW 5% and WiO 10%

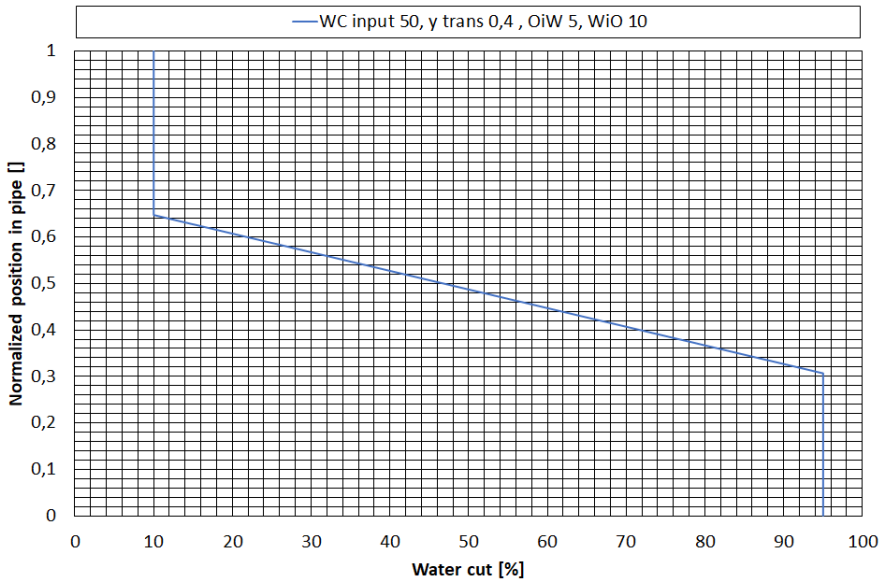


Figure 2.20: Linear transition water volume fraction, for WC inlet 50% transition zone 0,4 OiW 5%, WiO 10%

2.10.5 Numerical solving

Approximation of pipe area was compared to geometric determined cross sectional area of the pipe as given in Eq. 2.51.

$$A_{\text{geometrical}} = \pi \cdot \frac{D_{in}^2}{4} \quad (2.51)$$

$$Error_A = |A_{\text{geometrical}} - A_{\text{calculated}}| \quad (2.52)$$

$$Relative\ Error_A = \frac{Error_A}{A_{\text{calculated}}} \quad (2.53)$$

The validity of the water volume fraction distribution function generated was checked by comparing the total calculated by WC of the pipe, with the WC input as expressed in Eq. 2.54.

$$WC_{\text{total calculated}} = \int_0^{D_{in}} w(y) \cdot \alpha(y) \cdot dy \quad (2.54)$$

$$Error_{WC} = |WC_{\text{input}} - WC_{\text{total calculated}}| \quad (2.55)$$

$$Relative\ Error_{WC} = \frac{Error_{WC}}{WC_{\text{calculated}}} \quad (2.56)$$

To locate the point of interface i.e WC 50% that gave an error of acceptable level, presented in Eq. 2.55 in the distribution generated, Bisection Method presented by Mathews, Fink

[17] was used. Level of acceptable error was chosen to be relative error of less than 1%. If relative errors as presented in Eq. 2.53, 2.56 were above 1%, the discretization of the pipe was increased.

Chapter 3

Bottle separation tests

3.1 Method

The effect on adding crude oil to Exxsol™ D60 was studied by performing "bottle tests separations" at ambient temperature, 23 ± 1 °C. As a part of the experiment, a risk assessment was completed, attached in Appendix C.

Exxsol™ D60 with crude concentration of 200, 300, 400, 500, 600, 700 and 800 [mass-ppm] was chosen. The 800 ppm sample was made using a balance of type SARTORIUS CPA6202S. From this batch, the Exxsol™ D60 with added crude oil was diluted to concentration by adding pure Exxsol™ D60. Exxsol™ D60 with added crude oil and distilled water with 3.4 wt% NaCl was mixed to WC's of 25%, 50%, and 75% in DURAN® YOUTILITY Laboratory Bottle 125 ml. The combination of conditions for bottle separation tests are summarized in test matrix **Table 3.1**

Crude concentration [ppm]	WC _{in} [%]
200	25/50/75
300	25/50/75
400	25/50/75
500	25/50/75
600	25/50/75
700	25/50/75
800	25/50/75

Table 3.1: Test matrix for bottle separation tests

The mixture was stirred using a heidolph MR Hei-Standard magnetic stirrer at 750 rpm for 30 s. Then given time for the phases to separate. The separation was filmed using a camera CANON EOS 1300D to capture and analyze the separation process. A separation test was performed 3 times for each sample. 2 separate times were recorded.

T_{in} represents the time from the stirring of the magnetic mixer to stop, until the Exxsol™ D60 with crude oil, emulsion/water interface stabilized at fix height in the container, as illustrated in **Fig. 3.1**. T_{sep} represents the time from the stirring of the magnetic mixer to stop until the separation of the phases was completed. completed separation as when the mixture had returned to the original two pure phases, as illustrated in **Fig 3.2**. The range of the result is presented by given the max and min value, as "error bars", as presented in section 2.9.



Figure 3.1: Photo of the separation bottle depicting Exxsol™ D60 w/ 300 ppm crude oil, WC 50%. The black line is interface of clean oil, the brown layer between clean oil and transparent water at the bottom is an emulsion layer. Photo taken at T_{in} , time when separation of the phases was completed



Figure 3.2: Photo of the separation bottle depicting Exxsol™ D60 w/ 300 ppm crude oil, WC 50%. The black line is interface of clean oil and transparent water at the bottom. Photo taken at T_{sep} , time when separation of the phases was completed

3.2 Bottle separation test results

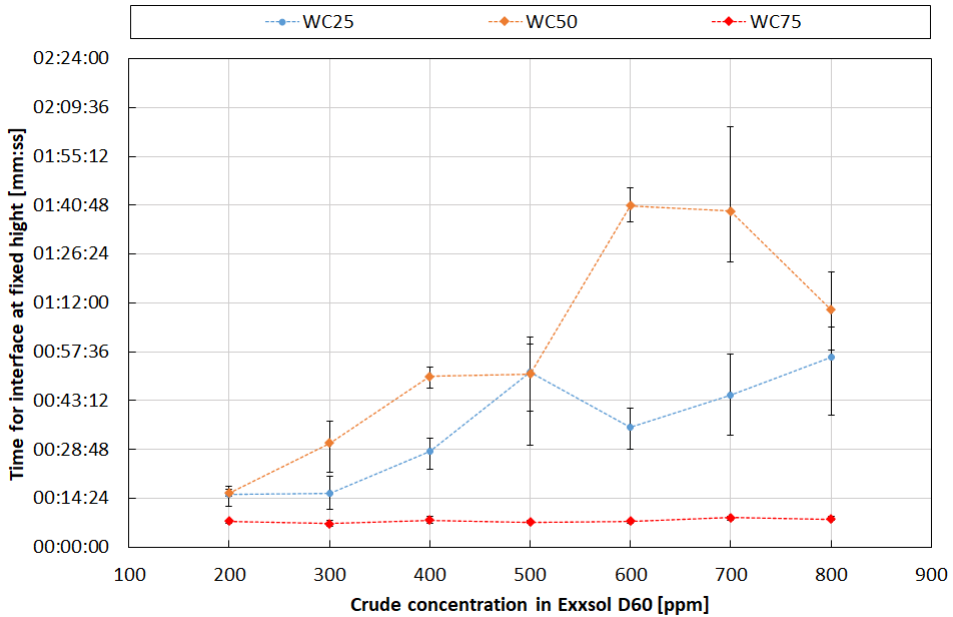


Figure 3.3: Time recorded for fixed interface, T_{in} at Crude concentration of 200, 300, 400, 500, 600, 700, 800 ppm in Exxsol™ D60, at WC 25%, 50%, 75%

The general trend for WC 50% and 25% was that T_{in} increased with increasing crude concentration in the Exxsol™ D60 as given in **Fig. 3.3**. T_{in} for WC 50% was higher than for WC 25% for most crude concentration, but the same at 500 ppm. T_{in} did not change as crude concentration increased for WC 75%.

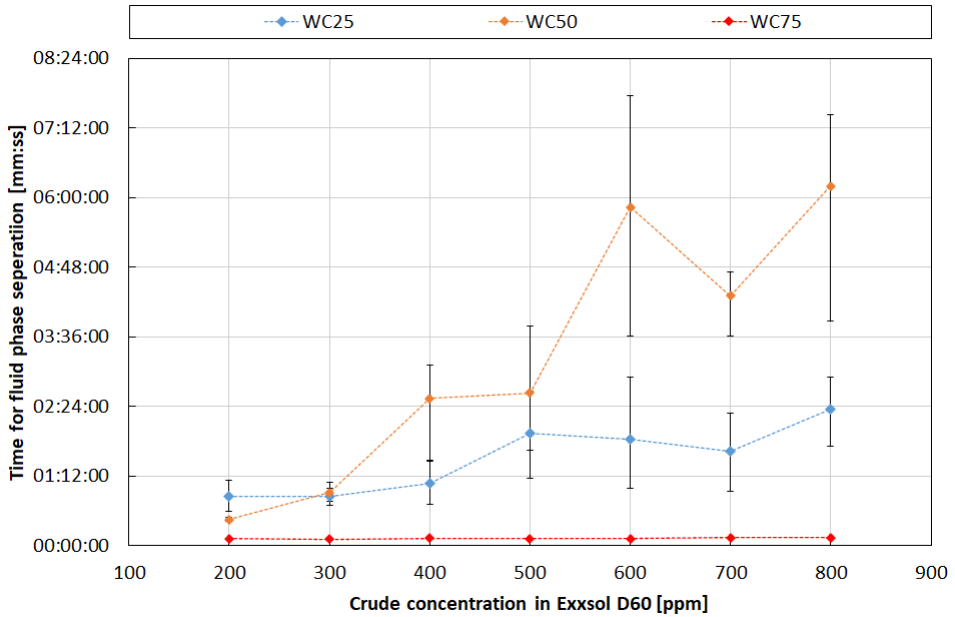


Figure 3.4: Time recorded phase separation, T_{sep} at Crude concentration of 200, 300, 400, 500, 600, 700, 800 ppm in Exxsol™ D60, at WC 25%, 50%, 75%

The general trend for WC 50% and 25% was that T_{sep} increased with increasing crude concentration in the Exxsol™ D60 as given in **Fig. 3.4**. T_{sep} for WC 50% was higher than for WC 25% for most crude concentration but the same for 300 ppm. For crude concentration of 200, T_{sep} was less for WC 50% than WC 25%. T_{sep} do not change as crude concentration increased for WC 75%.

Chapter 4

Experimental campaigns

A prototype of the Multiple Parallel Pipe Separator was previously designed and build as a part of Skjefstad work [26]. Skjefstad ran several experimental campaigns, the reader are referred to Skjefstads papers [27], [28] for a close descriptions of these campaigns.

As a part of this master project, the Multiple Parallel Pipe Separator prototype received some mechanical maintenance before running the experimental campaigns, to bring the system back to a functional state. However, the design was not altered in this process. This section introduces the system and describes the experimental campaign ran as a part of this master project.

4.1 Design

Fig. 4.1 illustrates the layout of the MPPS prototype. Fluid enters the separator unit at labeled flow \dot{Q}_{in} in Fig. 4.1., here the flow is diverted into two streams. Different flow inlet sections can be installed to alter how the flow is split. All experiments reporter was performed using a tangent to the pipe section at the inlet. This tangent inlet creates a rotation at the inlet, this rotation will push the denser water towards the wall and center the less dense oil in the center for the pipe at the inlet section. In the elbow or "bend" of the inlet section there is a device installed to stop the rotational flow and convert it into a layered flow configuration. Fluid flow then enters a downward inclined pipe section that leads the flow to the two parallel pipes. The downward inclined pipe section and the straight parallel pipes provide fluid residence time for gravity-driven phase separation. This residence will vary as the total flow rate in the separator varies. At the end of the straight parallel pipes, the fluid flow enters an upward inclined pipe section. In this upward inclined pipe section, there is tapping point for tapping fluid from the bottom side of the pipe section. Fluid dominated by the denser fluid e.g water is extracted at tapping points located at the upward inclined pipe section. Flow tapped at these tapping points are labeled \dot{Q}_w in Fig. 4.1. Tapping can be performed at different locations and different angles along the upward inclined pipe section. Flow not tapped at upward inclined pipe section enters the flow gathering pipe. Here the streams from the two parallels come together and are extracted stream labeled \dot{Q}_o in Fig. 4.1, and will be denoted oil outlet.

This fluid stream is expected to be dominated by the less dense component of the fluid mixture, e.g. Exxsol™D60.

Dimensions in millimeter of the prototype are given in **Fig. 4.2**

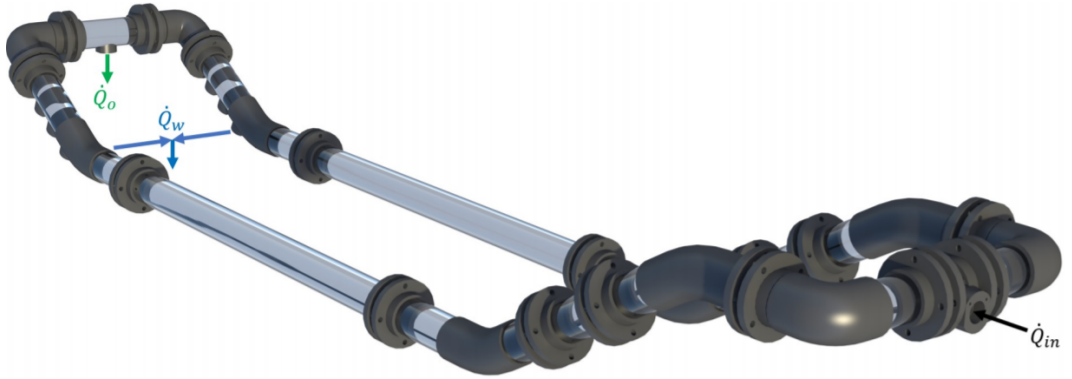


Figure 4.1: MMPS prototype [26]

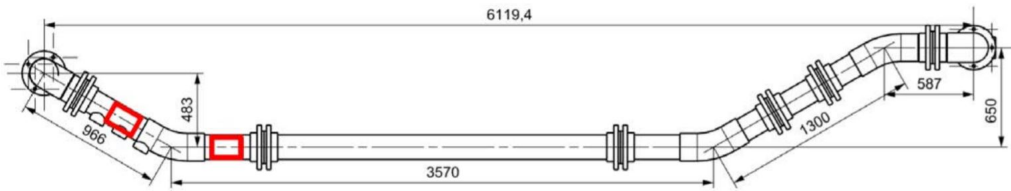


Figure 4.2: MMPS prototype dimensions [mm] [26]

The MPPS experimental setup had a control system that allows the operator of the system to specify test inlet WC, total inlet flow rate. The control system automatically adjusted the frequency of the water and pumps until desired operator-given values were reached. The main component is illustrated in the PI&D of the experimental setup **Fig. 4.3**. The main components were a storage tank, two small and two larger centrifugal pumps, piping, valves, and instrumentation. The storage tank had a storage capacity of approximately 6 m³. The storage tank provides storage for the liquid mixture and base separation of the phases. The extraction points of water and oil were separated by a 0,74 m weir plate to ensure extraction of separated liquids to the pumps and MPPS. Tapped flow from the tapping points and oil outlet flow combined after the upward inclined pipe section was transferred to the storage tank in pipes and hoses. Fluids from the MPPS tapping point and oil outlet were placed opposite of the fluid extraction points on the storage tank. This to give the fluid mixture residence time in the storage tank before reuse in the MPPS flow loop. The flow from the MPPS oil outlet and tapping points was driven into the storage tank by gravity, the MPPS system was placed above the storage tank. These fluid inlets were placed close to the centerline of the storage tank and thus close to the liquid-liquid

interface in the storage tank when filled with an equal amount of the two test liquids. This to provide possible oil droplets dispersed in water and water droplets dispersed in oil with a shorter horizontal distance to travel before reaching the respective water phase and oil phase. The centrifugal pumps provided a total flow rate and head to the system. Pump specifications is presented in **Table 4.1**.

Quantity	Model	Flow Rate	Head	Power
1	Pedrollo F65/200 AR	400-2100	22.0	57.5
1	Pedrollo F50/200 B	400-1700	15.0	52.0
2	Pedrollo F40/200 A	100-700	7.5	55.0

Table 4.1: Pump specifications

4.2 Regulation

The total liquid flow rate in the MPPS and WC inlet to MPPS was regulated by adjusting the frequency on the pumps, regulating the rotational speed. The water cut was regulated by adjusting the flow rates of water and oil. The LabVIEW operation panel included regulators for the WC inlet and total flow rate. The fluids were mixed in the piping after the Coriolis flowmeter and transported to the MMPS using pipe and tubes. The system formed a closed-loop with the liquid being extracted and returned to the storage tank. Thus liquid contamination was expected to rise throughout running the system because some droplets would not separate out of the "hosting" phase before being extracted and delivered to the MPPS separator.

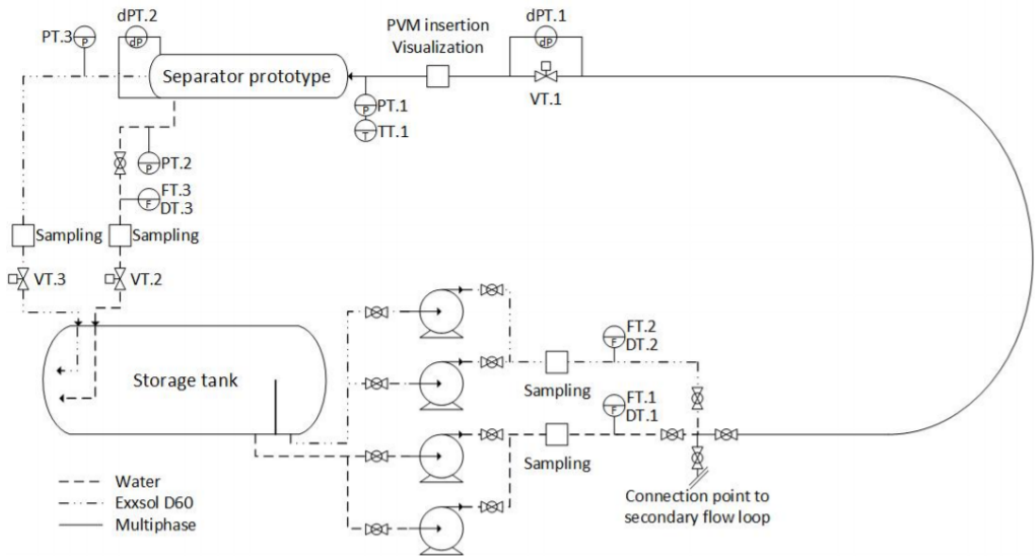


Figure 4.3: PI&D experimental system setup

4.3 Instrumentation and measurements

Recorded parameters, their corresponding tags in the PI& I of Fig. 4.3 and equipment details are presented in Table 4.2.

PI & I - Tag	Parameter	Unit	Instrument
FT.1	\dot{Q}_1	L/min	Micro Motion F200
FT.2	\dot{Q}_2	L/min	Micro Motion F200
FT.3	\dot{Q}_3	L/min	Sitrans FC430
DT.1	ρ_1	kg/m ³	Micro Motion F200
DT.2	ρ_2	kg/m ³	Micro Motion F200
DT.3	ρ_3	kg/m ³	Sitrans FC430
PT.1	P_1	barg	Sitrans P310
PT.2	P_2	barg	Sitrans P310
PT.3	P_3	barg	Sitrans P310
dPT.1	dP_1	mbar	Sitrans P310
dPT.2	dP_2	mbar	Sitrans P310
TT.1	T_1	° C	Ni1000 TK5000

Table 4.2: Recorded parameters

Micro Motion F200 and Sitrans FC430 are Coriolis flowmeters capable of measuring volume flow rate, mass flow rate, and density of liquid passing.

From density measured, ρ_i , WC_i was calculated using Eq. 4.1.

$$WC_i = \frac{\rho_i - \rho_o}{\rho_w - \rho_o} \quad (4.1)$$

Giving the WC presented in **Table 4.3**.

PI & I - Tag	Parameter	Unit	Calculated parameter
DT.1	ρ_1	kg/m ³	WC ₁
DT.2	ρ_2	kg/m ³	WC ₂
DT.3	ρ_3	kg/m ³	WC ₃

Table 4.3: WC calculated related to the corresponding tags in the PI&D of Fig.4.3

Because of the expected liquid contamination, the WC of the inlet was calculated using Eq. 4.2.

$$WC_{in} = \frac{WC_1 \cdot \dot{Q}_1 + WC_2 \cdot \dot{Q}_2}{\dot{Q}_1 + \dot{Q}_2} \quad (4.2)$$

The Extraction ratio (ER), relates the total flow rate input into MPPS, to the flow rate extracted at the tapping point. Related by the expression presented in Eq. 4.3

$$ER = \frac{\dot{Q}_1}{\dot{Q}_3} \quad (4.3)$$

4.3.1 Data acquisition system

The data acquisition system was developed and is described by Skjefstad [26]. No changes were made to the data acquisition system as a part of this project. Data is transferred to a computer from a Programmable logic controller (PLC) using an open platform communications server. Input data to the PLC is analog signal converted to 13 bit by an analog to digital converter (ADC). Coriolis flowmeters output signal in analog 4-20 mA. On the computer, the LabVIEW operation panel was set up to manage the data collection. In the LabVIEW operation panel, the operator inputted a sampling frequency, f given in measurement recorded per second (Hz) and a period time for collecting measurements, in second. The number of data points in a sampling set, n can be calculated using Eq. 4.4.

$$n = f(Hz) \cdot t(s) \quad (4.4)$$

LabVIEW generate a file with data. The file was stored on the computer and transformed to Excel file for data analysis.

4.3.2 Systematic error in experimental campaign

13 bit signal from the ADC gives a resolution error of $\pm 0.98 \mu\text{A}$.

The transducer error, U_t and measurement error, U_m are reported by Skjefstad [26]. The systematic error components related to the data collected and presented in this work are summarized in **Table 4.4**

Parameter	Unit	U_t	U_{res}	U_m	U_{sys}
\dot{Q}_1	L/min	$\pm 1.5\text{e}+00$	$\pm 6.0\text{e}-02$	$\pm 6.0\text{e}-01$	$\pm 1.6\text{e}+00$
\dot{Q}_2	L/min	$\pm 1.5\text{e}+00$	$\pm 6.0\text{e}-02$	$\pm 6.0\text{e}-01$	$\pm 1.6\text{e}+00$
\dot{Q}_3	L/min	$\pm 1.5\text{e}+00$	$\pm 6.0\text{e}-02$	$\pm 6.0\text{e}-01$	$\pm 1.6\text{e}+00$
$\dot{\rho}_1$	kg/m^3	$\pm 5.4\text{e}-01$	$\pm 1.8\text{e}-02$	$\pm 1.8\text{e}-01$	$\pm 5.7\text{e}-01$
$\dot{\rho}_2$	kg/m^3	$\pm 5.4\text{e}-01$	$\pm 1.8\text{e}-02$	$\pm 1.8\text{e}-01$	$\pm 5.7\text{e}-01$
$\dot{\rho}_3$	kg/m^3	$\pm 5.4\text{e}-01$	$\pm 1.8\text{e}-02$	$\pm 1.8\text{e}-01$	$\pm 5.7\text{e}-01$

Table 4.4: Systematic error components [26]

4.3.3 Random error in experimental campaign

Given the number of samples n , and a confidence level, C 95% as recommend by Moffat [23]. The \bar{t} was calculated to $\bar{t} = 1.96$ using the online calculator *Student T-value Calculator* by "Online calculators" [2]. The \bar{t} provide by *Student T-value Calculator* was compared to Table D in Moore et. al [25] and the *Student T-value Calculator* is by the author viewed as digitization of Table D in Moore et. al [25].

4.3.4 Calibration

Results presented from the experimental campaign are all based on measurements by the Coriolis flowmeters i.e the two Micro Motion F200 and the Sitrans FC430. The flow metes are pre-calibrated by the vendor and due to time constraints, it was not possible to re-calibrate. However, the vendor states that there is no need for a re-calibration within 10 years of operation of the flow meters. A statement and calibration certificates dated 2017 are supplied in Appendix A and Appendix B.

4.4 Exxsol™ D60 campaign

As a part of the experimental work, a risk assessment was performed, this is attached in Appendix D. After filling half the storage tank with premixed distilled water w/ 3.4 wt% NaCl, half with Exxsol™ D60 premixed with 0.015 g/L of the colorant Oil Red O ($C_{26}H_{24}N_4O$) The density of distilled water w/ 3.4 wt% NaCl was recorded running only water in the MPPS and density of Exxsol™ D60 running only Exxsol™ D60 in the MPPS was recorded. The following test points as presented in **Table 4.5** was recorded given flow rate, WC_{in} and Water Tapped(WT) as defined in Eq. 2.17

Qt [L/min]	WC _{in} [%]	WT [%]
300	30/50/70/90	10/30/50/60/80/70/90
500	30/50/70/90	10/30/50/60/80/70/90
700	30/50/70	10/30/50/60/80/70/90

Table 4.5: Unspiked Exxsol™ D60 Experimental campaign test matrix

Test points values of total flow rate and WC inlet of MPPS were set in the LabVIEW operation panel. The system was given time to reach these set points. The valves VT.2 and VT.3 as the nomenclature of Fig. 4.3 was adjusted to reach WT as required. Tapping was performed by tapping point normal to the upward-inclined section. LabVIEW operation panel did not include a WT calculation, so WT was calculated from WC of water stream inlet (WC_1), flow rate of water inlet (\dot{Q}_1), WC of Exxsol stream inlet (WC_2), flow rate of Exxsol inlet (\dot{Q}_2), WC tapped (WC_3) and flow rate tapped (\dot{Q}_3), as in the formula Eq.4.5 using Excel and the nomenclature of Fig.4.3.

$$WT = \frac{WC_3 \cdot \dot{Q}_3}{WC_2 \cdot \dot{Q}_2 + WC_1 \cdot \dot{Q}_1} \cdot 100 \quad (4.5)$$

The system was given time to reach steady state. A 30-second sample file recording parameters presented in Table 4.2 was recorded. The sampling frequency was set to 10 Hz, generating 300 individual measurements. Photos of the flow pattern were taken. The procedure repeated for the next set of test conditions as given in Table 4.5.

Initial result resulted in the collection of additional test points at the set of conditions where a need for mote date was identified. Resulting in additional test points gathered as presented in **Table 4.6** after the completion of the initial data collection.

Qt [L/min]	WC _{in} [%]	WT [%]
300	30	40/55/95
300	50/70/90	95
500	30	20/40/55
500	50	20/40/55
500	70	85/95
500	90	95
700	30	20/45/55
700	50	40/55

Table 4.6: Unspiked Exxsol™ D60 Experimental campaign infill test matrix

4.5 Exxsol™ D60 + 185 ppm crude oil campaign

Crude oil was added to the storage tank to spike the Exxsol™ D60. The oil pump was run to circulate the crude and Exxsol™ D60 in the MPPS, to mix the crude in the Exxsol™ D60. A sample of Exxsol™ D60 spiked w/ crude was collected to verify the concentration of crude in the Exxsol™ D60. The following test points as presented in **Table 4.7**. The campaign performed using same sampling frequency and procedure as described in Section 4.4.

Qt [L/min]	WC _{in} [%]	WT [%]
300	30/50/70/90	10/30/50/60/80/70/90
500	30/50/70/90	10/30/50/60/80/70/90
700	30/50/70	10/30/50/60/80/70/90

Table 4.7: Spiked Exxsol™ D60 Experimental campaign test matrix

The initial result resulted in the collection of additional test points in the set of conditions where a need for more data was identified. Resulting in additional test points gathered as presented in **Table 4.8** after the completion of the initial data collection.

Qt [L/min]	WC _{in} [%]	WT [%]
300	30/50/70/90	95
500	30	15/20
500	50	40/55
500	70/90	95
700	30	20
700	50	20/40

Table 4.8: Spiked Exxsol™ D60 Experimental campaign infill test matrix

Chapter 5

MPPS experimental results

The calculated drainage potential from the two experimental campaigns is presented in drainage potential curves. First drainage potential curve for Exxsol™ D60, also denoted unspiked oil and Exxsol™ D60 + 185 ppm crude, also denoted spiked oil, at the same inlet conditions, WC inlet and total inlet flow are presented in the same figure to illustrate the effect of adding crude to Exxsol™ D60 on the performance of the MPPS. Picture of the flow in the MPPS prior to tapping point is presented in figures for the given set of inlet conditions.

Secondly, the drainage potential curves for a fixed WC inlet and the same fluid mixture are presented over the range of different total flow rates, to illustrate the change of the drainage potential curves when the total flow rate was changing. Also to possibly identify if the response of drainage potential curves to total flow rate, is different when separating unspiked oil in the MPPS, compared to spiked oil in the MPPS.

The calculated points are illustrated as the rotated squares or "diamonds" points in the drainage potential curves. The points have the calculated uncertainty visualized as "error bars". The points are interconnected by straight dotted lines to exaggerate the trend of the data. The y-axis provides values in percentage of WT [%] and the x-axis provides the WC tapped stream [%] in percentage. Note that the span of the x-axis may be different for the different figures. This in order to clearly illustrate the general trend of the data in question, and "zoom in" on the data for the given figure.

The first figure of each section will be explained in detail to give the reader a basis for examining the figures, then observations regarding the results will be stated, to the figure in question.

5.1 Drainage potential for unspiked oil and spiked oil at equal inlet conditions

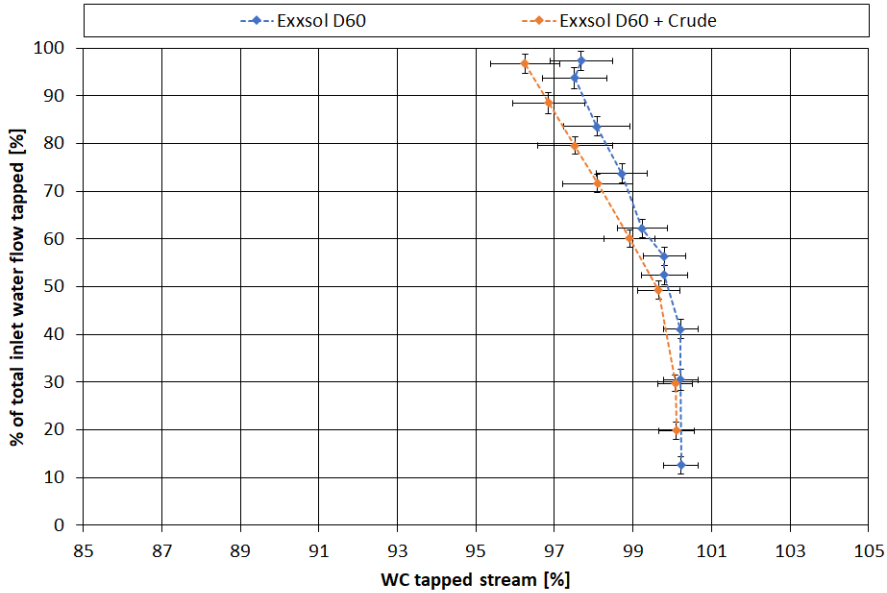


Figure 5.1: Drainage potential for spiked oil and distilled water w/ 3.4 wt% NaCl and unspiked oil and distilled water w/ 3.4 wt% NaCl at WC inlet 30%, total flow rate of 300 L/min.

Looking at WT 10-20% for both curves in **Fig. 5.1** observe that WC tapped stream of unspiked oil and spiked oil was similar and close to 100%. WC tapped stream of unspiked oil and spiked oil did not change as WT increase until WT 40-50%. At WT 40-50%, WC tapped stream decrease as WT increase for both cases. As more water was tapped increasing the WT, WC tapped stream was decreasing i.e more oil was being tapped alongside the water, lowering the WC tapped stream. However, WC tapped stream of spiked oil decreased more than unspiked oil, resulting in a difference of the drainage potential curves as WT increase. At WT above 90%, WC tapped stream was above 95% for spiked and unspiked oil and within 2% of each other.

5.1 Drainage potential for unspiked oil and spiked oil at equal inlet conditions

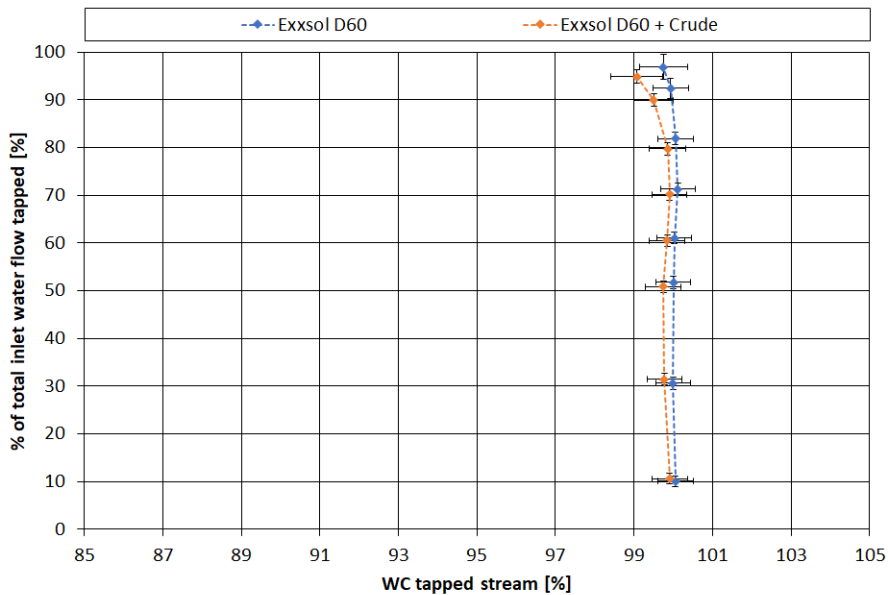


Figure 5.2: Drainage potential for spiked oil and distilled water w/ 3.4 wt% NaCl and unspiked oil and distilled water w/ 3.4 wt% NaCl at WC inlet 50%, total flow rate of 300 L/min.

At WT 10% in **Fig. 5.2** observe that WC tapped stream of unspiked oil and spiked oil was similar and close to 100%. WC tapped stream of spiked oil was less than of unspiked oil but within 1%. As WT increased WC tapped stream remains stable until WT 80%. A decrease in WC was observed above WT 80%. WC tapped stream of spiked oil decreased more than of unspiked oil, resulting in a difference of the drainage potential curves. At WT 95%, WC tapped stream was above 99% for spiked oil and unspiked oil.

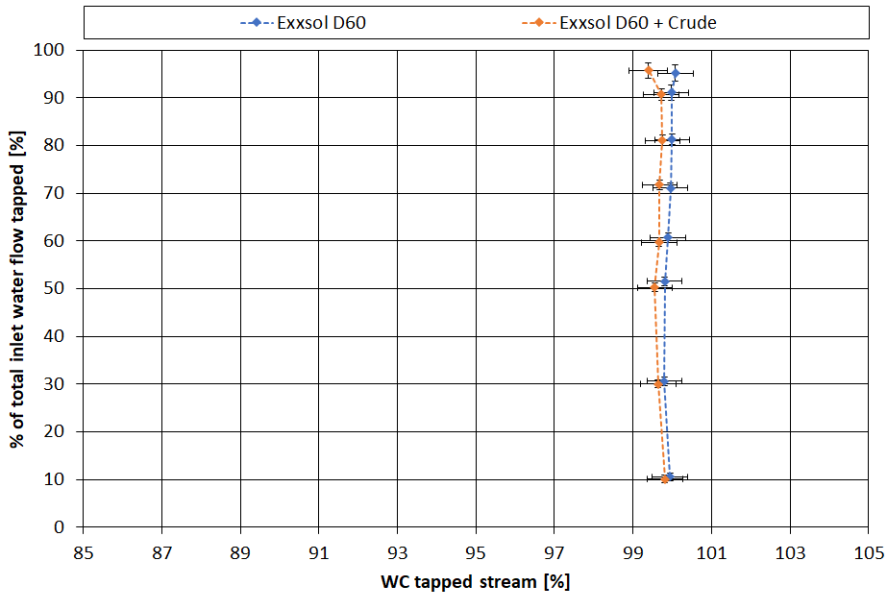


Figure 5.3: Drainage potential for spiked oil and distilled water w/ 3.4 wt% NaCl and unspiked oil and distilled water w/ 3.4 wt% NaCl at WC inlet 70%, total flow rate of 300 L/min.

At WT 10% in **Fig. 5.3** observe that WC tapped stream of unspiked oil and spiked oil was similar and close to 100%. WC tapped stream of spiked oil was less than of unspiked oil but within 1%. As WT increased the WC tapped stream remains stable until WT 90%. A small decrease in WC tapped stream was observed above WT 90% for spiked oil. WC tapped stream for unspiked oil remains stable, or WC tapped stream increases somewhat, resulting in a difference of the drainage potential curves. At WT 95%, WC tapped stream was above 99% for spiked oil and unspiked oil.

5.1 Drainage potential for unspiked oil and spiked oil at equal inlet conditions

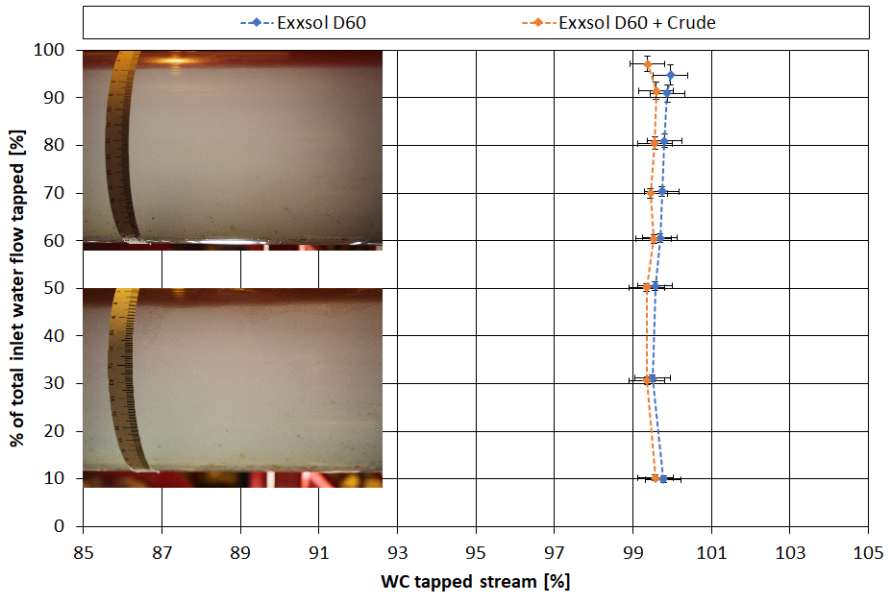


Figure 5.4: Drainage potential for spiked oil and distilled water w/ 3.4 wt% NaCl and unspiked oil and distilled water w/ 3.4 wt% NaCl at WC inlet 90%, total flow rate of 300 L/min. Picture of flow of unspiked oil top left, picture of flow of spiked oil bottom left

At WT 10% in **Fig. 5.4** observe that WC tapped stream of unspiked oil and spiked oil was similar and close to 100%. WC tapped stream of spiked oil was less than of unspiked oil but within 1%. As WT increased the WC tapped stream remains stable until WT 90%. A small decrease in WC tapped stream was observed above WT 90% for spiked oil. WC for unspiked oil remains stable, or WC increases somewhat, resulting in a difference of the drainage potential curves. At WT 95%, WC tapped stream is above 99% for spiked oil and unspiked oil.

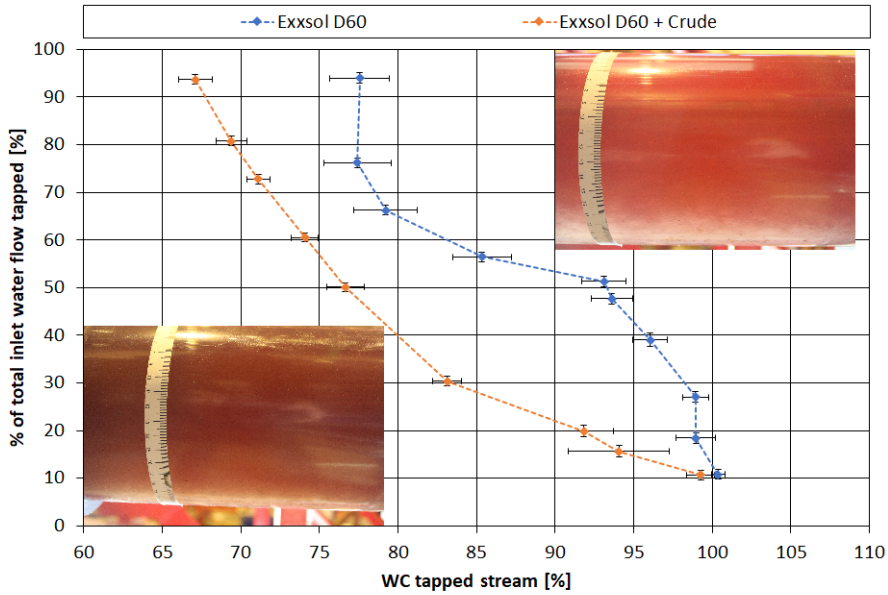


Figure 5.5: Drainage potential for spiked oil and distilled water w/ 3.4 wt% NaCl and unspiked oil and distilled water w/ 3.4 wt% NaCl at WC inlet 30%, total flow rate of 500 L/min. Picture of flow of unspiked oil top right, picture of flow of spiked oil bottom left

At WT 10% in **Fig. 5.5** observe that WC tapped stream of unspiked oil and spiked oil was similar and close to 100%. WC tapped stream for unspiked oil remains stable until WT 30%. WC tapped stream decrease as WT increase until WT 50%. From WT 50% WC tapped stream decrease more as WT increase. AT WT 75% WC tapped stabilize between WC tapped stream 75 - 80%.

WC tapped stream for spiked oil decreased as WT increased for all WT. WC tapped stream decreased more at low WT, the decrease WC tapped stream was less as WT was above 50%. At WT 95% WC tapped stream was 67%.

5.1 Drainage potential for unspiked oil and spiked oil at equal inlet conditions

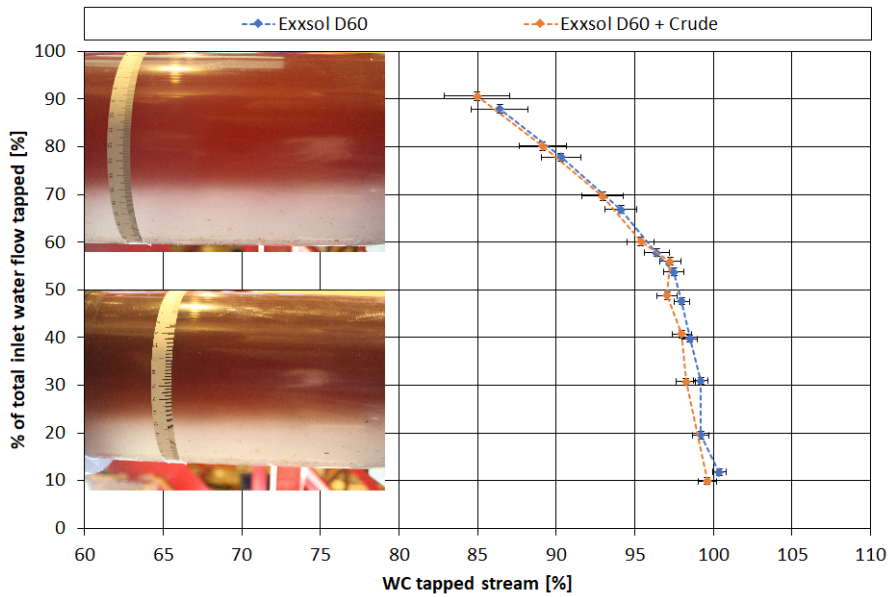


Figure 5.6: Drainage potential for spiked oil and distilled water w/ 3.4 wt% NaCl and unspiked oil and distilled water w/ 3.4 wt% NaCl at WC inlet 50%, total flow rate of 500 L/min. Picture of flow of unspiked oil top left, picture of flow of spiked oil bottom left

At WT 10% in **Fig. 5.6** observe that WC tapped stream of unspiked oil and spiked oil was similar and close to 100%. WC tapped stream of spiked oil was less than of unspiked oil but within 1%. As WT increase the WC tapped stream decreased. At and above WT 50%, WC tapped stream decrease more as WT increase, for spiked oil and unspiked oil.

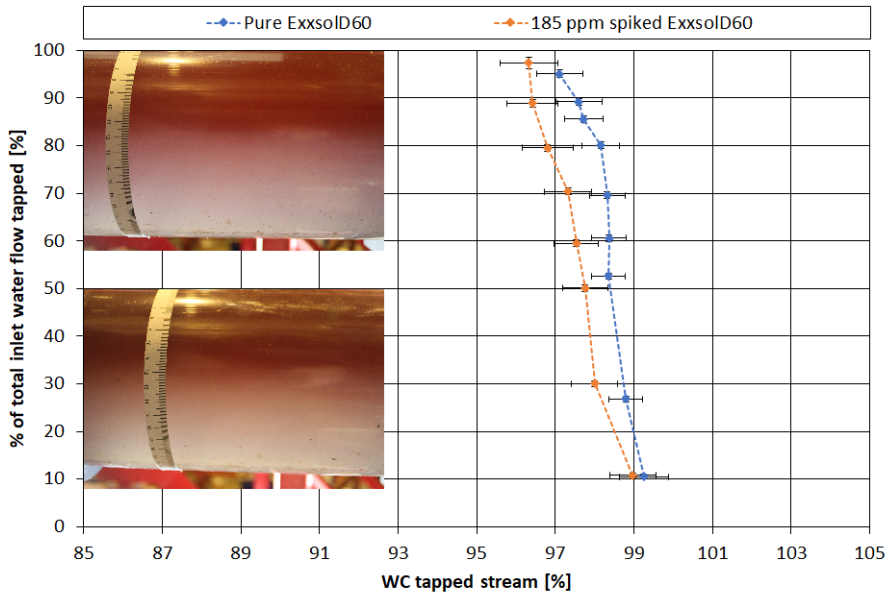


Figure 5.7: Drainage potential for spiked oil and distilled water w/ 3.4 wt% NaCl and unspiked oil and distilled water w/ 3.4 wt% NaCl at WC inlet 70%, total flow rate of 500 L/min. Picture of flow of unspiked oil top left, picture of flow of spiked oil bottom left

At WT 10% in **Fig. 5.7** observe that WC tapped stream of unspiked oil and spiked oil was similar and less than 100%. WC tapped stream of spiked oil was observable less than of unspiked oil but within 1%. As WT increased the WC tapped stream decreased for both cases. WC tapped stream for spiked oil decreased more at WT 30 than unspiked oil. The difference of the two drainage potential curves was similar from WT 30% as WT increases. At WT 95% WC tapped stream is above 95% for spiked oil and unspiked oil.

5.1 Drainage potential for unspiked oil and spiked oil at equal inlet conditions

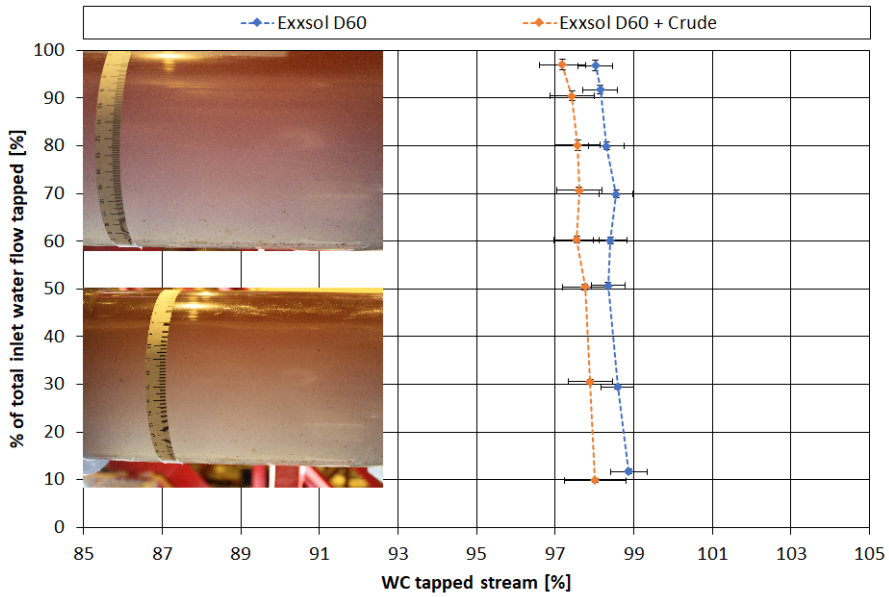


Figure 5.8: Drainage potential for spiked oil and distilled water w/ 3.4 wt% NaCl and unspiked oil and distilled water w/ 3.4 wt% NaCl at WC inlet 90%, total flow rate of 500 L/min. Picture of flow of unspiked oil top left, picture of flow of spiked oil bottom left

At WT 10% in **Fig. 5.8** observe that WC tapped stream of unspiked oil and spiked oil was less than 100%. WC tapped stream of spiked oil was less than of unspiked oil but within 1%. As WT increased the WC tapped stream slightly decreased for both cases. The difference of the two drainage potential curves was similar for all WT as WT increased. At WT 95% WC tapped stream was above 97% for spiked oil and unspiked oil.

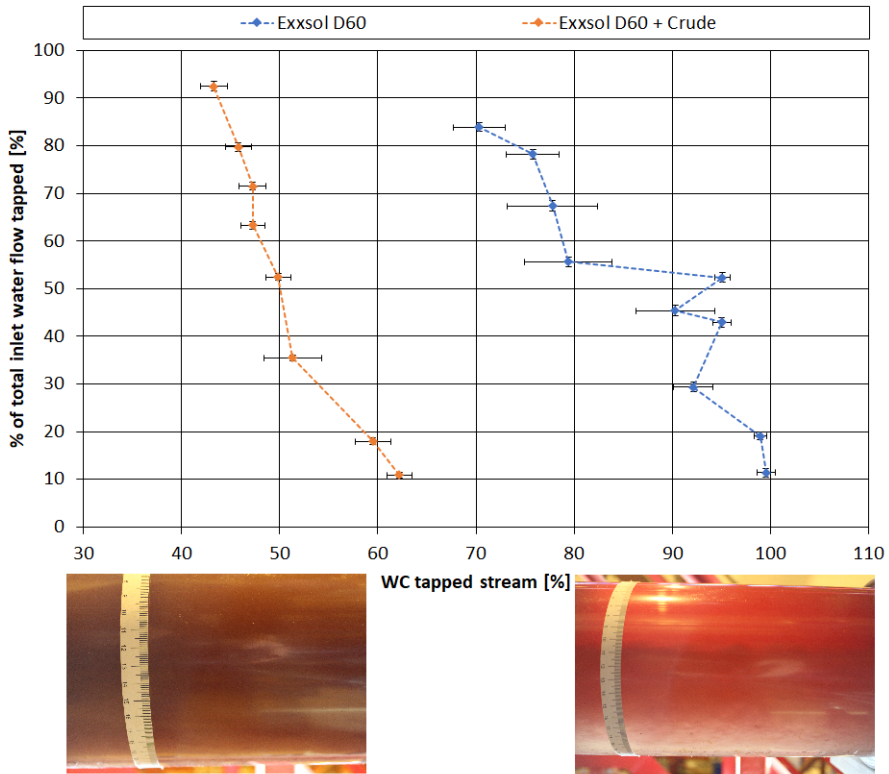


Figure 5.9: Drainage potential for spiked oil and distilled water w/ 3.4 wt% NaCl and unspiked oil and distilled water w/ 3.4 wt% NaCl at WC inlet 30%, total flow rate of 700 L/min. Picture of flow of unspiked oil bottom right, picture of flow of spiked oil bottom left

At WT 10% in **Fig. 5.9** observe that WC tapped stream of unspiked oil was close to 100% and WC tapped stream of spiked oil was 62%. For spiked oil WC tapped stream decreased as WT increased, the decrease in WC tapped stream was more as WT was below 40%, above WT 40% WC tapped stream decreased as WT increase, but not as much. At WT 95% WC tapped steam was 44%.

WC tapped stream for the case of unspiked oil decreased as WT increase to WT 30%, then WC tapped stream moved up and down as WT increased. WC tapped stream decreased as WT increased from 55 to 80%. At WT 85% WC tapped steam decreased more than for the lower WT 70% and 80%. At WT 85% WC tapped steam was 70%.

The difference between the two drainage potential curves was the most at WT 10% to 30%. Then WC tapped stream for unspiked oil decreased more than for spiked oil and consequently, the difference of the two drainage potential curves was less for WT above 50%.

5.1 Drainage potential for unspiked oil and spiked oil at equal inlet conditions

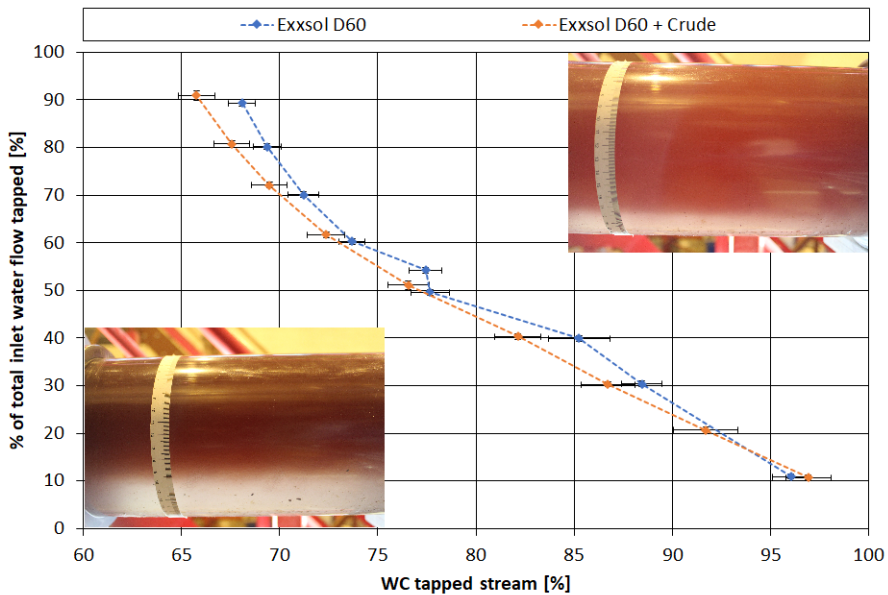


Figure 5.10: Drainage potential for spiked oil and distilled water w/ 3.4 wt% NaCl and unspiked oil and distilled water w/ 3.4 wt% NaCl at WC inlet 50%, total flow rate of 700 L/min. Picture of flow of unspiked oil top left, picture of flow of spiked oil bottom left

At WT 10% in **Fig. 5.10** observe that WC tapped stream of unspiked oil and spiked oil was similar and less than 100%. WC tapped stream of spiked oil was more than of unspiked oil but within 1%. For all other WT, WC tapped stream of spiked oil was less than of unspiked oil. As WT increased the WC tapped stream decreased for spiked oil and unspiked oil.

The difference of the two drainage potential curves was similar for all WT, but more for WT 80% and 90%. At WT 90% WC tapped stream was between 65% and 70% for spiked oil and unspiked oil.

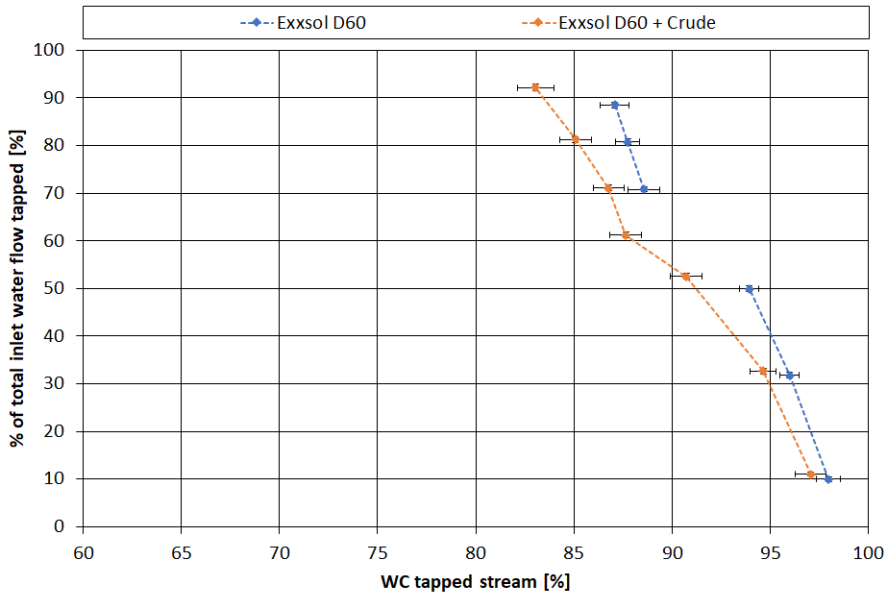


Figure 5.11: Drainage potential for spiked oil and distilled water w/ 3.4 wt% NaCl and unspiked oil and distilled water w/ 3.4 wt% NaCl at WC inlet 70%, total flow rate of 700 L/min

At WT 10% in **Fig. 5.11** observe that WC tapped stream of unspiked oil and spiked oil was similar and less than 100%. WC tapped stream of spiked oil was less than of unspiked oil but within 1%. As WT increased WC tapped stream decreased for spiked oil and unspiked oil. The decrease of WC tapped stream was more for spiked oil than for unspiked oil consequently the difference of the two drainage potential curves increased as WT increased. Missing data point at WT 60% for unspiked oil due to quality issues. At WT 90% WC tapped stream was above 85% for unspiked oil and below 85% for spiked oil.

5.2 Drainage potential for fixed WC inlet and same fluid mixture over a range total flow rates

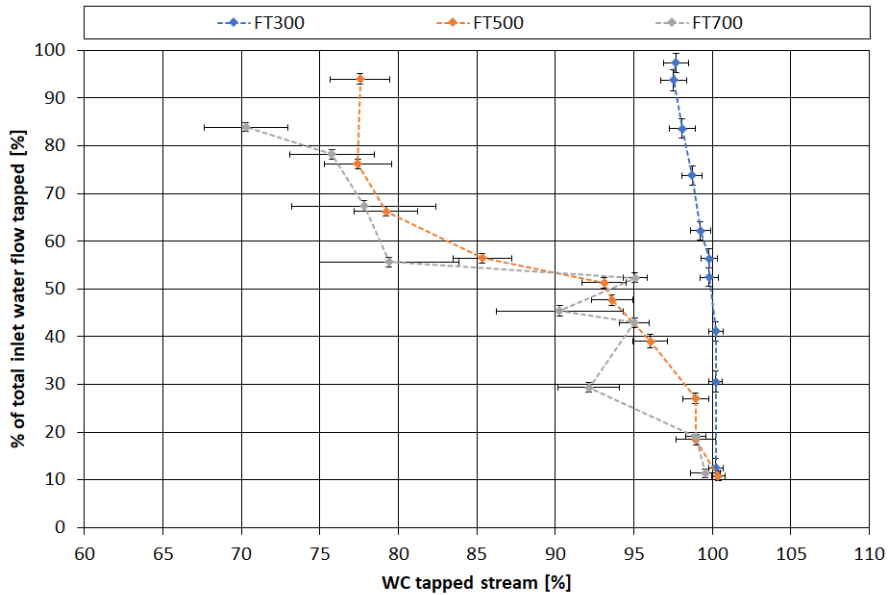


Figure 5.12: Drainage potential for unsiked oil and distilled water w/ 3.4 wt% NaCl at WC inlet 30%, total flow rate of 300, 500, 700 L/min

At WT 10% of **Fig. 5.12** WC tapped stream was similar and close to 100% for all total flow rates. For total flow rate of 300 L/min, WC tapped stream was stable as WT increased until WT 50%. WC tapped stream decreased as WT increases above 50% for total flow rate of 300 L/min. As more water was tapped, more unsiked oil was tapped alongside the water, lowering the WC tapped stream.

For total flow rate of 500 L/min, WC tapped stream decreased as WT increase. For total flow rate of 700 L/min, WC tapped stream moves up and down from WT 20% to 50%. From WT 50 total flow rate of 700 L/min moves similar to total flow rate of 500 L/min.

The difference between drainage potential curves of total flow rate of 300 L/min and flow rates of 500 L/min, 700 L/min increased as WT increased.

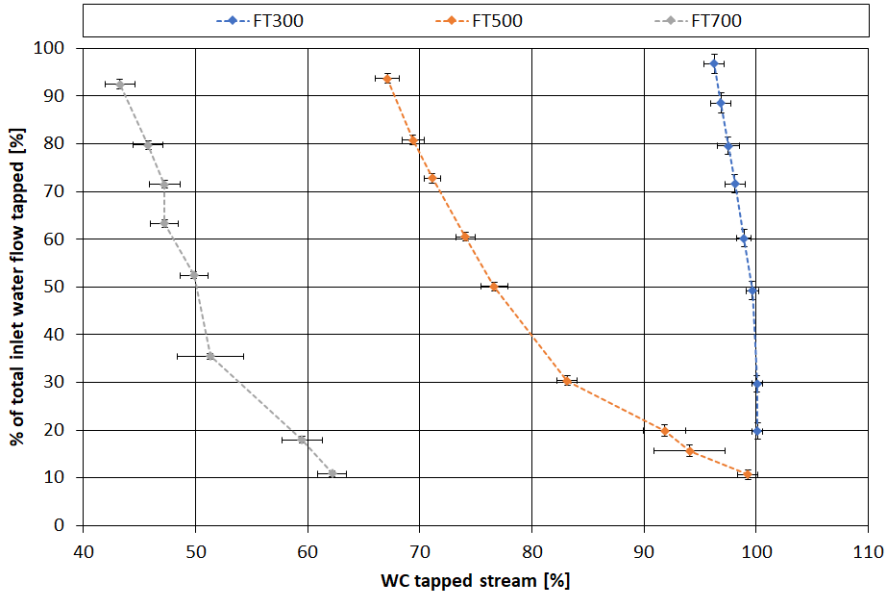


Figure 5.13: Drainage potential for spiked oil and distilled water w/ 3.4 wt% NaCl, WC inlet 30%, total flow rates 300, 500, 700 L/min

At WT 10% of **Fig. 5.13** WC tapped stream was similar and close to 100% for total flow rates 300 L/min and 500 L/min. For total flow rate of 300 L/min WC tapped stream was stable as WT increased, until WT 40%. WC tapped stream decreased as WT increased above 40% for total flow rate of 300 L/min.

At WT 10% for total flow rate of 700 L/min, WC tapped stream was 62%. For total flow rates of 500 L/min and 700 L/min, WC tapped stream decreased as WT increased, more at the lower WT. Drainage potential curves for total flow rates 500 L/min and 700 L/min show similar development as WT increase, and keep a similar difference between drainage potential curves.

5.2 Drainage potential for fixed WC inlet and same fluid mixture over a range total flow rates

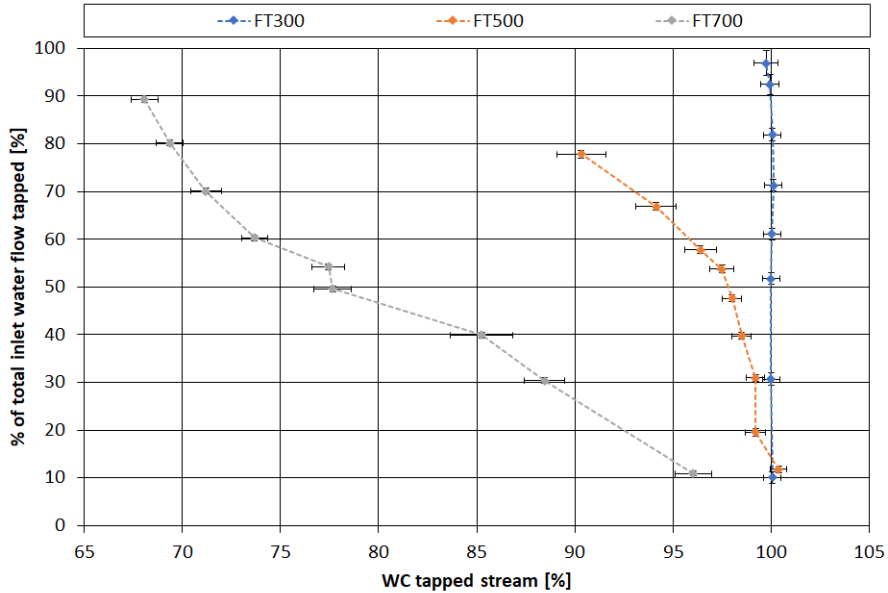


Figure 5.14: Drainage potential for unspiked oil and distilled water w/ 3.4 wt% NaCl at WC inlet 50%, total flow rates 300, 500, 700 L/min

At WT 10% of **Fig. 5.14** WC tapped stream was similar and close to 100% for total flow rates 300 L/min and 500 L/min. For total flow rate of 300 L/min, WC tapped stream was stable as WT increased.

For total flow rate of 500 WC tapped stream decreased as WT increased, WC tapped stream decreased more for higher WT. The difference between the drainage potential curves of 300 L/min and 500 L/min increased as WT increased. At WT 10% for total flow rate of 700 L/min, WC tapped stream was less than 100%. WC tapped stream decreased as WT increased, more at lower WT.

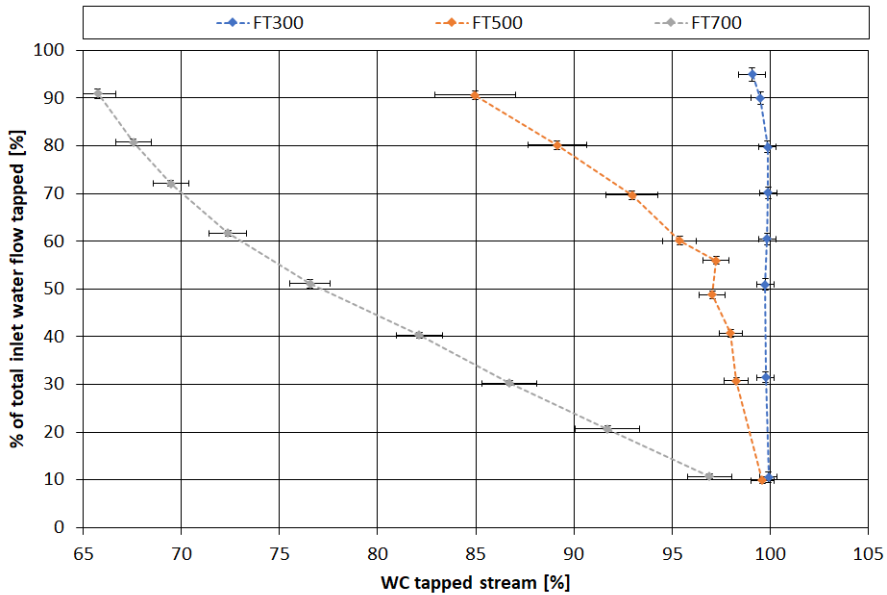


Figure 5.15: Drainage potential for spiked oil and distilled water w/ 3.4 wt% NaCl at WC inlet 50%, total flow rates 300, 500, 700 L/min

At WT 10% of **Fig. 5.15** WC tapped stream was similar and close to 100% for total flow rates 300 L/min and 500 L/min. For total flow rate of 300 L/min, WC tapped stream was stable as WT increased.

For total flow rate of 500 L/min, WC tapped stream decreased as WT increased, WC tapped stream decreased more for higher WT. The difference between the drainage potential curves for 300 L/min and 500 L/min increased as WT increased. At WT 10% for total flow rate of 700 L/min, WC tapped stream was less than 100%. WC tapped stream decreased as WT increased, more at lower WT.

5.2 Drainage potential for fixed WC inlet and same fluid mixture over a range total flow rates rates

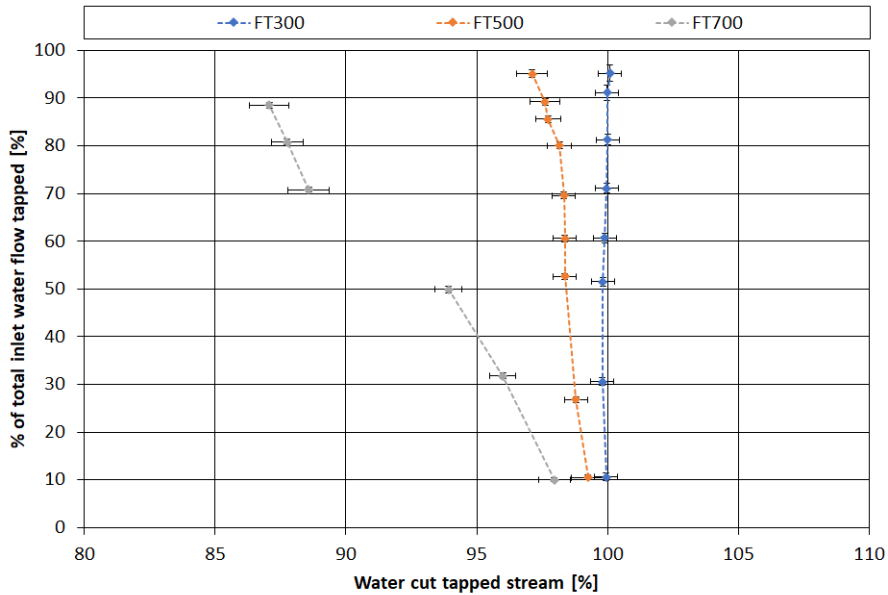


Figure 5.16: Drainage potential for uns spiked oil and distilled water w/ 3.4 wt% NaCl at WC inlet 70%, total flow rates 300, 500, 700 L/min

At WT 10% of **Fig. 5.16** WC tapped stream was similar and close to 100% for total flow rates 300 L/min and 500 L/min. For total flow rate of 300 L/min, WC tapped stream was stable as WT increased.

For total flow rate of 500 L/min, WC tapped stream decreased as WT increased, WC tapped stream decreased more for higher WT. The difference between the drainage potential curves for total flow rate of 300 L/min and total flow rate 500 L/min increased as WT increased.

At WT 10% for total flow rate of 700 L/min, WC tapped stream was less than 100% but within 2%. For total flow rate of 700 WC tapped stream decreased as WT increased, WC tapped stream decreased more for higher WT. Missing data point at WT 60%. WC tapped stream decreased more for total flow rate of 700 L/min than for total flow rate of 500 L/min, thus the difference between the drainage potential curves increased as WT increased.

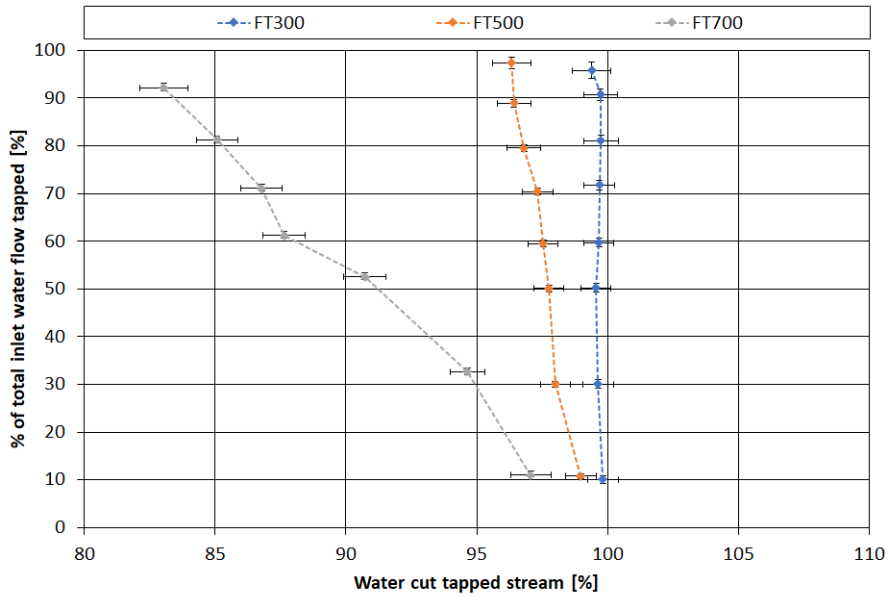


Figure 5.17: Drainage potential for spiked oil and distilled water w/ 3.4 wt% NaCl at WC inlet 70%, total flow rates 300, 500, 700 L/min

At WT 10% of **Fig. 5.17** WC tapped stream was close to 100% for total flow rate of 300 L/min. For total flow rate of 300 L/min, WC tapped stream was stable as WT increased, until WT 95% where WC tapped stream decreased.

At WT 10% WC tapped stream was less than 100% but within 2% for total flow rate of 500 L/min and less than but within 5% for total flow rate of 700 L/min. For total flow rate of 500 L/min, WC tapped stream decreased as WT increased, WC tapped stream decreased more for higher WT. The difference between the drainage potential curves for 300 L/min and 500 L/min increased as WT increased.

For total flow rate of 700 L/min, WC tapped stream decreased as WT increased, WC tapped stream decreased more for higher WT. WC tapped stream decreased more for total flow rate of 700 L/min than for total flow rate of 500 L/min, thus the difference between the drainage potential curves increased as WT increased.

5.2 Drainage potential for fixed WC inlet and same fluid mixture over a range total flow rates

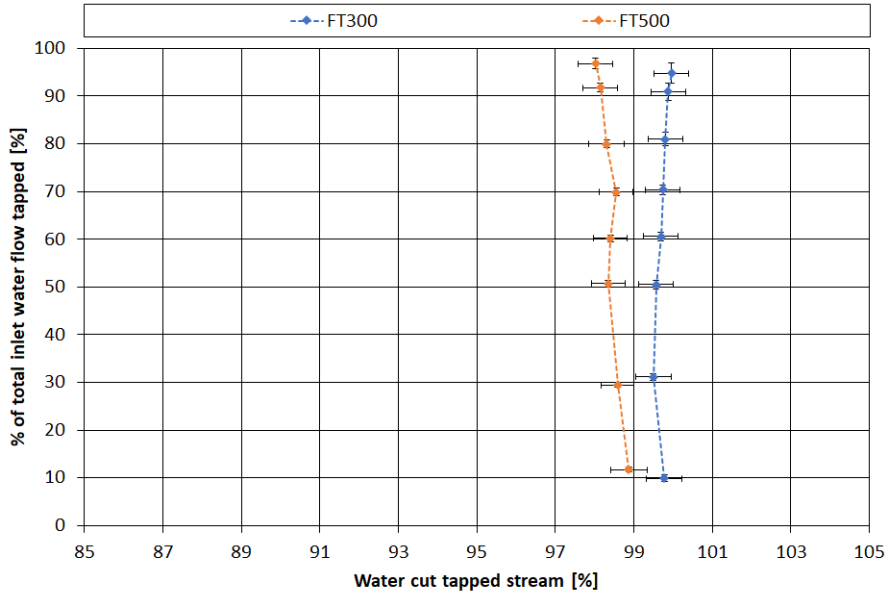


Figure 5.18: Drainage potential for unspiked oil and distilled water w/ 3.4 wt% NaCl at WC inlet 90%, total flow rates 300, 500 L/min

At WT 10% of **Fig. 5.18** WC tapped stream was close to 100% for total flow rate of 300 L/min. For total flow rate of 300 L/min, WC tapped stream was stable as WT increased.

At WT 10% of WC tapped stream was close to 100% for total flow rate of 500 L/min. For total flow rate of 500 L/min, WC tapped stream was stable as WT increased, until WT 70%. Then WC tapped stream decreased somewhat as WT increased.

The difference between the drainage potential curves was stable until WT 70%. From WT 70% the difference increased as WT increased.

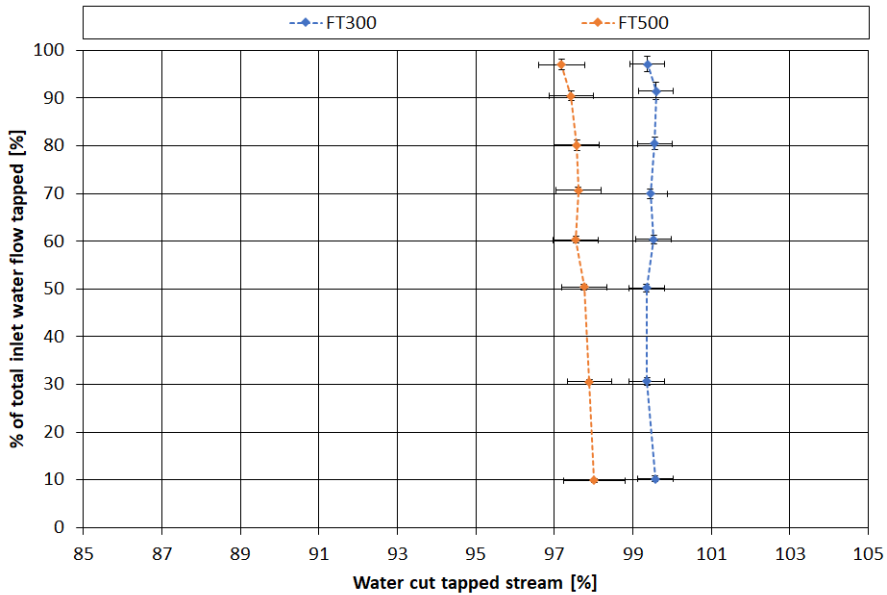


Figure 5.19: Drainage potential for spiked oil and distilled water w/ 3.4 wt% NaCl at WC inlet 90%, total flow rates 300, 500 L/min

At WT 10% of **Fig. 5.19** WC tapped stream was close to 100% for total flow rate of 300 L/min. For total flow rate of 300 L/min, WC tapped stream was stable as WT increased.

At WT 10% of WC tapped stream was less than 100% but within 2% for total flow rate of 500 L/min. For total flow rate of 500 L/min, WC tapped stream decreased as WT increased.

The difference of the drainage potential curves increased as WT increased.

The combination of total flow rate of 700 L/min and WC inlet 90% was planned to be tested as a part of both MPPS spiked oil campaign and unspiked campaign. However, the current MPPS regulation system was not able to deliver this set of conditions in a stable manner, thus this combination of this set of inlet conditions was discarded.

Chapter 6

Project thesis numerical modeling results

6.1 Drainage potential curves from numerical modeling

Drainage potential curves presented by Harstad [16] by use of the numerical model given in Section 2.10 is given in this chapter. To form a basis for comparing the numerical model-generated drainage potential curves and the curves drainage potential generated from the experimental data from MPPS campaigns presented Chapter 5.

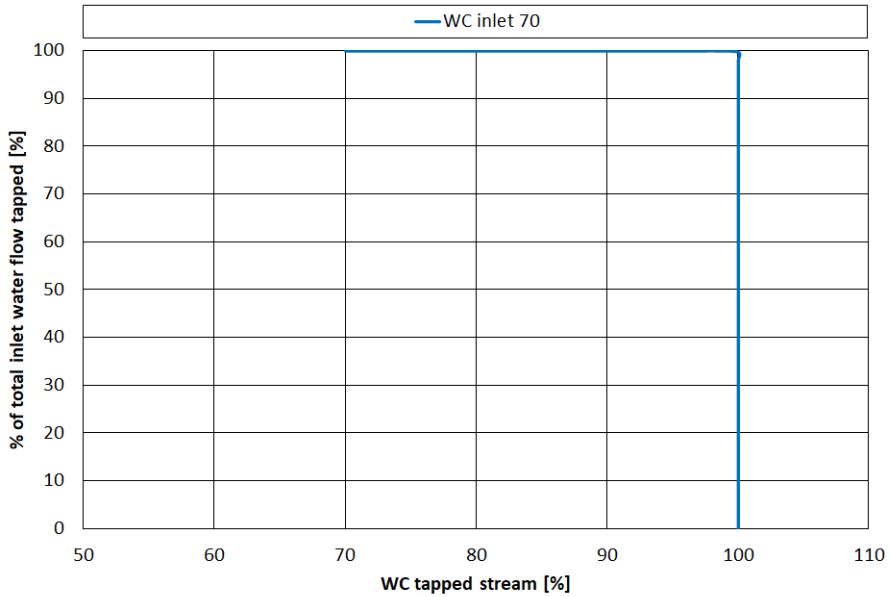


Figure 6.1: Drainage potential curve given step water volume fraction function distribution $\alpha(y)$ WC inlet 70% [16]

The model-generated drainage potential curve presented in **Fig. 6.1** shows a WC tapped stream of 100% as WT increase. This represents tapping of a pure water flow. At WT 100% the WC tapped stream drops as oil is being tapped alongside the water.

6.1 Drainage potential curves from numerical modeling

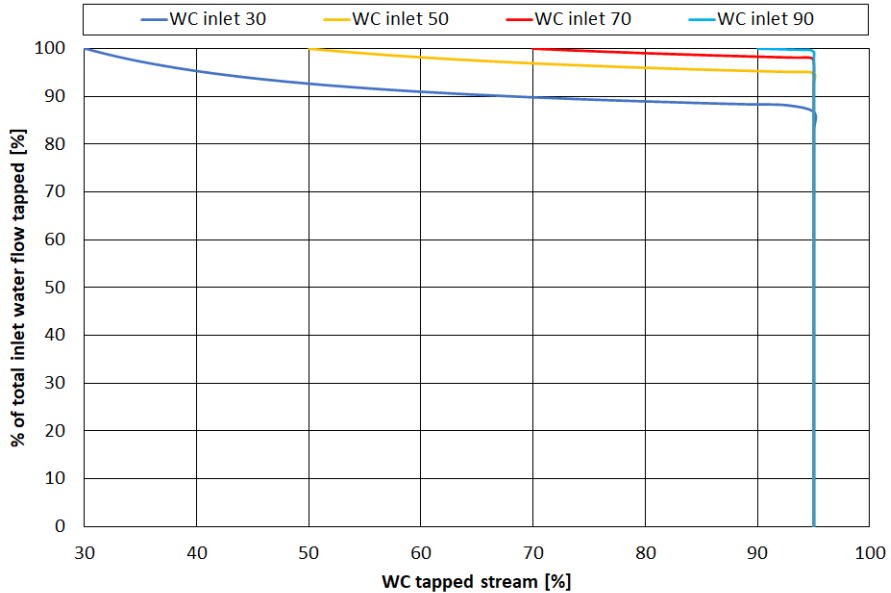


Figure 6.2: Drainage potential curve given step water volume fraction function distribution $\alpha(y)$ with uniform contamination OiW 5%, WiO 5% WC inlet 30%, 50%, 70%, 90% [16]

The model-generated drainage potential curves presented in **Fig. 6.2** shows a WC tapped stream of 95% as WT increase, due to the 5% OiW contamination. The WC tapped stream drops as the model simulates the tapping of the oil phase with 5% WiO contamination. The difference in at what WT this drop in WC tapped stream occur, was determined by the WC inlet.

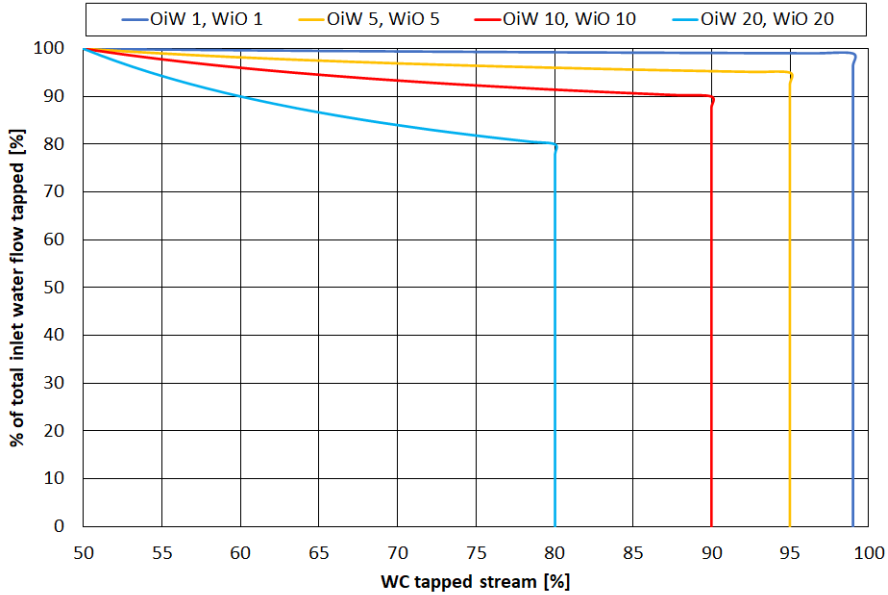


Figure 6.3: Drainage potential curve given step water volume fraction function distribution $\alpha(y)$ with uniform contamination OiW 1% WiO 1%, OiW 5% WiO 5%, OiW 10% WiO 10%, OiW 20% WiO 20%, WC inlet 50% [16]

The model-generated drainage potential curves presented in **Fig. 6.3** show a stable WC tapped stream below 100% determined by the OiW contamination, as WT increase. The WC tapped stream drops as the model simulates the tapping of the oil phase with WiO contamination. For the curves simulated with more WiO contamination, the drop in WC tapped stream occurs at lower WT. This because more of the WT is present as WiO contamination in the oil phase, and thus tapping of the WiO contamination oil phase happened at lower WT.

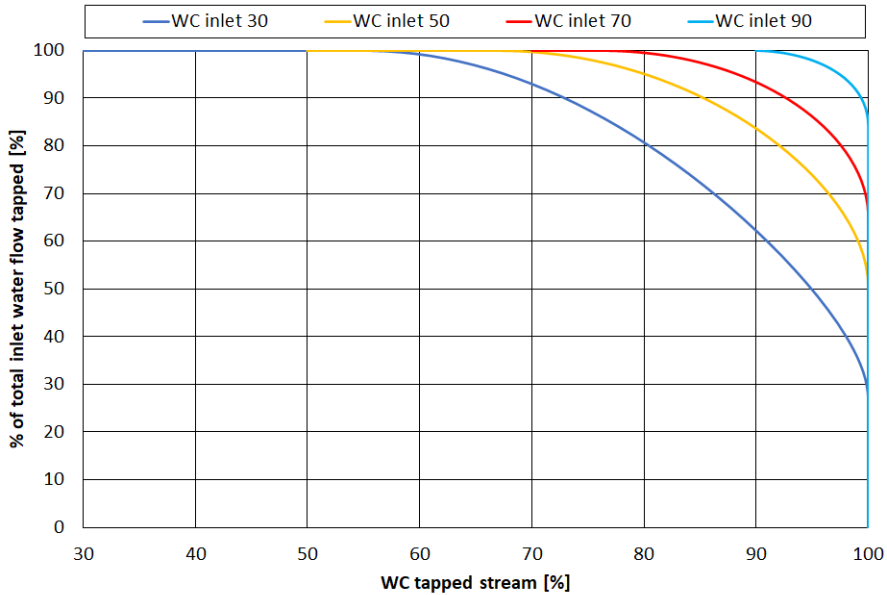


Figure 6.4: Drainage potential curve given linear transition water volume fraction function distribution $\alpha(y)$ given normalized width of transition zone 0,4 WC inlet 30%, 50%, 70%, 90% [16]

The model-generated drainage potential curves presented in **Fig. 6.4** show a stable WC tapped stream at 100%, as WT increase. The WC tapped stream drops as the model simulates the tapping of the linear transition from water to oil. The difference in at what WT this drop in WC tapped stream occurs, was determined by the WC inlet as more of the total water was present in the transition zone for lower WC inlets.

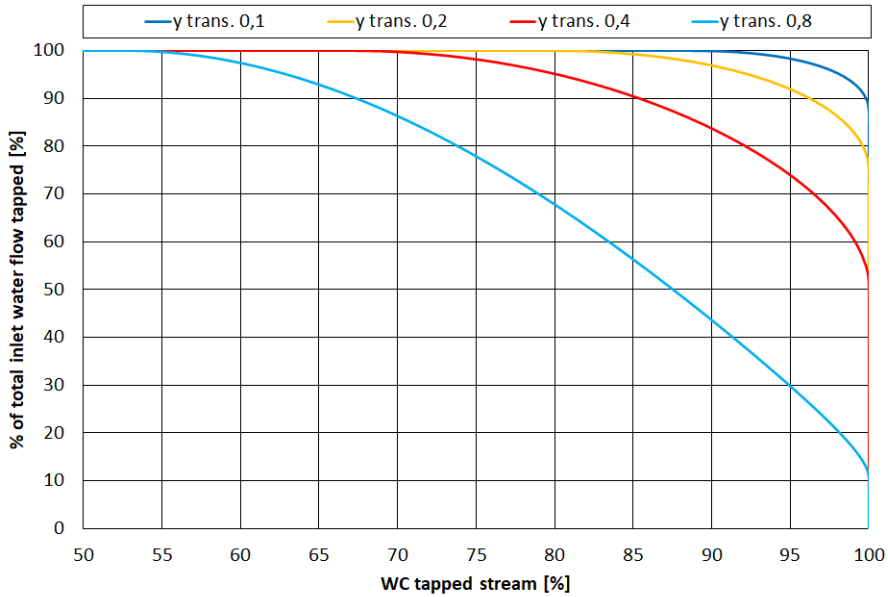


Figure 6.5: Drainage potential curve given linear transition water volume fraction function distribution $\alpha(y)$ given normalized width of transition zone 0,1 , 0,2 , 0,4 , 0,8 WC inlet 50% [16]

The model-generated drainage potential curves presented in **Fig. 6.5** show a stable WC tapped stream at 100%, as WT increase. The WC tapped stream drops as the model simulates the tapping of the linear transition from water to oil. The difference in at what WT this drop in WC tapped stream occur, was determined by the normalized height of the transition as more of the total water was present in the larger transition zones.

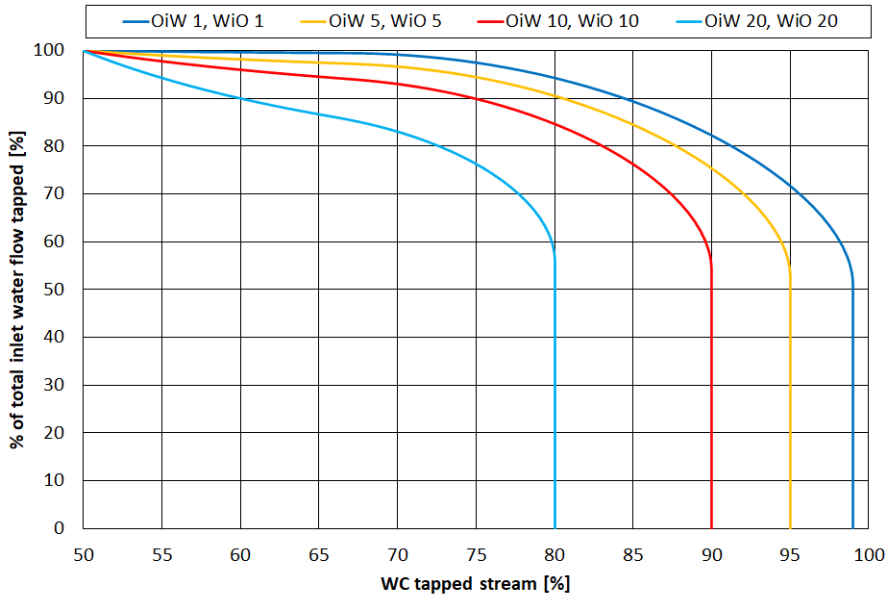


Figure 6.6: Drainage potential curve given linear transition water volume fraction function distribution $\alpha(y)$ with uniform contamination OiW 1% WiO 1%, OiW 5% WiO 5%, OiW 10% WiO 10%, OiW 20% WiO 20% given normalized width of transition zone 0,4 WC inlet 50% [16]

The model-generated drainage potential curves presented in **Fig. 6.6** show a stable WC tapped stream below 100% determined by the OiW contamination, as WT increase. The WC tapped stream drops at the same WT, as the model simulates the tapping of the linear transition from water to oil.

Chapter 7

Discussion

7.1 Bottle separation tests results

As the concentration of crude oil in Exxsol™ D60 was increased in the bottle separation tests, T_{in} (the time required for the interface to reach a constant height) for WC 50% and 75% generally increased as presented in Fig. 3.3. For WC 50% there was little or no change for T_{in} as the concentration of crude in Exxsol™ D60 was increased from 400 ppm to 500 ppm. Also for WC 50%, T_{in} decreased as the concentration of crude in Exxsol™ D60 was increased from 700 ppm to 800 ppm. For WC 25%, T_{in} decrease as crude concentration in Exxsol™ was increased from 500 ppm to 600 ppm.

For WC 75% there was little to no change in T_{in} suggesting that the effect of adding crude to Exxsol™ D60 on T_{in} is limited at WC 75%.

As the concentration of crude oil in Exxsol™ D60 was increased in the bottle separation tests, T_{sep} (the time required for the phases to separate) for WC 25% and 50% generally increased as presented in Fig. 3.4. For WC 50% there was little or no change to T_{sep} as the concentration of crude in Exxsol™ D60 was increased from 400 ppm to 500 ppm. Also for WC 50% T_{sep} decrease as the concentration of crude in Exxsol™ D60 was increased from 600 ppm to 700 ppm. For WC 75% there was little to no change in the T_{sep} suggesting that the effect on T_{sep} of adding crude to Exxsol™ D60 is limited at WC 75%.

Three bottle separation tests were performed for each set of conditions. The interpretation of the recorded footage was done manually, and can thus lead to errors and differences in interpretation, especially for the time of fixed interface, T_{in} . However, the results presented in Fig. 3.3 and Fig. 3.4 indicate that adding of crude oil to Exxsol™ D60 increased T_{in} and T_{sep} for WC 25% and 50%, generally there was an increase with increasing crude concentration in Exxsol™ D60. Adding crude oil to Exxsol™ D60 do not change T_{in} and T_{sep} for WC 75%.

Bottle separation tests show that T_{in} and T_{sep} was higher for WC 50% than WC 25%, for all concentration of crude in Exxsol™ D60, except for 200 ppm and 500 ppm for T_{in} and except for 200 ppm for T_{sep} . Bottle separation tests show that T_{in} and T_{sep} was higher for WC 25% than WC 75% for all concentration of crude in Exxsol™ D60.

A larger number of tests for each set of conditions, and bottle separation tests for different WC may be performed to better understand the effect of adding crude to Exxsol™ D60 to bottle separation performance.

7.2 MPPS experimental results

As presented in Fig. 5.1 through Fig. 5.11 adding crude to Exxsol™ D60 gave a lower WC tapped stream for most WT, with the exception of WT 10% for some set condition e.g in Fig. 5.3 and Fig. 5.4. Thus the performance of the MPPS was less favorable as spiked oil was mixed with distilled water w/ 3.4 wt% NaCl compared to unspiked oil mixed with distilled water w/ 3.4 wt% NaCl. The effect of adding crude to Exxsol™ D60 on the performance of the MPPS was stronger at unfavorable flow conditions as high total flow rate and low inlet WC. This can be observed when comparing drainage potential curves in Fig. 5.4 where the difference in WC tapped stream was within 1%, and drainage potential curves in Fig. 5.9 where the difference in WC tapped stream was between 40 and 50% WC tapped stream.

Adding crude to Exxsol™ D60 may create more stable emulsions as the crude include heavy polar components according to Kokal [20]. Looking at the photos of flow in the MPPS presented in Fig. 5.7 and Fig. 5.9 it looked like the emulsion occupied a large portion of the pipe section when flowing spiked oil compared to unspiked oil. More water in the emulsion phase means that as WT increase, more of the emulsion was tapped to achieve the desired WT, and WC tapped stream decreased as more oil in the emulsion phase was tapped alongside the water in the emulsion phase.

As presented in Fig. 5.12 through Fig. 5.17 an increase in total flow rate from 300 L/min to 500 L/min and 700 L/min in the MPPS gave a less favorable performance of the MPPS. This development can be explained by the fact that increased total flow rate reduces the residence time in the MPPS and gave the liquid-liquid system less time to reach phase separation. This change was seen for spiked oil mixed with distilled water w/ 3.4 wt% NaCl and unspiked oil mixed with distilled water w/ 3.4 wt% NaCl. The less favorable performance of the MPPS as total flow rate increase was more substantial at WC inlet 30% as presented in Fig. 5.12 and Fig. 5.13 compared to WC inlet 70% as presented in Fig. 5.16 and Fig. 5.17.

The difference in WT value at data points collected and presented across figures for spiked oil and unspiked oil cases is related to the fact that the presented WT value was calculated after the experiments were concluded. During the experiments, an inaccurate preliminary WT was used to decide where to collect data points.

7.3 Comparison between experimental and model-generated drainage potential curves

The drainage potential curves of:

- Fig. 5.12 for total flow rate of 300 L/min and WT below 50%
- Fig. 5.13 for total flow rate of 300 L/min and WT below 50%
- Fig. 5.14 for total flow rate of 300 L/min
- Fig. 5.16 for total flow rate of 300 L/min
- Fig. 5.18 for total flow rate of 300 L/min
- Fig. 5.18 for total flow rate of 500 L/min and WT below 70%
- Fig. 5.19 for total flow rate of 500 L/min and WT below 50%

all resemble model-generated curves shown in Fig. 6.1, obtained assuming stratified flow and pure water and oil layer. When looking at the flow photos of all of these cases there is a clear layer of water at the bottom of the pipe.

The drainage potential curves of:

- Fig. 5.12 for total flow rate of 500 L/min
- Fig. 5.12 for total flow rate of 700 L/min
- Fig. 5.15 for total flow rate of 300 L/min

all resemble model-generated curves presented in Fig. 6.5, obtained assuming a linear transition from water to oil between a pure water and oil layer. Linear transition from water to oil was an attempt to simulate an emulsion layer in the pipe. When looking at the available photos of the flow, an emulsion layer can be seen between the pure water and oil layer.

The drainage potential curves of:

- Fig. 5.17 for total flow rate of 300 L/min
- Fig. 5.19 for total flow rate of 300 L/min

resemble model-generated curve "y trans. 0,1" presented in Fig. 6.5, obtained assuming pure water and oil flow with a linear transition from water to oil occupying 0,1 normalized height of the pipe. When looking at the available photos of the flow, an emulsion layer is not clearly visible.

The drainage potential curves of:

- Fig. 5.16 for total flow rate of 700 L/min
- Fig. 5.17 for total flow rate of 700 L/min

also resemble model-generated curves presented in Fig. 6.5, obtained assuming a linear transition from water to oil between a pure water and oil layer. However WC tapped stream does not decrease as fast with increasing WT as predicted by the model.

The drainage potential curves of:

- Fig. 5.14 for total flow rate 500 L/min
- Fig. 5.15 for total flow rate 500 L/min

resemble model-generated curves presented in Fig. 6.6, obtained assuming OiW contaminated water flow and linear transition to oil. However, the decline from stable WC tapped stream was at lower WT than the model predicted. This may indicate that emulsion occupied a larger portion of the pipe. When looking at the available photos of the flow, an emulsion layer can be seen between the pure water and oil layer.

The drainage potential curves presented in Fig. 5.16 for total flow rate of 500 L/min and WT below 80% resemble model-generated curves presented in Fig. 6.3, obtained assuming OiW contaminated water flow. When looking at the available photos of the flow, OiW contamination can not be clearly seen.

The drainage potential curves of:

- Fig. 5.12 for total flow rate of 300 L/min and WT above 50%
- Fig. 5.13 for total flow rate of 300 L/min and WT above 50%
- Fig. 5.16 for total flow rate of 500 L/min and WT above 80%
- Fig. 5.17 for total flow rate of 500 L/min
- Fig. 5.18 for total flow rate of 500 L/min and above WT 50%
- Fig. 5.19 for total flow rate of 500 L/min and above WT 50%

shows a "straight-line" decline in WC tapped stream as WT increase. This behavior of the drainage potential curve was not captured in the modeling results. When looking at the available photos of the flow, there seems to be contamination of the water phase, close to the interface. The "straight-line" decline in WC tapped stream as WT increases, maybe a product of increasing OiW contamination in the water phase.

7.3 Comparison between experimental and model-generated drainage potential curves

The drainage potential curves of:

- Fig. 5.13 for total flow rate of 500 L/min
- Fig. 5.13 for total flow rate of 700 L/min
- Fig. 5.14 for total flow rate of 700 L/min
- Fig. 5.15 for total flow rate of 700 L/min

shows a decrease of WC tapped stream as WT increased. WC tapped decreases more at low WT, this behavior was not captured in the modeling results. When looking at the available photos of the flow, an emulsion layer can be seen between the pure water and oil layer.

Note that total flow rate of 300 L/min with spiked oil as presented in Fig. 5.15, Fig. 5.17 and Fig. 5.19 fit better with modeling result for linear transition from water to oil as in Fig. 6.6, the modeling equivalent to emulsion flow at liquid-liquid interface. And for total flow rate 300 L/min of unspiked oil as presented in Fig. 5.14, Fig. 5.16 and Fig. 5.18 fit better with modeling result of tapping from pure water flow as in Fig. 6.1. Suggesting that adding 185 ppm crude to Exxsol™ D60 helps emulsion to form at total flow rate of 300 L/min and WC inlet of 50, 70, 90%.

Generally, the model-generated curves fit good for tapping of a pure water and oil flow as in Fig. 6.1. Some cases of emulsion layer between pure water and oil flow fit the model-generated curves for a linear transition from water to oil as in Fig. 6.5.

However, tapping of emulsions seen in the photos corresponds to the different behavior of the experimental drainage potential curves, suggesting that different emulsions have a different distribution of water and oil. All emulsion flows was not captured by the model-generated curves when compared to the experimental drainage potential curves.

Chapter 8

Conclusion

Bottle separation tests for Exxsol™ D60 added 200, 400, 500, 600, 700, and 800 ppm crude oil and distilled water w/ 3,4 wt% NaCl at WC 25, 50 and 75% were performed. The results indicate that adding crude oil to Exxsol™ D60 increased T_{in} and T_{sep} for WC 25% and 50%, generally there was an increase in T_{in} and T_{sep} with increasing crude concentration in Exxsol™ D60. Adding of crude oil to Exxsol™ D60 did not change T_{in} and T_{sep} for WC 75%.

Experimental campaigns on MPPS with unspiked oil mixed with distilled water w/ 3,4 wt% and spiked oil mixed with distilled water w/ 3,4 wt% were performed. Adding crude to Exxsol™ D60 gave a lower WC tapped stream for most WT. The performance of the MPPS was less favorable as spiked oil was mixed with distilled water w/ 3.4 wt% NaCl compared to unspiked oil mixed with distilled water w/ 3.4 wt% NaCl. The effect of adding crude oil to Exxsol™ D60 on the performance of the MPPS was stronger at unfavorable flow conditions as high total flow rates e.g 700 L/min and low inlet WC e.g 30, 50%.

The experimental drainage potential curves were compared with drainage potential curves generate by numerical models developed by Harstad [16] as part of the project thesis. The model-generated drainage potential curves fit good for a tapping of a pure water and oil flow. For flow with an emulsion layer, the model-generated drainage potential curves do not capture all the different behaviors observed of the experimental drainage potential curves.

8.1 Recommendation for further work

For further work more bottle separation tests for different WC can be performed to better understand the effect of adding crude oil to Exxsol™ D60 over more WC's. More repetitions of the set of conditions presented in this work can be performed to more data, and get a better estimation of errors in the result.

Experimental campaign on MPPS with Exxsol™ D60 + higher concentrations of crude e.g 400 and 800 ppm mixed with distilled water w/ 3,4 wt% can be performed to investigate if the trend of higher separation times at the crude concentration increase, as observed in the bottle separation test holds for MPPS experiments. Exxsol™ D60 + higher concentrations of crude are also expected to behave closer to a crude + brine mixture, as will be the expected fluid mixture from a well stream.

Drainage potential curves where WC tapped stream decrease as WT increase and the decrease of WC tapped was larger for low WT was not captured in the modeling results and further investigation to understand and model such a drainage process may be completed.

Bibliography

- [1] NTNU. 2019 TPG4135, Production Technology Field Processing and Systems. Presented 7 January 2019, Trondheim, Norway.
- [2] Student t-value calculator. <https://goodcalculators.com/student-t-value-calculator/>. [Online; Accessed 20-January-2021].
- [3] Aktivitetsforskriften. <https://www.ptil.no/regelverk/alle-forskrifter/aktivitetsforskriften/XI/60/>, 2010. [Online; Accessed 19-March-2020].
- [4] Annual report 2018. Technical report, SUBPRO, March 2019. [Online; Accessed 20-March-2020].
- [5] Miljørapport 2019. <https://www.norskoljeoggass.no/miljo/miljorapporter/miljorapport-2019/>, September 2019. [Online; Accessed 18-March-2020].
- [6] Ressursrapport felt og funn 2019. <https://www.npd.no/globalassets/1-mpd/publikasjoner/ressursrapport-2019/ressursrapport-2019.pdf>, September 2019. [Online; Accessed 18-March-2020].
- [7] Sensor terminology. <https://www.ni.com/en-no/innovations/white-papers/13/sensor-terminology.html#section-1895225590>, July 2020. [Online; Accessed 26-January-2021].
- [8] A. R. Ganji A. J. Wheeler. *Introduction to Engineering Experimentation*. Pearson Higher Education, Upper Saddle River, New Jersey, third edition, 2010.
- [9] M. Bothamley. Offshore processing options vary widely. *Oil & Gas Journal*, 102:47–55, 2004.
- [10] H. B. Bradley, editor. *Petroleum Engineering Handbook*. Society of Petroleum Engineers, Richardson, TX, U.S.A., third edition, 1987.
- [11] N. Brauner. *Modelling and Experimentation in Two-Phase Flow*. Springer-Verlag, Wien, first edition, 2003.
- [12] B. Ratcliffe C. Ratcliffe. *Doubt-Free Uncertainty In Measurement An Introduction for Engineers and Students*. Springer, New York, first edition, 2015.

-
- [13] Y. A. Cengel and J. M. Cimbala. *Fluid Mechanics, Fundamentals and Applications*. McGraw-Hill, Avenue of the Americas, New York, second si units edition, 2010.
- [14] S. Osisanya C.O. Olotu. Development of a user friendly computer program for designing conventional oilfield separators. In *Nigeria Annual International Conference and Exhibition*, Lagos, Nigeria, 2013.
- [15] E. K. Knudsen Ellertsen. Experimental study of oil-water pipe flow and separation. Specialization project, December 2017.
- [16] S. Harstad. Bulk oil-water pipe separation: performance of single tap and spiking experiments. Specialization project, June 2020.
- [17] K. D. Fink J. H. Mathews. *Numerical Methods Using MATLAB*. Pearson, Upper Saddle River, New Jersey, fourth edition, 2004.
- [18] J.P Brill J.L. Trallero, C. Sarica. A study of oil/water flow patterns in horizontal pipes. *SPE Production & Facilities*, pages 165–172, 1997.
- [19] S. Keleşoğlu. *Flow Behaviour of Water-in-North Sea Acidic Crude Oil Emulsions and Preparation of Synthetic Reference Acidic Oils and Their Emulsions*. PhD thesis, Norwegian University of Science and Technology, December 2010.
- [20] S. Kokal. Crude oil emulsions: Everything you wanted to know but were afraid to ask. SPE DISTINGUISHED LECTURER SERIES.
- [21] M. Golan M. Stanko. Simplified hydraulic desing mehodology for a subsea inline oil-water for pipe separator. In *Offshore Technology Conference*, Rio da Janeiro, Brazil, 2015.
- [22] K. Arnold M. Stewart. *Gas-Liquid And Liquid-Liquid Separators*. Gulf Professional Publishing, 30 Corporate Drive, Suite 400, Burlington, MA 01803, USA, first edition, 2008.
- [23] R.J. Moffat. Describing the uncertainties in experimental results. *Experimental thermal and fluid science*, 1:3–17, 1988.
- [24] G. Mogseth. Functional verification of the worlds first full field subsea separation system - tiora. In *Offshore Technology Conference*, Huston, TX, USA, 2008.
- [25] B. A. Craig P. S. Moore, G. P. McCabe. *Introduction to the Practice of STATISTICS, International edition*. W.H Freeman and Company, 41 Madison Avenue, New York, seventh edition, 2012.
- [26] H. S. Skjefstad. *Development and assessment of a multi-pipe oil-water bulk separator concept for subsea applications*. PhD thesis, Norwegian University of Science and Technology, November 2019.
- [27] H. S. Skjefstad and M. Stanko. An experimental study of a novel parallel pipe separator design for subsea oil-water bulk separation. In *SPE Asia Pacific Oil & Gas Conference and Exhibition*, Brisbane, Australia, 2018.
-

-
- [28] H. S. Skjefstad and M. Stanko. Experimental performance evaluation and design optimization of a horizontal multi-pipe separator for subsea oil-water bulk separation. *Journal of Petroleum Science and Engineering*, 176:203–219, 2019.
- [29] R. Zwanzig. Hydrodynamic fluctuations and stokes' law friction. *JOURNAL OF RESEARCH of the National Bureau of Standards-B. Mathematics and Mathematical Physics*, 68B:143–145, 1964.

**Appendix A - Calibration certificate for Micro Motion F200
and Sitrans FC430**

Micro Motion, Inc.

Mass Flowmeter Calibration Certificate

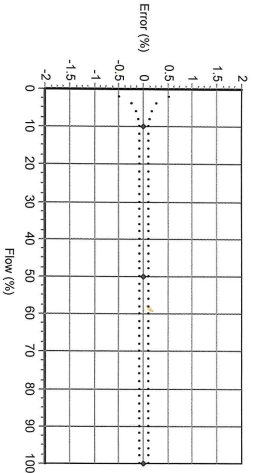
15018910

Product Code	Serial ID	Order ID	Line	Item	Customer Tag
F200S369C2E2NZKZZ	15018910	22045314	2.1	1	
PUCR800	33369466				

Process

Process ID : 2.41668262
 Process Time : 2017.06.15 11:01:58
 Process Stand : S8F2A8SSCE
 Stand Uncertainty : +/-0.030%
 Fluid : H2O
 100% Rate : 725.7477 KG/MIN
 Pickoff : 1
 Max Rate P/T : 17.14 PSIG/19.5 C

Detail



Results

Status : PASS
 D1 : 0
 D2 : 1
 K1 : 3375.878
 K2 : 3885.176
 DT : 4.5
 FD : 6000
 DTG : 0
 DFG1 : 0
 DFG2 : 0
 FlowCal : 1518.84.56
 FFG : 0
 FTG : 0
 DensCal : 033760388854.50
 FCF : 1518.8
 FT : 4.56

Flow (%)	Flow Rate (kg/min)	Meter Total (kg)	Reference Total (kg)	Error (%)	Specification (±%)
100.0	725.7477	751.9714	751.8981	0.010	0.100
10.0	72.57477	98.63879	98.62951	0.009	0.100
50.0	362.8739	373.6875	373.6937	-0.002	0.100
100.0	725.7477	753.7616	753.7493	0.002	0.100

STOJLE T. Technican
 This certificate is produced by an electronic data system and is valid without signature
 Traceable to one or more of the following National Metrology Institutes: NIM-China, NIST-USA, and VSL-The Netherlands
 15.0.0.140 2017.06.15 11:15:33 1/1

Micro Motion, Inc.

Transmitter Configuration Report

19005565

Product Code	Serial ID	Order ID	Line	Item	Customer Tag
E200S369C2EZNKZZ	15018910	22045314	2.1	1	
5700R12HEFAZZZ	19005565	22045314	2.48	1	
PDCR800	3369466				

Process

Process ID : 2.41674782
 Process Time : 2017.06.15 15:28:10
 Process Stand : MMTV_XMTR_CONFIG@SSCE

Sensor

D1 : 0
 D2 : 1
 DRQ1 : 0
 DRQ2 : 0
 DT : 4.5
 DTG : 0
 Density Meter Factor : 1
 Density Press Comp Factor : 0
 FCF : 1518.8
 FD : 6000
 FFQ : 0
 FT : 4.56
 FTG : 0
 Flow PCP : 19.99998
 Flow PCF : 0
 K1 : 3375.878
 K2 : 3885.176
 Mass Flow Meter Factor : 1
 Temperature Cal Factor : 1.00000T-.00000
 Volume Flow Meter Factor : 1

Units

Special Mass Flow Text : NONE
 Special Mass Time Unit : SEC
 Special Mass Total Text : NONE
 Special Volume Base Unit : LITER
 Special Volume Conv Factor : 1
 Special Volume Flow Text : NONE
 Special Volume Time Unit : SEC
 Special Volume Total Text : NONE
 Temperature Unit : DEGC
 Velocity Unit : MTR/S
 Volume Flow Unit : L/MIN

I/M/D Channel Assignments

Channel A Assignment : ANALOG 1
 Channel B Assignment : ANALOG 2
 Channel C Assignment : NONE
 Channel C Power : INTERNAL
 Channel D Assignment : NONE
 Channel D Power : EXTERNAL

Assignments

Discrete Output 1 Assignment : FWD / REV
 Discrete Output 2 Assignment : FWD / REV
 Discrete Output 3 Assignment : FWD / REV
 Event 1 Variable : DENSITY
 Event 2 Variable : DENSITY

Frequency1 Scaling Method : FREQUENCY/FLOW
 Frequency Variable 1 : MASS FLOW RATE
 Frequency Variable 2 : MASS FLOW RATE
 mA1 Variable : MASS FLOW RATE
 mA2 Variable : DENSITY
 mA3 Variable : TEMPERATURE

Ranges

15.0.0.138 2017.06.15 15:49:31 1/2

Units

Density Unit : G/CM3
 GSV Flow Unit : SCFM
 Mass Flow Unit : KG/MIN
 Pressure Unit : PSI
 Special GSV Base Time Unit : MIN
 Special GSV Base Volume Unit : STANDARD_CUBIC_FEET
 Special GSV Conv Factor : 1
 Special GSV Flow Unit Text : NONE
 Special GSV Total Text : NONE
 Special Mass Base Unit : GRAM
 Special Mass Conv Factor : 1

Micro Motion, Inc.

Transmitter Configuration Report

19005565

Ranges

Other

Event 1 Setpoint : 0
 Event 1 Type : LOW ALARM
 Event 2 Setpoint : 0
 Event 2 Type : LOW ALARM
 Frequency1 Hertz : 1000
 Frequency1 Output Mode : SINGLE
 Frequency1 Pulses/Unit : 82.67336
 Frequency1 Rate : 725.7477
 Frequency1 Units/Pulse : 0.0120958
 Frequency2 Hertz : 1000
 Frequency2 Pulses/Unit : 59.99999
 Frequency2 Rate : 1000
 Frequency2 Units/Pulse : 0.0166667
 mA1 LRV : 0
 mA1 URV : 725.7477
 mA2 LRV : 0
 mA2 URV : 5
 mA3 LRV : -240
 mA3 URV : 450

Faults

Frequency1 Fault Behavior : DOWNSCALE
 Frequency1 Fault Value : 14500
 Frequency2 Fault Behavior : DOWNSCALE
 Frequency2 Fault Value : 14500
 RS485 Fault Behavior : NONE
 mA1 Fault Behavior : DOWNSCALE
 mA1 Fault Value : 2
 mA2 Fault Behavior : DOWNSCALE
 mA2 Fault Value : 2
 mA3 Fault Behavior : DOWNSCALE
 mA3 Fault Value : 2

Other

Calibration Process ID : 2.41668262
 Core Software Rev : 420
 Density Cutoff : 0.2
 Density Damping : 1.28
 Density High Limit : 5
 Density Low Limit : 0
 Direction : 5700 ENABLED
 Fault Dwell Time : 0
 Feature Bits : 197120
 Flow Damping : 0.64
 HART Device ID : 3348975

Micro Motion, Inc.

Mass Flowmeter Calibration Certificate

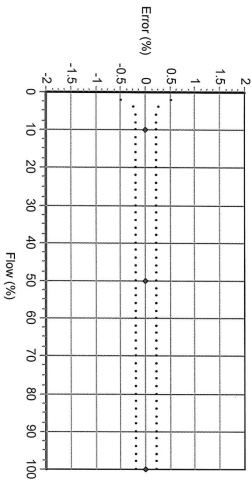
15018877

Product Code	Serial ID	Order ID	Line	Item	Customer Tag
F200S369C2E2MVKZ	15018877	22045314	1.1	1	

Process

Process ID : 9.23670276
 Process Time : 2017.05.23 12:53:01
 Process Stand : TSM2G@SSCCL
 Stand Uncertainty : +/-0.030%
 Fluid : H2O
 100% Rate : 725.7477 KG/MIN
 Pickoff : 1
 Max Rate P/T : 50.7 PSIG/25 C

Detail



Results

Status : PASS
 D1 : 0
 D2 : 1
 K1 : 3390.66
 K2 : 3899.263
 DT : 4.5
 FD : 6000
 DTG : 0
 DFQ1 : 0
 DFQ2 : 0
 FlowCal : 1530.34.56
 FFG : 0
 FTG : 0
 DensCal : 03391038994.50
 FCF : 1530.3
 FT : 4.56

Flow (%)	Flow Rate (kg/min)	Meter Total (kg)	Reference Total (kg)	Error (%)	Specification (±%)
100.0	725.7477	712.8294	712.8368	-0.001	0.200
10.0	72.57477	70.65759	70.66615	-0.012	0.200
50.0	362.8739	369.8471	369.8633	-0.004	0.200
100.0	725.7477	714.3535	714.3505	0.000	0.200

CRISTIAN CIMPEAN

Technician

This certificate is produced by an electronic data system and is valid without signature.

Traceable to one or more of the following National Metrology Institutes: NIM-China, NIST-USA, and VSL-The Netherlands

15.0.0.138 2017.06.16 10:40:30 1/1

Micro Motion, Inc.

Transmitter Configuration Report

19005564

Product Code	Serial ID	Order ID	Line	Item	Customer Tag
F200S369C2EZNKZZ	15018977	22045314	1.1	1	
5700R12HEFAZZAAAZZ	19005564	22045314	1.48	1	
PDCR800	33369436				

Process
 Process ID : 2.41690863
 Process Time : 2017.06.16 11:43:53
 Process Stand : MMTV_XMTR_CONFIGSSCE

Sensor

D1 : 0
 D2 : 1
 DFQ1 : 0
 DFQ2 : 0
 DT : 4.5
 DTG : 0
 Density Meter Factor : 1
 Density Press Comp Factor : 0
 FCF : 1530.3
 FD : 6000
 FFQ : 0
 FT : 4.56
 FTG : 0
 Flow PCP : 19.99998
 Flow PCF : 0
 K1 : 3390.66
 K2 : 3899.263
 Mass Flow Meter Factor : 1
 Temperature Cal Factor : 1.000000T.000000
 Volume Flow Meter Factor : 1

Units

Special Mass Flow Text : NONE
 Special Mass Time Unit : SEC
 Special Mass Total Text : NONE
 Special Volume Base Unit : LITER
 Special Volume Conv Factor : 1
 Special Volume Flow Text : NONE
 Special Volume Time Unit : SEC
 Special Volume Total Text : NONE
 Temperature Unit : DEGC
 Velocity Unit : MTR/S
 Volume Flow Unit : L/MIN

MVD Channel Assignments

Channel A Assignment : ANALOG 1
 Channel B Assignment : INTERNAL
 Channel C Assignment : NONE
 Channel C Power : INTERNAL
 Channel D Assignment : NONE
 Channel D Power : EXTERNAL

Units

Density Unit : G/GUOM
 GSV Flow Unit : SCFM
 Mass Flow Unit : KG/MIN
 Pressure Unit : PSI
 Special GSV Base Volume Unit : STANDARD_CUBIC_FEET
 Special GSV Conv Factor : 1
 Special GSV Flow Unit Text : NONE
 Special GSV Total Text : NONE
 Special Mass Base Unit : GRAM
 Special Mass Conv Factor : 1

Assignments

Discrete Output 1 Assignment : FWD / REV
 Discrete Output 2 Assignment : FWD / REV
 Discrete Output 3 Assignment : FWD / REV
 Event 1 Variable : DENSITY
 Event 2 Variable : DENSITY
 Frequency/Scaling Method : FREQUENCY/FLOW
 Frequency Variable 1 : MASS FLOW RATE
 Frequency Variable 2 : MASS FLOW RATE
 mA1 Variable : MASS FLOW RATE
 mA2 Variable : DENSITY
 mA3 Variable : TEMPERATURE

Ranges

Micro Motion, Inc.

Transmitter Configuration Report

19005564

Ranges

Event 1 Setpoint : 0
Event 1 Type : LOW ALARM
Event 2 Setpoint : 0
Event 2 Type : LOW ALARM

Other

LD Coil : 0
LD Type : 0
Mass Flow Cutoff : 2.0736
Pressure Comp Line Pressure : 0
Pressure Compensation State : OFF
Slug Duration : 0
Tag :
Temperature Damping : 4.8
Transmitter Software Rev : 13
Volume Flow Cutoff : 2.0736

Frequency1 Hertz : 1000
Frequency1 Output Mode : SINGLE
Frequency1 Pulses/Unit : 82.67336
Frequency1 Rate : 725.7477
Frequency1 Units/Pulse : 0.0120958
Frequency2 Hertz : 1000
Frequency2 Pulses/Unit : 59.99999
Frequency2 Rate : 1000
Frequency2 Units/Pulse : 0.01666667
mA1 LRV : 0
mA1 URV : 725.7477
mA2 LRV : 0
mA2 URV : 5
mA3 LRV : -240
mA3 URV : 450

Faults

Frequency1 Fault Behavior : DOWNSCALE
Frequency1 Fault Value : 14500
Frequency2 Fault Behavior : DOWNSCALE
Frequency2 Fault Value : 14500
RS485 Fault Behavior : NONE
mA1 Fault Behavior : DOWNSCALE
mA1 Fault Value : 2
mA2 Fault Behavior : DOWNSCALE
mA2 Fault Value : 2
mA3 Fault Behavior : DOWNSCALE
mA3 Fault Value : 2

Other

Calibration Process ID : 9.23670276
Core Software Rev : 420
Density Cutoff : 0.2
Density Damping : 1.28
Density High Limit : 5
Density Low Limit : 0
Direction : 5700 ENABLED
Fault Dwell Time : 0
Feature Bits : 197120
Flow Damping : 0.64
HART Device ID : 3348942

SIEMENS**Industry Sector**

**Factory Calibration Certificate / Werkskalibrierungszertifikat /
Certificat d'étalonnage usine**

Topic / Thema / Sujet: SITRANS F Flowmeter / Durchflussmessgerät / Débitmètre

Object / Betreff / Objet:

Customer order / Kundenauftrag / Commande client : N1740736
 Siemens order / Siemensauftrag / Commande Siemens : 0001531239/000010
 Flowmeter type / Durchflussmessgerättyp / Type de débitmètre : SITRANS FC400
 Nominal sensor diameter / Messaufnehmer-Nennweite / Diamètre nominal de capteur : DN 50 (2")
 Product order No. / Produktbestellnummer / N° de référence d'appareil : 7ME46134CA014DA3-Z
 Options ordered / Bestellten Optionen / Options commandées : A02+B11+E06+F40
 Sensor serial No. / Messaufnehmer Seriennummer / N° de série de capteur : FDKJ6190005780

Technical data / Technische Daten / Données techniques:

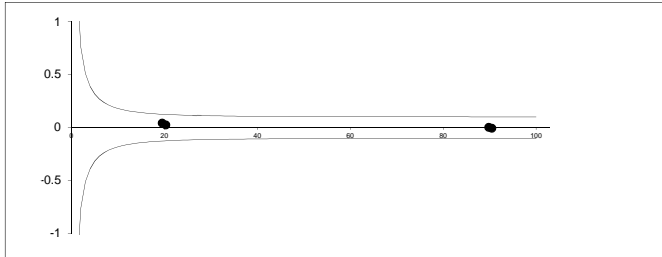
Calibration factor / Kalibrierungsfaktor / Facteur d'étalonnage : 1526589000
 Calibration medium / Kalibriermedium / Moyen de calibration : Water / Wasser / Eau
 Calibrated full scale flow / Kalibrierter Messbereichsendwert / Fin de plage de mesure : 50000 kg/h / 110231 lb/h
 étalonnée
 Calibration rig / Kalibrierstand / Plate-forme d'étalonnage : CAL00130

Standards / Normen / Normes:

ISO 4185-1980

Results / Ergebnisse / Résultats:

Point # Messpunkt nr Point mesure n°	Flowrate Durchfluss Débit [%]	Fluid temperature Flüssigkeitstemperatur Température du fluide		Reference flow value Referenz Durchflusswert Débit de référence		Flowmeter output / Durchflussmessgerätausgang / Sortie de débitmètre		Error Fehler / Erreur [%]
		[°C]	[°F]	[kg/h]	[lb/h]	[kg/h]	[lb/h]	
1	90	23.2	73.8	44905.7593	99000.2527	44906.8389	99002.6329	0.00
2	90	23.3	73.9	45231.4219	99718.2158	45228.7035	99712.2228	-0.01
3	20	23.3	73.9	9756.2305	21508.8064	9760.4530	21518.1155	0.04
4	20	23.3	73.9	10144.5193	22364.8367	10147.0267	22370.3646	0.02



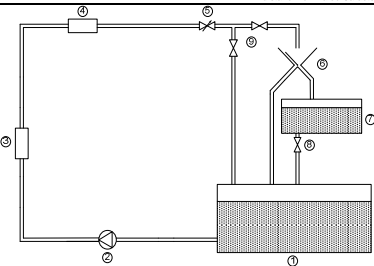
Summary of the results / Zusammenfassung der Ergebnisse: / Sommaire des résultats obtenus :

- The measured values are within the specified limits / Die gemessenen Werte liegen innerhalb der Toleranzen / Les résultats de mesure se trouvent dans les tolérances définies

Siemens A/S, Flow Instruments	Issued by / Erstellt von / émis par MD	Date / Datum / Date 2017-06-22
-------------------------------	---	-----------------------------------

SIEMENS**Industry Sector**

**Factory Calibration Certificate / Werkskalibrierungszertifikat /
Certificat d'étalonnage usine**

Test rig characteristics Prüfstand Merkmale / Caractéristiques de la plate-forme de test	
	Test rig ID / Prüfstand ID / ID de la plate-forme de test
	CAL00130
	Fluid / Flüssigkeit / Fluide
	Water / Wasser / Eau
	Fluid temperature / Flüssigkeit Temp. / Temp. du fluide
	15-30 °C / 59-86 °F
	Test rig capacity / Prüfstand Kapazität / Capacité de la plate-forme
	DN 25...80 / 1"...3"
	Max. Flowrate / Max. Durchfluss / Débit max.
	50000 kg/h / 110231 lb/h
	Min. Flowrate / Min. Durchfluss. / Débit min
	220 kg/h / 485.02 lb/h
	Max. Mass / Max.Masse / Masse max.
	600 kg / 1322.77 lb
	Uncertainty / Ungenauigkeit / Incertitude
	< 0.05%

- 1) Reservoir / Tank / Réservoir
 2) Pump / Pumpe / Pompe
 3) One or more reference meters / Ein oder mehrere Referenz Messgeräte / un ou plusieurs débitmètres de référence
 4) Meter under test / Messgerät unter Prüfung / Débitmètre en test
 5) Control valve / Kontrollventil / Vanne de régulation
 6) Diverter / Kippschaltung / Bascule
 7) Weighing tank / Gewichtsmessungstank / Cuve de mesure
 8) Drain valve / Abflussventil / Vanne de vidange
 9) Valve to switch between reference meter method and static/dynamic weighing method / Ventile zum switchen zwischen Referenz Methode und statische/dynamische Gewichtsmessung Methode / Vanne de basculement entre méthode avec débitmètres de référence et méthode par pesée statique or dynamique

Traceability / Rückverfolgbarkeit / Traçabilité

The Siemens flowmeter calibration process is ISO9001-certified, ensuring the entire calibration procedure is controlled to the highest quality standards.

All primary measuring instrumentation used by the Siemens Flow Laboratory during the performance of its calibrations, has been calibrated with international standards traceability referring directly to the physical unit of measurement according to the International System of Units (SI). Therefore the calibration certificate ensures recognition of the test results worldwide, including the US (NIST traceability).

Der Siemens Kalibrierungsprozess für Durchflussmessgeräte ist ISO9001 zertifiziert, sicherstellend, dass das ganze Kalibrierungsverfahren nach den höchsten Qualitätsstandards kontrolliert ist.

Alle Hauptmessinstrumente, die zur Durchführung der Kalibrierungen vom Siemens Durchfluss Laboratorium genutzt werden, sind kalibriert, um eine Rückverfolgbarkeit auf internationale Normen sicherzustellen. Dies bezieht sich direkt auf die Maßeinheit gemäß dem Internationalen Einheitensystem (SI). Das Kalibrierungszertifikat gewährleistet daher die Anerkennung der Prüfergebnisse weltweit, einschließlich in den USA (NIST-Rückverfolgbarkeit).

Le processus d'étalonnage des débitmètres Siemens est certifiée ISO9001 et est contrôlé périodiquement selon les normes qualités en vigueur les plus élevées.

Tous les instruments de mesure primaires utilisés dans les laboratoires Siemens Flow durant les opérations d'étalonnage ont été étalonnés en conformité avec les normes internationales relatives à l'unité de mesure physique, conformément au système international d'unités (SI). Le certificat d'étalonnage garantit ainsi que les résultats obtenus lors des essais sont conformes aux normes internationales, y compris NIST (USA).

Siemens A/S, Flow Instruments

Coriolisvej 1-3
DK-6400 Sønderborg
Denmark

Tel (+45) 29 49 32 32

SIEMENS**Industry Sector****Factory Calibration Certificate / Werkskalibrierungszertifikat /
Certificat d'étalonnage usine****Object / Betreff / Objet:**

Customer order / Kundenauftrag / Commande client	:	N1740736
Siemens order / Siemensauftrag / Commande Siemens	:	0001531239/000010
Flowmeter type / Durchflussmessgerättyp / Type de débitmètre	:	SITRANS FC400
Nominal sensor diameter / Messaufnehmer-Nennweite / Diamètre nominal de capteur	:	DN 50 (2")
Product order No. / Produktbestellnummer / N° de référence d'appareil	:	7ME46134CA014DA3-Z
Options ordered / Bestellten Optionen / Options commandées	:	A02+B11+E06+F40
Sensor serial No. / Messaufnehmer Seriennummer / N° de série de capteur	:	FDKJ6190005780

Technical data / Technische Daten / Données techniques:

Calibration rig / Kalibrierstand / Plate-forme d'étalonnage	:	20001973
A Constant / Konstante A / Constante A	:	-2.399724E+03
B constant / Konstante B / Constante B	:	8.045804E+08
Density TC / Dichte TC / CT densité	:	-4.417412E-04
D Constant / Konstante D / Constante D	:	1.500000E-05

Density results / Dichte Ergebnisse / Résultats de la densité:

Point # Messpunkt nr. Point mesure n°	Calibration medium Kalibriermedium Moyen de calibration	True density Wahre Dichte Densité réelle		Flowmeter output / Durchflussmessgerätausgang / Sortie de débitmètre			
		[kg/m ³]	[lb/ft ³]	Density Dichte / Densité		Error Fehler / Erreur	
1	Warm water	981.45	61.270	981.47	61.271	0.0	0.00
2	Cold water	997.55	62.275	997.69	62.284	0.1	0.01

Temperature results / Temperatur Ergebnisse / Résultats de la température:

Point # Messpunkt nr. Point mesure n°	Calibration medium Kalibriermedium Moyen de calibration	True Temperature Wahre Temperatur Température réelle		Flowmeter output / Durchflussmessgerätausgang / Sortie de débitmètre			
		[°C]	[°F]	Temperature Temperatur / Température		Error Fehler / Erreur	
1	Warm water	63.3	145.9	63.4	146.1	0.06	0.11
2	Cold water	22.7	72.9	22.8	73.0	0.11	0.20

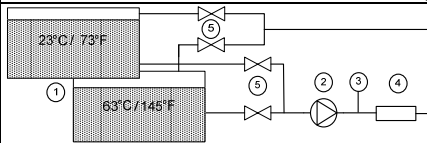
Summary of the results / Zusammenfassung der Ergebnisse: / Sommaire des résultats obtenus .:

- The measured values are within the specified limits / Die gemessenen Werte liegen innerhalb der Toleranzen / Les résultats de mesure se trouvent dans les tolérances définies

Siemens A/S, Flow Instruments	Issued by / Erstellt von / émis par MD	Date / Datum / Date 2017-06-22
-------------------------------	---	-----------------------------------

SIEMENS**Industry Sector**

Factory Calibration Certificate / Werkskalibrierungszertifikat / Certificat d'étalonnage usine

Test rig characteristics <small>Prüfstand Merkmale / Caractéristiques de la plate-forme de test</small>		
 <p style="font-size: small; margin-top: 5px;"> 1) Reservoir / Tank / Réservoir 2) Pump / Pumpe / Pompe 3) Temperature sensor / Temperatursensor / Capteur de température 4) Meter under test / Messgerät unter Prüfung / Débitmètre en test 5) Control valve / Kontrollventil / Vanne de régulation </p>	Test rig ID / Prüfstand ID / ID de la plate-forme de test	20001973
Fluid / Flüssigkeit / Fluide	Water / Wasser / Eau Air / Luft / l'air	
Fluid temperature / Flüssigkeit Temp. / Temp. du fluide	23 & 63 °C / 73 & 145 °F	
Test rig capacity / Prüfstand Kapazität / Capacité de la plate-forme	DN 15...150 / 1/2" .. 6"	

Density calibration / Dichtekalibrierung / Etalonnage densité

Density measurements on Siemens massflow meters are calculated on the basis of media temperature and period of the sensor.

$$\text{Density} = A + B(1 + \alpha)T^2$$

A,B = Calibration constants, a = Density TC, t = Fluid temperature, T = period time of sensor

Dichtemessungen bei Siemens Massedurchflussmessgeräten werden anhand der Medientemperatur und des Messaufnehmer-Zeitraums berechnet.

$$\text{Dichte} = A + B(1 + \alpha)T^2$$

A,B = Kalibrierungskonstanten, a = Dichte TC, t = Temperatur der Flüssigkeit, T = Zeitraum des Messaufnehmer

Les débitmètres massiques de Siemens mesurent la densité par rapport à la température du milieu et à la période du capteur.

$$\text{Densité} = A + B(1 + \alpha)T^2$$

A,B = constantes d'étalonnage, a = CT densité, t = température fluide, T = période temps du capteur

Siemens A/S, Flow Instruments

Coriolisvej 1-3
 DK-6400 Sønderborg
 Denmark

Tel (+45) 29 49 32 32

Appendix B - Re-calibration statement

SIEMENS		Page	of
Siemens Flow Instruments A/S		1	1

To whom it may concern.

SITRANS FM MAGFLO:

As our sensors have no moving parts and using newest technology, by meaning of digital electronic and auto off set, it is not necessary to perform recalibration of our flow meter within normal life time which is > 10 years.

John Hansen
SIEMENS Flow Instruments A/S
Service and Product Specialist



Appendix C - Risk assessment for laboratory experiments (Norwegian)

RISIKOANALYSE

I Excel, blir rar i PDF Men lagt til

Enhet/Institutt:	PTS, Reservoalab
Ansvarlig linjeleder (navn):	
Ansvarlig for aktiviteten som risikovurderes (navn):	Sigurd Harstad
Deltakere (navn):	

Sigurd Harstad, Hamidreza Asaadian

Beskrivelse av den aktuelle aktiviteten, området mv.:

Klaregjøre prøver av Exxsol D60 , råolje og vann. Måle seperasjonstid

Aktivitet/arbeidsoppgave	Mulig uønsket hendelse
<i>Klaregjøre hovedprøve av råolje og Exxsol D60</i>	<i>Exxsol, råolje i øyne, på hud. Avdamping fra Exxsol/Råolje</i>
	<i>Exxsol, råolje i øyne, på hud. Avdamping fra Exxsol/Råolje</i>
Måle seperasjonstid	
<i>Rengjøre utstyr</i>	<i>Exxsol, toulen, råolje i øyne, på hud</i>

Eksisterende risikoreducerende tiltak	Vurdering av sannsynlighet (S)	Vurdering av konsekvens (K) <i>Vurder en konsekvenskategori om gangen. N alltid vurderes.</i>		
	(1-5)	Menneske (1-5)	Øk/materiell (1-5)	Ytre miljø (1-5)
<i>Vernebriller, labfrakk, hansker og er alltid på under håndtering av fluider. Jobbe i avtrekk om mulig</i>	2	2	1	2
<i>Vernebriller, labfrakk, hansker og er alltid på under håndtering av fluider Påse at prøver holdes i lukkede beholdere og korken er skurdd på</i>	2	2	1	2
<i>Vernebriller, labfrakk, hansker og er alltid på under håndtering av fluider</i>	2	3	1	2

Dato opprettet:	07.09.2020
Sist revidert:	10.okt

<i>Menneske skal</i>	Risikoverdi (S x K)	Forslag til forebyggende og/eller korrigerende tiltak <i>Prioriter tiltak som kan forhindre at hendelsen inntreffer (sannsynlighetsreducerende tiltak) foran skjerpet beredskap (konsekvensreducerende tiltak)</i>	Restrisiko etter tiltak (S x K)
Omdømme (1-5)			
1	4	<i>Før oppstart: Gjennomføre dokumentert HMS-opplæring med områdeansvarlig</i>	3
1	4	<i>Før oppstart: Gjennomføre dokumentert HMS-opplæring med områdeansvarlig.</i>	3
1	6	<i>Før oppstart: Gjennomføre dokumentert HMS-opplæring med områdeansvarlig. Toulén behandles i avtekk</i>	3

Appendix D - Risk assessment for MPPS experiments (Norwegian)

RISIKOANALYSE

I Excel, blir rar i PDF Men lagt til

Enhet/Institutt:	PTS,PTS Hallen
Ansvarlig linjeleder (navn):	
Ansvarlig for aktiviteten som risikovurderes (navn):	Sigurd Harstad
Deltakere (navn):	

Sigurd Harstad, Hamidreza Asaadian

Beskrivelse av den aktuelle aktiviteten, området mv.:

Fyller opp MPPS testrig med Exxsol D60, saltvann og råolje. Gjennomføre eksperimenter på anlegget

Aktivitet/arbeidsoppgave	Mulig uønsket hendelse
<i>Flytte Exxsol D60 fra lager til lagertank</i>	<i>Exxsol i øyne, på hud. Avdamping fra Exxsol. Klemfare, bruk av truck</i>
<i>Destillere vann</i>	<i>Varmt vann på hud, brannskade. Vann i øyne</i>
<i>Blande vann og salt</i>	<i>Varmt vann på hud, brannskade. Vann i øyne. Salt i øyne</i>
<i>Fylle Saltvann i lagertank</i>	<i>Varmt vann på hud, brannskade. Vann i øyne. Salt i øyne</i>
<i>Gjennomføre eksperimenter med Exxsol D60 og saltvann</i>	<i>Exxsol i øyne, på hud. Avdamping fra Exxsol. Lekasje. Fall ned fra stillas</i>

Eksisterende risikoreducerende tiltak	Vurdering av sannsynlighet (S)	Vurdering av konsekvens (K) <i>Vurder en konsekvenskategori om gangen. N alltid vurderes.</i>		
	(1-5)	Menneske (1-5)	Øk/materiell (1-5)	Ytre miljø (1-5)
<i>Vernebriller, kjeledress, hansker og er alltid på under håndtering av fluider. Kun godkjent personell bruker truck</i>	2	3	1	3
<i>Vernebriller, kjeledress, hansker og er alltid på under håndtering av fluider. Legge opp slager før man starte destilasjonsanlegg, unngå håndtering av varme slanger</i>	2	1	1	1
<i>Vernebriller, kjeledress, hansker og er alltid på under håndtering av fluider.</i>	2	2	1	2
<i>Vernebriller, kjeledress, hansker og er alltid på under håndtering av fluider.</i>	2	2	1	2
<i>Vernebriller, kjeledress, hansker og er alltid på under håndtering av fluider.</i>	2	3	1	3

Dato opprettet:	15.10.2020
Sist revidert:	17.des

<i>Menneske skal</i>	Risikoverdi (S x K)	Forslag til forebyggende og/eller korrigerende tiltak <i>Prioriter tiltak som kan forhindre at hendelsen inntreffer (sannsynlighetsreducerende tiltak) foran skjerpet beredskap (konsekvensreducerende tiltak)</i>	Restrisiko etter tiltak (S x K)
Omdømme (1-5)			
1	6	<i>Før oppstart: Gjennomføre dokumentert HMS-opplæring med områdeansvarlig. Planlegge bruk av truck og bli enig om hvordan gjøre dette</i>	3
1	2	<i>Før oppstart: Gjennomføre dokumentert HMS-opplæring med områdeansvarlig. Få opplæring i bruk av apparatet, kjenne til vasker for kjøling av brannskader og nøddusj.</i>	2
1	4	<i>Før oppstart: Gjennomføre dokumentert HMS-opplæring med områdeansvarlig.</i>	3
1	4	<i>Før oppstart: Gjennomføre dokumentert HMS-opplæring med områdeansvarlig.</i>	3
1	6	<i>Før oppstart: Gjennomføre dokumentert HMS-opplæring med områdeansvarlig. Teste anlegget med ferskvann for å kontrollere at det ikke lekker. Gjennomføre oppstarte sammen med Overingenør som kjenner anlegget og oppstart. Holde i rekkverk i leider, påse at ingenting ligger i leider eller på stillas</i>	3

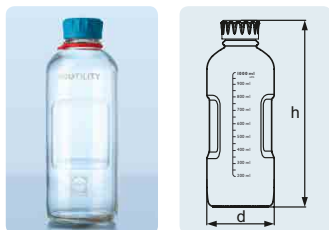
Appendix E - Documentation for laboratory equipment

DURAN©YOUTILITY Laboratory Bottle 125 ml

01 LABORATORY GLASS BOTTLES AND ACCESSORIES

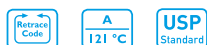
DURAN® YOUTILITY Laboratory Bottle

GL 45



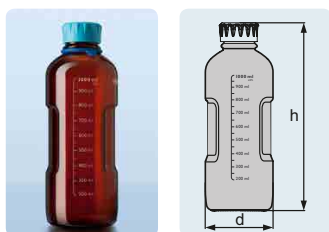
The specially shaped gripping zones on both sides of the bottle enable easier and safer handling. With the new DURAN® YOUTILITY bottle thread opening or closing the bottle is significantly faster. The thread is fully compatible with DIN GL 45 closures and other accessories. The slimmer DURAN® YOUTILITY bottle shape allows a more optimal use of limited space in autoclaves and laboratory refrigerators. A pre-defined labelling area is compatible with the dedicated DURAN® self-adhesive YOUTILITY bottle labels. Nominal volume is shown at the top of the easy-to-read graduation scale for fast determination of the volumes. Each DURAN® YOUTILITY bottle is supplied as a complete system, with a pouring ring (PP) and a GL 45 cap (PP).

Cat. No.	Capacity (mL)	DIN Thread (GL)	d (OD) (mm)	h (mm)	Pack Unit
with screw-cap and pouring ring from PP					
21 881 28 54	125	45	55	124	4
21 881 36 53	250	45	66	158	4
21 881 44 52	500	45	78	193	4
21 881 54 57	1 000	45	93	253	4



DURAN® YOUTILITY Laboratory Bottle Amber

GL 45, USP <660> and USP <671> (Spectral Transmission) compliant



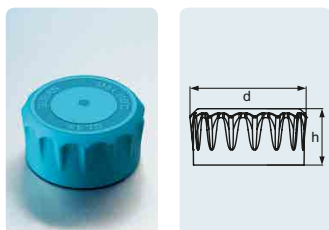
The specially shaped gripping zones on both sides of the bottle enable easier and safer handling. With the new DURAN® YOUTILITY bottle thread opening or closing the bottle is significantly faster. The thread is fully compatible with DIN GL 45 closures and other accessories. The slimmer DURAN® YOUTILITY bottle shape allows a more optimal use of limited space in autoclaves and laboratory refrigerators. A pre-defined labelling area is compatible with the dedicated DURAN® self-adhesive YOUTILITY bottle labels. Nominal volume is shown at the top of the easy-to-read graduation scale for fast determination of the volumes. The glass bottle body is moulded from the tried and tested DURAN® borosilicate 3.3 pharmacopoeial Type 1 neutral glass. DURAN® glass offers very good chemical resistance and high temperature resistance. Each DURAN® YOUTILITY bottle is supplied as a complete system, with a pouring ring (PP) and a GL 45 cap (PP).

Cat. No.	Capacity (mL)	DIN Thread (GL)	d (OD) (mm)	h (mm)	Pack Unit
with screw-cap and pouring ring from PP					
21 886 28 59	125	45	55	124	4
21 886 36 58	250	45	66	158	4
21 886 44 57	500	45	78	193	4
21 886 54 53	1 000	45	93	253	4



DURAN® YOUTILITY Screw Cap from PP

GL 45



The DURAN® YOUTILITY Screw Cap GL 45 is manufactured from a food-grade polypropylene (PP). Ergonomically shaped screw cap with optimised grooves and ridges for a more efficient and easier tightening or removal. The faster opening and closing thread of the YOUTILITY screw cap is fully compatible with DIN GL 45 bottle threads. The optimised cap sealing system ensures a liquid tight seal. A pre-defined labelling area on the cap is compatible with the dedicated DURAN® self-adhesive YOUTILITY labels.

Cat. No.	DIN Thread (GL)	d (OD) (mm)	h (mm)	Colour	Pack Unit
screw cap					
29 229 28 02	45	53	25	cyan	10
pouring ring					
29 241 28 08	45		4	cyan	16



DURAN® YOUTILITY

DESIGNED FOR YOU



**DURAN
WHEATON
KIMBLE**

Excellence in your hands

SARTORIUS CPA6202S

Model		CPA6202S	CPA6202P	GPA5202/ CPA5202S-DS	CPA4202S	CPA3202S/ GPA3202	CPA2202S/ CPA2202S-DS
Weighing capacity	g	6,200	1,500/ 3,000/6,200	5,200	4,200	3,200	2,200
Readability	g	0.01	0.01/0.02/ 0.05	0.01	0.01	0.01	0.01
Tare range (subtractive)	g	-6,200	-6,200	-5,200	-4,200	-3,200	-2,200
Repeatability (std. deviation)	±g	0.01	0.01/0.01/ 0.03	0.01	0.01	0.01	0.01
Linearity	±g	0.02	0.02/0.02/ 0.05	0.02	0.02	0.02	0.02
Response time (average)	s	≤ 1.5					
Operating temperature range	°C	10° to 30° (50° to 86°F)					
Allowable ambient operating temperature	°C	0° to 40° (32° to 104°F)					
Sensitivity drift within +10 to +30°C	±%/K	2 · 10 ⁻⁶					
External calibration weight (of at least accuracy class...)	g	5,000 (E2)	5,000 (F1)	5,000 (E2)	2,000 (E2)	2,000 (F1)	2,000 (F1)
Net weight, approx.	kg	4.7	4.7	6	4.7	4.7	4.7/6
Weighing pan size	mm	190×204	190×204	190×204/ ∅ 130	190×204	190×204	190×204/ ∅ 130
Weighing pan area	cm ²	388	388	388/133	388	388	388/133
Dimensions (W×D×H)	mm	213× 342× 88	213× 342× 88	213× 342× 88/340	213× 342× 88	213× 342× 88	213× 342× 88/340
AC power source/ power requirements	V~	AC adapter STNG6, 230 V or 115 V, +15% to - 20% (protection rating IP20)					
Frequency	Hz	48 - 60					
Power consumption (average)	VA	maximum 16; typical 8					
Approx. hours of operation with the YRB05Z rechargeable battery pack	h	27					
Selectable weight units		Grams, kilograms, carats, pounds, ounces, Troy ounces, Hong Kong taels, Singapore taels, Taiwanese taels, grains, pennyweights, milligrams, parts per pound, Chinese taels, mommes, Austrian carats, tola, baht and mesghal					
Built-in interface		RS-232C-S/V24-V28; 7-bit; parity: even, odd, mark, or space; transmission rates: 150 to 19,200 baud; 1 or 2 stop bits; software/hardware handshake					

Model		CPA 10001	CPA 8201	CPA 5201	CPA 34001S	CPA 34001P	CPA 16001S	CPA 12001S	CPA 34000	
Weighing capacity	kg	10	8.2	5.2	34	8/16/34	16	12	34	
Readability (scale interval)	g	0.1	0.1	0.1	0.1	0.1/0.2/0.5	0.1	0.1	1	
Tare range (subtractive)	kg	-10	-8.2	-5.2	-34	-34	-16	-12	-34	
Repeatability (std. deviation)	±g	0.1	0.1	0.1	0.1	0.1/0.2/0.5	0.1	0.1	0.5	
Linearity	±g	0.2	0.2	0.2	0.2	0.3/0.3/0.3	0.2	0.2	1	
Response time (average)	s	≤ 1	≤ 1	≤ 1	≤ 2	≤ 2	≤ 2	≤ 2	≤ 1.5	
Operating temperature range	°C	10° to 30° (50° to 86°F)								
Allowable ambient operating temperature	°C	0° to 40° (32° to 104°F)								
Sensitivity drift within 10° to 30°C	±g/K	4 · 10 ⁻⁶	4 · 10 ⁻⁶	4 · 10 ⁻⁶	2 · 10 ⁻⁶	2 · 10 ⁻⁶	2 · 10 ⁻⁶	2 · 10 ⁻⁶	2 · 10 ⁻⁶	
External calibration weight (of at least accuracy class...)	kg	5 (F1)	5 (F2)	5 (F2)	10 (F1)	10 (F2)	10 (F1)	10 (F1)	10 (F2)	
Net weight, approx.	kg	4.7	4.7	4.7	16	16	16	16	16	
Weighing pan size	mm	190×204	190×204	300×400		300×400	300×400	300×400	300×400	
Dimensions (WxD×H)	mm	213× 342× 90	213× 342× 90	213× 342× 90	313× 532× 120	313× 532× 120	313× 532× 120	313× 532× 120	313× 532× 120	
AC power source/ power requirements	V~	AC adapter STNG6, 230 V or 115 V, +15% to - 20% (protection rating IP20)								
Frequency	Hz	48 - 60								
Power consumption (average) VA		maximum 16; typical 8								
Approx. hours of operation with a rechargeable battery pack	h	40	40	40	22	22	22	22	22	
Selectable weight units		Grams, kilograms, carats, pounds, ounces, Troy ounces, Hong Kong taels, Singapore taels, Taiwanese taels, grains, pennyweights, milligrams, parts per pound, Chinese taels, mommes, Austrian carats, tola, baht and mesghal								
Cable length between display unit/weighing platform	m	-	-	-	1.2	1.2	1.2	1.2	1.2	
Built-in interface		RS-232C-5/V24-V28; 7-bit; parity: even, odd, mark, or space; transmission rates: 150 to 19,200 baud; 1 or 2 stop bits; software/hardware handshake								



* Three-sided weighing pan: \varnothing = diameter of inner circle.
The cross-hatched section can be fully utilized.

Model		CPA26P -OCE	CPA225D -OCE	CPA324S -OCE	CPA224S -OCE, CPA224 -PCE	CPA124S -OCE, CPA124S -PCE	CPA64 -OCE
Type		BC BL 100	BC BL 100	BC BL 100	BC BL 100	BC BL 100	BC BL 100
Accuracy class ¹⁾		Ⓢ	Ⓢ	Ⓢ	Ⓢ	Ⓢ	Ⓢ
Maximum capacity, Max ¹⁾	g	5/21	100/220	320	220	120	64
Scale interval d ¹⁾	mg	0.002/0.01	0.01/0.1	0.1	0.1	0.1	0.1
Tare range (subtractive)	g	≤ 100% of the maximum capacity					
Verification scale interval, e ¹⁾	g	0.001	0.001	0.001	0.001	0.001	0.001
Minimum capacity, Min ¹⁾	g	0.0002	0.001	0.01	0.01	0.01	0.01
Response time (average)	s	10	≤ 6/3	≤ 3	≤ 2	≤ 2	≤ 2
Range of use according to CD ¹⁾	g	0.0002–21	0.001–220	0.01–320	0.01–220	0.01–120	0.01–64
Allowable ambient operating temperature:							
– with "isoCAL" function	°C	+10° to +30° (+50° to +86°F)					
– without "isoCAL" function	°C	+15° to +25° (+59° to +77°F)					
External calibration weight (of at least accuracy class...)	g	20 (E2)	200 (E2)	200 + 100 (E2)	200 (E2)	100 (E2)	50 (E2)
Net weight, approx.	kg	7.6	7.6	6.5	6.5	6.5	6.5
Weighing pan size (inner diameter)	mm	50 Ø	80 Ø*	80 Ø*	80 Ø*	80 Ø*	80 Ø*
Weighing pan area	cm ²	20	64*	64*	64*	64*	64*
Weighing chamber height (weighing pan to draft shield cover)	mm	162	232	232	232	232	232
Dimensions (W×D×H)							
– Balance	mm	213×342×270	213×342×340	213×342×340	213×342×340	213×342×340	213×342×340
– Electronics box	mm	134×51×155	134×51×155	–	–	–	–
AC power source/ power requirements	V~	AC adapter STNG6, 230 V or 115 V, +15%...– 20% (protection rating IP20)					
Frequency	Hz	48 – 60					
Power consumption (average)	VA	maximum 16; typical 8					
Approx. hours of operation with the YRB05Z rechargeable battery pack	h	20	20	22	22	22	22
Selectable weight units		Grams, carats, milligrams					
Built-in interface		RS-232C-5/V24-V28; 7-bit; parity: even, odd, mark, or space; transmission rates: 150 to 19,200 baud; 1 or 2 stop bits; software/hardware handshake					

¹⁾ CD= Council Directive 90/384/ECC for non-automatic weighing instruments; applicable to the European Economic Area



* Three-sided weighing pan: Ø = diameter of inner circle.
The cross-hatched section can be fully utilized.

Model		CPA1003S-OCE	CPA623S-OCE	CPA523S-PCE	CPA423S-OCE
Type		BD BL 100	BD BL 200	BD BL 200	BD BL 200
Accuracy class ¹⁾		Ⓘ	Ⓙ	Ⓚ	Ⓛ
Maximum capacity, Max ¹⁾	g	1,000	620	520	420
Scale interval, d ¹⁾	g	0.001	0.001	0.001	0.001
Tare range (subtractive)	g	≤ 100% of the maximum capacity			
Verification scale interval, e ¹⁾	g	0.01	0.01	0.01	0.01
Minimum capacity, Min ¹⁾	g	0.1	0.02	0.02	0.02
Response time (average)	s	≤ 1.5			
Range of use according to CD ¹⁾	g	0.1–1,000	0.02–620	0.02–520	0.02–420
Allowable ambient operating temperature:					
– with “isoCAL” function		+10 to +40°C (+50° to +104°F)	+0° to +40°C (+32° to +104°F)	+0° to +40°C (+32° to +104°F)	+0° to +40°C (+32° to +104°F)
– without “isoCAL” function		+15 to +25°C (+50° to +77°F)	+10° to +30°C (+50° to +86°F)	+10° to +30°C (+50° to +86°F)	+10° to +30°C (+50° to +86°F)
Net weight, approx.	kg	6.5	4.6	4.6	4.6
Weighing pan size (inner diameter)*	mm	110 ∅			
Weighing pan surface*	cm ²	120			
Weighing chamber height (weighing pan to draft shield cover)	mm	240	50	50	50
Dimensions (WxDxH)	mm	213x342x340	213x342x153	213x342x153	213x342x153
AC power source/ power requirements	V~	AC adapter STNG6 230 V or 115 V, +15% to – 20% (protection rating IP20)			
Frequency	Hz	48 – 60			
Power consumption (average)	VA	maximum 16; typical 8			
Approx. hours of operation with the YRB05Z rechargeable battery pack	h	27			
Selectable weight units		Grams, carats			
Built-in interface		RS-232C-S/V24-V28; 7-bit; parity: even, odd, mark, or space; transmission rates: 150 to 19,200 baud; 1 or 2 stop bits; software/hardware handshake			

¹⁾ CD= Council Directive 90/384/ECC for non-automatic weighing instruments; applicable to the European Economic Area



* Three-sided weighing pan: ∅ = diameter of inner circle.
The cross-hatched section can be fully utilized.

Model		CPA323S-OCE	CPA223S-OCE	GC1603S-OCE	GC803S-OCE
Type		BD BL 200	BD BL 200	BC BL 100	BC BL 100
Accuracy class ¹⁾		II	II	I	I
Maximum capacity, Max ¹⁾		320 g	220 g	1,600 ct	800 ct
Scale interval, d ¹⁾		0.001 g	0.001 g	0.001 ct	0.001 ct
Tare range (subtractive)		≤ 100% of the maximum capacity			
Verification scale interval, e ¹⁾		0.01 g	0.01 g	10 mct	10 mct
Minimum capacity, Min ¹⁾		0.02 g	0.02 g	0.1 ct	0.1 ct
Response time (average)	s	≤ 1.5	≤ 1.5	≤ 2	≤ 2
Range of use according to CD ¹⁾		0.02–320 g	0.02–220 g	0.1–1,600 ct	0.1–800 ct
Allowable ambient operating temperature:					
– with "isoCAL" function	°C	+0° to +40° (+32° to +104°F)		+10° to +30° (+50° to +86°F)	
– without "isoCAL" function	°C	+10° to +30° (+50° to +86°F)		+15 to +25 (59°F to 77°F)	
External calibration weight (of at least accuracy class)	g			200 + 100 (E2)	100 (E2)
Net weight, approx.	kg	4.6	4.6	6.1	6.1
Weighing pan size (inner diameter)*	mm	110 ∅	110 ∅	80 ∅	80 ∅
Weighing pan area*	cm ²	120	120	64	64
Weighing chamber height (weighing pan to draft shield cover)	mm	50	50	162	162
Dimensions (WxDxH)	mm	213x342x153	213x342x153	213x342x270	213x342x270
AC power source/ power requirements	V~	AC adapter STNG6 230 V or 115 V, +15% to –20% (protection rating IP20)			
Frequency	Hz	48 – 60			
Power consumption (average)	VA	maximum 16; typical 8			
Approx. hours of operation with the YRB05Z rechargeable battery pack	h	27	27	22	22
Selectable weight units		Grams, carats		Grams, milligrams, carats	
Built-in interface		RS-232C-5/V24-V28; 7-bit; parity: even, odd, mark, or space; transmission rates: 150 to 19,200 baud; 1 or 2 stop bits; software/hardware handshake			

¹⁾ CD= Council Directive 90/384/ECC for non-automatic weighing instruments; applicable to the European Economic Area



* Three-sided weighing pan: ∅ = diameter of inner circle. The cross-hatched section can be fully utilized.

Model		CPA6202S -OCE	CPA6202P -OCE	GPA5202 -OCE	CPA4202S -OCE, CPA4202S -PCE	CPA3202S -OCE, CPA3202S -PCE, GPA3202 -OCE	CPA2202S -OCE
Type		BD BL 200	BD BL 200	BD BL 200	BD BL 200	BD BL 200	BD BL 200
Accuracy class ¹⁾		II	II	II	II	II	II
Maximum capacity, Max ¹⁾	g	6,200	1,500/3,000/ 6,200	5,200	4,200	3,200	2,200
Scale interval, d ¹⁾	g	0.01	0.01/0.02/ 0.05	0.01	0.01	0.01	0.01
Tare range (subtractive)	g	≤ 100% of the maximum capacity					
Verification scale interval, e ¹⁾	g	0.1	0.1	0.1	0.1	0.1	0.1
Minimum capacity, Min ¹⁾	g	0.5	0.5	0.5	0.5	0.5	0.5
Response time (average)	s	≤ 1.5					
Range of use according to CD ¹⁾	g	0.5–6,200	0.5–6,200	0.5–5,200	0.5–4,200	0.5–3,200	0.5–2,200
Allowable ambient operating temperature:							
- with "isoCAL" function	°C	+0° to +40° (+32° to +104°F)					
- without "isoCAL" function	°C	+10° to +30° (+50° to +86°F)					
Net weight, approx.	kg	4.7					
Weighing pan size	mm	190×204					
Weighing pan area*	cm ²	388					
Dimensions (W×D×H)	mm	213×342×88					
AC power source/ power requirements	V~	AC adapter STNG6 230 V or 115 V, +15% to - 20% (protection rating IP20)					
Frequency	Hz	48 – 60					
Power consumption (average)VA		maximum 16; typical 8					
Approx. hours of operation with the YRB05Z rechargeable battery pack	h	27					
Selectable weight units		Grams, kilograms, carats					
Built-in interface		RS-232C-S/V24-V28; 7-bit; parity: even, odd, mark, or space; transmission rates: 150 to 19,200 baud; 1 or 2 stop bits; software/hardware handshake					

¹⁾ CD= Council Directive 90/384/ECC for non-automatic weighing instruments;
applicable to the European Economic Area

heidolph MR Hei-Standard



➤ Technical data

MR Hei-Standard, MR Hei-Tec, MR Hei-Connect

Supply power	230 V 50/60 Hz	or 115 V 50/60 Hz
Power consumption (W)	825	or 625
Protective class (IEC 61140)	1 ⊕	
Protection class (IEC 60529)	IP 32	
Sound pressure level (dB(A)) (based on IEC 61010)	< 70	
Drive	EC-motor	
Overheat protection	no	
Operating mode	continuous	
Speed range (rpm)	100 - 1,400	
Speed accuracy (%)	±2	
Stirring capacity, max (H ₂ O) (l)	20	
Temperature control	Micro controller	
Heating power (W)	800	or 600
Hotplate temperature (° C)	20 - 300	
Accuracy hotplate (° C)	±5	
Safety circuit hotplate (° C)	>25 set temperature hotplate	
External sensor	Pt 1000	
Pt 1000 temperature max. (° C)	300	
Temperature accuracy with external temperature sensor (° C)	±1	
Safety circuit hotplate via temperature sensor Pt 1000 (° C)	>25 set temperature Pt 1000	
Load capacity, max. (kg)	25	
Plate diameter (Ø) (mm)	145	
Dimensions (l x w x h) (mm)	277 x 173 x 94	
Weight (kg)	2.9	

Model	MR Hei-Standard	MR Hei-Tec	MR Hei-Connect
Timer	-	-	yes
Interface			RS 232
Speed setting	analog	digital	digital
Accuracy temperature setting (° C)	±5	±1	±1

* Accuracy determined with following parameters: 800 ml water in 1 l beaker, form H according to DIN 12 331; temperature 50 °C; magnetic stirring bars 40 mm; speed 600 rpm; sensor depth 60 mm.

Appendix F - MATLAB script

Drainage potential curve script

```
1 % Sigurd Harstad
2 % 17.4.2020
3 % Posjekt
4 % Drainage curve model, draf 2, Sigurd Harstad
5
6 close all
7 clear all
8 clc
9
10 %% Logical
11 TRUE=1;
12 FALSE=0;
13
14 %Goal
15 %  $\alpha_{wc} = \int (0-D) \alpha(y) * W(y) dy$ 
16 %% Area of pipe
17 % needs a fuction of width of pipe W(y) to find
18 % inputs
19 D_in=1; %[m] % Inner diamter of pipe
20 y=linspace(0,D_in,1e4); % discretization the pipe into
    segments
21 width=zeros(1,length(y)); % empty array for width
22
23 A=zeros(1,length(y));% empty array for segment area , A=
    segment area
24 width=width_func(y,D_in); % call width function
25 %% Area of pipe using midpoint rule methode
26 for i=1:length(y)
27     if i==1
28         A(i)=(width(i))*(y(i)); % first entry
29     else
30         A(i)=((width(i)+width(i-1))/2)*(y(i)-y(i-1)); %
            midpoint value for area
31     end
32 end
33 Ageo=(D_in^2/4)*pi; % Gemoetric determine area , in order to
    compare aprox .
34 Aitt=sum(A); % Total area of pipe , using aprox
35 error=abs(Ageo-Aitt); % compare gemetric and aprox
36 relerror=error/Aitt; % determine relativ error of aprox
    area of pipe
```

```

37
38 %% Water cut
39
40 %% Uniforme water cut
41 if (FALSE)
42     % WC_in=input('Input Water cut into system [0-1]')
43     WC_in=0.3;
44     alfa_i=WC_in; % uniform water cut
45     alfa=zeros(1,length(y));
46     for i=1:length(y)
47         alfa(i)=alfa_i;
48     end
49 end
50
51 %% Straified flow uncontaminated phases
52 % alfa = 1 in lower part, alfa = 0 in upper part
53 if(FALSE)
54     WC_in=0.9;
55     alfa=step_alfa(y,WC_in,A);
56 end
57 %% Stratified flow contaminated phases
58 % cont_w = contaminated of water (oil in water)
59 % cont_o = contaminated of oil (water in oil)
60 % alfa = 1-cont_w in lower part, alfa = 0+cont_w in upper
    part
61 if(FALSE)
62     WC_in=0.5;
63     cont_o=0.2; % WiO
64     cont_w=0.2; % OiW
65     alfa=step_cont_alfa(y,WC_in,A,cont_o,cont_w);
66 end
67
68 %% Stratified flow contaminated phases random contamination
69 % cont_w = mean contaminated of water (oil in water)
70 % cont_o = mean contaminated of oil (water in oil)
71 % alfa = 1-cont_w in lower part, alfa = 0+cont_w in upper
    part
72 if(FALSE)
73     WC_in=0.5;
74     cont_o=0.1; % WiO
75     cont_w=0.1; % OiW
76     alfa=step_cont_rand_alfa(y,WC_in,A,cont_o,cont_w);
77 end
78
79 %% Lin transiton from water to oil

```

```

80 if(FALSE)
81     WC_in=0.9;
82     y_inter=0.4;
83     alfa=lin_trans_alfa(y,Wc_in,A,y_inter);
84
85 end
86 %% Lin transiton from water to oil w/ contamination
87 if(TRUE)
88     WC_in=0.5;
89     y_inter=0.4;
90     cont_o=0.2; % WiO
91     cont_w=0.2; % OiW
92     alfa=lin_trans_alfa_cont(y,Wc_in,A,y_inter ,cont_o ,
93         cont_w);
94
95 end
96 %% Random water cut
97 if(FALSE)
98     WC_in=0.5;
99     alfa=rand(1,length(y));
100 end
101
102 %% Othe water cute
103 if(FALSE)
104     % not in use
105 end
106
107 %% Water content
108 v_liquid=2; %[m/s]
109 %q = A* v
110 q_water_arr=zeros(1,length(y));
111 q_liq_arr=zeros(1,length(y));
112 for i=1:length(y)
113     if i==1
114         q_water_arr(i)=(width(i))*(y(i))*(alfa(i))*v_liquid
115             ;
116         q_liq_arr(i)=(width(i))*(y(i))*v_liquid;
117     else
118         q_water_arr(i)=((width(i)+width(i-1))/2)*(y(i)-y(i-1))
119             *((alfa(i)+alfa(i-1))/2)*v_liquid;
120         q_liq_arr(i)=((width(i)+width(i-1))/2)*(y(i)-y(i-1))*
121             v_liquid;
122     end
123 end

```

```

121 %% Water drainage
122
123 cnt2=1;
124 h=0:0.01:D_in;
125 q_water_tapped=zeros(1,length(h));
126 q_water_total=zeros(1,length(h));
127 pst_q_tot_tapped=zeros(1,length(h));
128 wc_tapped_calc=zeros(1,length(h));
129
130 while h(cnt2)<D_in
131     cnt=1;
132     q_liq_tap_arr=zeros(1,length(y));
133     q_water_tap_arr=zeros(1,length(y));
134     while y(cnt)<h(cnt2)
135         q_liq_tap_arr(cnt)=q_liq_arr(cnt);
136         q_water_tap_arr(cnt)=q_water_arr(cnt);
137         cnt=cnt+1;
138     end
139     q_water_tapped(cnt2)=sum(q_water_tap_arr);
140     q_water_total(cnt2)=sum(q_water_arr);
141     pst_q_tot_tapped(cnt2)=100*((q_water_tapped(cnt2))/
        q_water_total(cnt2));
142     if (sum(q_liq_tap_arr))==0
143         wc_tapped_calc(cnt2)=alfa(1)*100;
144     else
145         wc_tapped_calc(cnt2)=100*(sum(q_water_tap_arr))/(sum(
            q_liq_tap_arr));
146     end
147     cnt2=cnt2+1;
148 end
149
150 if h(cnt2)==D_in % all liquid is drained
151     q_water_tapped(cnt2)= Aitt*v_liquid*WC_in;
152     q_water_total(cnt2)=q_water_tapped(cnt2);
153     pst_q_tot_tapped(cnt2)=100*(q_water_tapped(cnt2))/(
        q_water_total(cnt2));
154     wc_tapped_calc(cnt2)=100*WC_in;
155 end
156
157 %% Results
158
159 fprintf('Area of pipe from gemetri %.4f [m2]\n',Ageo) %
    print area of pipe geo
160 fprintf('Area of pipe from aprox %.4f [m2]\n',Aitt) % print
    area of pipe calc

```

```

161 fprintf('Relative error in aprox and gemotri %.4E []\n',
        relerror) % print relative error of area
162 figure
163 plot(wc_tapped_calc , pst_q_tot_tapped , '-b')
164 axis([-5,110,-5,110])
165 xlabel('Water cut of tapped stream [%]')
166 ylabel('Water tapped of totalt water in stream [%]')
167 grid on
168 title('Drainage pot. plot')
169
170 temp2=y/D_in; % normilize postion y in pipe by the the
        diameter
171 figure
172 plot(alfa , temp2 , '--r')
173 clear temp2
174 axis([-1,2,0,1])
175 xlabel('Water cut[]')
176 ylabel('Normalized position in pipe')
177 grid on
178 title('Water content at position')
179
180 WC_end_chech=sum(A.* alfa )/sum(A);
181 WC_error=abs(WC_in-WC_end_chech);
182 WC_rel=WC_error/WC_end_chech;
183 a=100*WC_in;
184 b=100*WC_end_chech;
185
186 fprintf('Water cut input %.4f [%%] \n',a) %print WC input
187 fprintf('Water cut calculatet %.4f [%%] \n',b) %print WC
        calc.
188 fprintf('Relative error in Water cut calculated %.4E []\n',
        WC_rel) %print relative error of WC
189 clear a b
190 %% Export water cut curve results to Excel
191 % Store values generated in Excel
192 if(FALSE)
193     t=clock;
194     store1=[y(:) , alfa (:) ];
195     xlswrite('C:\Users\sigur\Documents\Student\NTNU\
        Projekt\Resulteter\04_06_2020_model_results3.xls',t
        , 'Ark1' , 'A1:F1')
196     xlswrite('C:\Users\sigur\Documents\Student\NTNU\
        Projekt\Resulteter\04_06_2020_model_results3.xls' ,
        WC_in , 'Ark1' , 'A2')
197     xlswrite('C:\Users\sigur\Documents\Student\NTNU\

```

```

        Projekt\Resulteter\04_06_2020_model_results3.xls',
        store1, 'Ark1', 'A3:B1002')
198     clear store1
199 end
200 %% Export drainage curve results to Excel
201 % Store values generated in Excel
202 if(FALSE)
203     t=clock;
204     store1=[wc_tapped_calc(:), pst_q_tot_tapped(:)];
205     xlswrite('C:\Users\sigur\Documents\Student\NTNU\
        Projekt\Resulteter\06_06_2020_model_results3.xls', t
        , 'Ark4', 'A1:F1')
206     xlswrite('C:\Users\sigur\Documents\Student\NTNU\
        Projekt\Resulteter\06_06_2020_model_results3.xls',
        WC_in, 'Ark4', 'A2')
207     xlswrite('C:\Users\sigur\Documents\Student\NTNU\
        Projekt\Resulteter\06_06_2020_model_results3.xls',
        store1, 'Ark4', 'A3:B103')
208
209 end
210 %% Error seacht

```

Step water volume fraction function script

```

1  function [ alfa ]= step_alfa (y, WC_tot, A)
2  % Input: y, postion from in [m] lower edgt of pipe, y=0.
3  % diamter of pipe [m]
4  % WC_tot totalt water cut
5  % A, array of Area
6  % Output. Water content alfa(y) as a function of position y
   , distance from
7  % y=0, lower pipe
8  %n=length(y);
9  d=y(end);
10 if y>d
11     disp('postiton outside of pipe, y larger then d,
        diameter of pipe')
12     return
13 end
14 error=1;
15
16 delta=10e-5;
17 a=y(1);
18 b=y(end);
19 h=rand;

```

```

20 f=@(h) WC_tot-(sum(A.*(1-heaviside(y-h)))/sum(A));
21
22 [c,err,yc]=bisect(f,a,b,delta);
23
24 alfa=(1-heaviside(y-c));
25 return

```

Step with uniform phase contamination water volume fraction function script

```

1 function [alfa]=step_cont_alfa(y,WC_tot,A,cont_o,cont_w)
2 % Input: y, position from in [m] lower edgt of pipe, y=0.
3 % diamter of pipe [m]
4 % WC_tot totalt water cut
5 % A, array of Area
6 % Output. Water content alfa(y) as a function of position y
7 % , distance from
8 % y=0, lower pipe
9 %n=length(y);
10 d=y(end);
11 if y>d
12     disp('postiton outside of pipe, y larger then d,
13         diameter of pipe')
14     return
15 end
16 error=1;
17
18 delta=10e-6;
19 a=y(1);
20 b=y(end);
21 h=rand;
22 f=@(h) WC_tot-(sum(A.*(max((1-heaviside(y-h)-cont_w),cont_o
23     )))))/sum(A);
24 [c,err,yc]=bisect(f,a,b,delta);
25
26 alfa=max((1-heaviside(y-c)-cont_w),cont_o);
27 return

```

Step with random phase contamination water volume fraction function script

```
1 function [ alfa ]=step_cont_rand_alfa (y ,WC_tot ,A, cont_o , cont_w
   )
2 % Input: y, position from in [m] lower edgt of pipe , y=0.
3 % diamter of pipe [m]
4 % WC_tot totalt water cut
5 % A, array of Area
6 % Output. Water content alfa(y) as a function of position y
   , distance from
7 % y=0, lower pipe
8 %n=length(y);
9 d=y(end);
10 if y>d
11     disp('postiton outside of pipe , y larger then d,
           diameter of pipe')
12     return
13 end
14 error=1;
15
16 delta=10e-6;
17 a=y(1);
18 b=y(end);
19 h=rand;
20 f=@(h) WC_tot-(sum(A.*(max((1-heaviside(y-h)-cont_w),cont_o
   )))))/sum(A);
21
22 [c, err ,yc]=bisect(f,a,b,delta);
23
24 n=length(y);
25 cont_w2=cont_w*rand(1,n)+(cont_w/2);
26 cont_o2=cont_o*rand(1,n)+(cont_o/2);
27 alfa=max((1-heaviside(y-c)-cont_w2),cont_o2);
28
29 return
```

Uniform water volume fraction function script

```
1 function [ alfa ]=lin_alfa (y,d,WC_tot,n)
2 % Input: y, postion from in [m] lower edgt of pipe , y=0.
3 % diamter of pipe [m]
4 % WC_tot totalt water cut , sum of all alfa must be equal to
   WC_in
5 % n slicing of pipe , given from griding of from area
6 % Output. Water content alfa(y) as a function of position y
   , distance from
7 % y=0, lower pipe
8
9 if y>d
10     disp('postiton outside of pipe , y larger then d,
           diameter of pipe ')
11     return
12 end
13
14 holder1=linspace(0,d,n)
15 holder2=linspace(0,y)
16
17 return
```

Linear transition from water to oil script

```
1 function [ alfa ]=lin_trans_alfa (y,WC_tot,A,y_inter)
2 % Input: y, array of distans for low side pipe
3 % diamter of pipe [m]
4 % WC_tot totalt water cut
5 % A, array of Area
6 % Output. Water content alfa(y) as a function of position y
   , distance from
7 % y=0, lower pipe
8 d=y(end);
9 if y>d
10     disp('postiton outside of pipe , y larger then d,
           diameter of pipe ')
11     return
12 end
13
14 error=1;
15
16 delta=10e-5;
17 a=y(1);
18 b=y(end);
```

```

19 h=rand;
20 d_inter=y_inter;
21
22 %sub_alfa=lin_trans_disp(y,h,d_inter);
23 f=@(h) WC_tot- (sum(A.*(lin_trans_disp(y,h,d_inter)))/sum(
    A));
24
25
26 [c,err,yc]=bisect(f,a,b,delta);
27
28 alfa=lin_trans_disp(y,c,d_inter);
29
30
31 return

```

Linear transition sub function

```

1 function [sub_alfa]=lin_trans_disp(y,h,d_inter)
2 % y = position in pipe
3 % h = positon of "interface" the point where the domintans
    fluid switsh
4 % d_inter = width of trasistion zone over interface
5
6
7 n=length(y);
8 intermid=zeros(1,n);
9 for i=1:n
10 if (y(i)>h-d_inter/2 && y(i)<h+d_inter/2)
11     intermid(i)=1;
12 end
13 m=sum(intermid);
14 end
15 sub_alfa=zeros(1,n);
16
17 for i=1:n
18     if i==1
19         sub_alfa=1;
20     else
21         if (y(i)<h-d_inter/2)
22             sub_alfa(i)=1;
23         elseif (y(i)>h+d_inter/2)
24             sub_alfa(i)=0;
25         else
26             sub_alfa(i)=sub_alfa(i-1)-1/m;
27         end
28     end

```

```

29
30 end
31 return

```

Linear transition from water to oil with phase contamination script

```

1 function [ alfa ]=lin_trans_alfa_cont (y, WC_tot, A, y_inter ,
      cont_o , cont_w)
2 % Input: y, array of distans for low side pipe
3 % diamter of pipe [m]
4 % WC_tot totalt water cut
5 % A, array of Area
6 % Output. Water content alfa(y) as a function of position y
      , distance from
7 % y=0, lower pipe
8 d=y(end);
9 if y>d
10     disp('postiton outside of pipe, y larger then d,
           diameter of pipe')
11     return
12 end
13
14 error=1;
15
16 delta=10e-5;
17 a=y(1);
18 b=y(end);
19 h=rand;
20 d_inter=y_inter;
21
22 %sub_alfa=lin_trans_disp (y,h,d_inter);
23 f=@(h) WC_tot-(sum(A.*(max((lin_trans_disp (y,h,d_inter)-
      cont_w), cont_o)) ./ sum(A)));
24
25 %f=@(h) WC_tot-(sum(A.*(max((1-heaviside (y-h)-cont_w),
      cont_o)))) ./ sum(A);
26
27
28 [c, err , yc]=bisect (f, a, b, delta);
29
30 alfa=max (lin_trans_disp (y, c, d_inter)-cont_w , cont_o);
31
32
33 return

```

Width function script

```
1 function [W]=width_func(y,d)
2 %input y = hight from y=0, lowest point of pipe
3 % d= diamter of pipe in [m]
4 % output, width of a pipe, given in [m]
5 r=d/2;
6 if y>d
7     disp('postiton outside of pipe, y larger then d,
8         diameter of pipe')
9     return
10 end
11 if y<r
12     d=r-y;
13     W=2*r*sin(acos(d/r));
14 elseif y==r
15     W=2*r;
16 else
17     d=y-r;
18     W=2*r*sin(acos(d/r));
19 end
20 return
```

Bisection Method script

```
1 function [c, err , yc]=bisect(f,a,b,delta)
2 %Input - f is the function input as a string    f
3 %- a and b are the left and right endpoints
4 %- delta is the tolerance
5 %Output - c is the zero
6 %- yc=f(c)
7 %- err is the error estimate for c
8
9 ya=feval(f,a);
10 yb=feval(f,b);
11 if ya*yb>0
12     disp('no sultion found in bisec search')
13     return
14 end
15
16 max1=1+round((log(b-a)-log(delta))/log(2));
17
18 for k=1:max1
19     c=(a+b)/2;
20     yc=feval(f,c);
```

```
21
22  if yc==0
23  a=c;
24  b=c;
25  elseif yb*yc>0
26  b=c;
27  yb=yc;
28  else
29  a=c;
30  ya=yc;
31  end
32  if b-a < delta
33      break
34  end
35  end
36  c=(a+b)/2;
37  err=abs(b-a);
38  yc=feval(f,c);
39  return
```

